University of Southampton

Faculty of Environmental and Life Sciences

School of Ocean and Earth Science

Functional response of the Antarctic sea urchin, *Sterechinus neumayeri*, to environmental change and extreme events in the context of a warming climate

by

Rebecca De Leij

Thesis for the degree of Doctor of Philosophy

December 2021

University of Southampton

Abstract

Faculty of Environmental and Life Sciences
School of Ocean and Earth Science

Thesis for the degree of Doctor of Philosophy

Functional response of the Antarctic sea urchin, *Sterechinus neumayeri*, to environmental change and extreme events in the context of a warming climate

by
Rebecca de Leij

Gradual increases in mean ocean temperature are one of many broad-scale changes currently experienced in marine systems in response to anthropogenic forcing. Extreme climate events, such as marine heatwaves are forecast to escalate in many areas of the climate system under future global change scenarios. Species will have varying capacities to adapt, persist, and ultimately survive under these scenarios of environmental change. The allocation of energy to fundamental biological functions, in addition to the ability to acclimate to gradual change and recover from acute change, is key to this capacity. In the context of the current climate and that of the future, a better understanding of how organisms allocate energy as a response to environmental drivers is needed.

In this thesis I focus on the common Antarctic sea urchin, *Sterechinus neumayeri*; a representative species for studying environmental change impacts due to its inherent thermal sensitivity and overall significance as one of the most functionally important Antarctic shallow marine species and the most dominant echinoid in the nearshore benthic community. I explore how *S. neumayeri* allocates energy, in terms of reproductive investment and key biological functions, in the current climate, as well as during temperature extremes and for the climate predicted for 2100. I use a combination of approaches, including a timeseries of field-based observations and laboratory-based mesocosm experiments to simulate both gradual and acute extreme warming. My results show for the first time that endogenous rhythms against a backdrop of multifactorial shifts in the environment are key drivers of energy allocation in terms of reproduction. In addition, I show that the onset rate of acute warming is more important than absolute temperature in limiting key biological functions, and I provide evidence that a thermally

sensitive species like *S. neumayeri* may have an improved ability to cope with acute warming following acclimation to gradual temperature increases predicted for 2100.

Collectively, these results show that within the boundaries of natural variability, it is likely that species have the energetic capacity to buffer and cope with changes to the environment. However, as our global climate changes over the coming decades, the natural variability range of regional temperatures will shift in conjunction with extreme events, and as such, energetic investment and functional performance will depend on a matrix of factors such as warming onset rate and thermal history. Clearly, even some of the most thermally constrained species have the capacity to acclimate and recover from thermal stress, and although there will always be an energetic cost to this, the ability to acclimate and recover will undoubtedly benefit those who have this capacity in the future.

Table of Contents

Table of Tables

Table of Figures

Table of Figures

Research Thesis: Declaration of Authorship

Print name: Rebecca de Leij

Title of thesis: Functional response of the Antarctic sea urchin, *Sterechinus neumayeri*, to environmental change and extreme events in the context of a warming climate

I declare that this thesis and the work presented in it are my own and has been generated by me as the result of my own original research.

I confirm that:

1. This work was done wholly or mainly while in candidature for a research degree at this University;
2. Where any part of this thesis has previously been submitted for a degree or any other qualification at this University or any other institution, this has been clearly stated;
3. Where I have consulted the published work of others, this is always clearly attributed;
4. Where I have quoted from the work of others, the source is always given. With the exception of such quotations, this thesis is entirely my own work;
5. I have acknowledged all main sources of help;
6. Where the thesis is based on work done by myself jointly with others, I have made clear exactly what was done by others and what I have contributed myself;
7. Parts of this work have been published as:

De Leij, R., Peck, L. S., & Grange, L. J. (2021). Multiyear trend in reproduction underpins interannual variation in gametogenic development of an Antarctic urchin. *Scientific Reports*, 11(1), 1–13. https://doi.org/10.1038/s41598-021-98444-4

De Leij, R., Grange, L. J., & Peck, L. S. (2022). Functional thermal limits are determined by rate of warming during simulated marine heatwaves. *Marine Ecology Progress Series,* 685, 183-196. https://doi.org/https://doi.org/10.3354/meps13980

Signature: .....Date: .....

Acknowledgements

First and foremost, I would like to thank my supervisors Laura and Lloyd. Your support, enthusiasm, guidance, and kindness has been unfailing throughout the last four years and I am so very grateful to have had such fantastic supervisors to make this experience so enjoyable. You both allowed me to discover myself as a scientist, to learn and grow through my PhD experience with gentle guidance and reassurance whenever needed. To quote: “The best teachers are those who show you where to look but don’t tell you what to see”. You both have been the best teachers.

I would like to thank Madlaina Michelotti, Henry Ernst and Katie Margerum for their contributions to the histology work, and to the BAS Rothera Marine Team from 2012 - 2018, for collecting and preserving specimens and collecting the RaTS data. Thanks also to the Rothera Marine Team of 2020/21 Antarctic season, for the support provided during the experimental period of this work, in particular, the laboratory manager, Aurelia Reichardt for her technical guidance and assistance in the aquarium, and Dr. Simon Morley for his expertise and assistance during the Antarctic season. A huge thank you to the BAS aquarium manager, Becs Smith, for all her work involved in the long-term acclimation of my urchins and for supporting me through the experimental work in Cambridge.

A very special thank you to my husband, Mike. For being at the end of the phone and there at the end of each day to listen to the trials and tribulations that come with undertaking a PhD. You have been my biggest champion, encouragement and emotional support through this journey and your faith in me has kept me going through some of the toughest bits. Thank you. I cannot forget to thank my other emotional support, Enzo. My daily companion who has slept faithfully at my feet whilst I write, who has provided much needed fun and laughter in my breaks and is truly the best dog one could ask for.

Thank you to my Dad. You have been my biggest inspiration in your love of science and the natural world. Thank you for showing me how exciting nature is and nurturing my curiosity as a child. You have gone beyond that of a ‘typical’ parent role, from reading all of my reports for my bachelor’s degree, to always being ready and enthused to talk about science and my research. I would not be sitting here, writing the last words of my PhD, if it weren’t for you.

Finally, thank you to my wonderful Mum, for never willing me to be anything but happy. I wish you had been here to see me through this journey, but I have no doubt that you would be proud of this achievement.

Definitions and Abbreviations

AAnp	Adjusted area of nutritive phagocytes relative to gonad tissue total area
AAo	Adjusted area of oocytes relative to gonad tissue total area
ACC	Antarctic Circumpolar Current
AFDM	Ash-Free Dry Mass
AIC	Akaike information criterion
ANOVA	Analysis of Variance
Anp	Percentage area of nutritive phagocytes
Ao	Percentage area of oocytes
BAS	British Antarctic Survey
Chl-a	Chlorophyll-a
CI	Confidence Interval
CT_{max}	Critical Thermal Maximum
DM	Dry Mass
ECD	Equivalent Circular Diameter
ENSO	El Niño Southern Ocean Oscillation
GAM	Generalised Additive Modelling
GER	Gut Evacuation Rate
GHG	Green House Gas
GI	Gonad Index
LOESS	Locally weighted smoothing
MHW	Marine Heatwave
MSLP	Mean atmospheric sea level pressure
NP	Nutrient Phagocytes
OCLTT	Oxygen and Capacity Limited Thermal Tolerance Hypothesis

RaTS	Rothera Oceanographic and Biological Time Series
RO	Reverse Osmosis purified
SAM	Southern Annular Mode
SD	Standard Deviation
SE	Standard Error
SOI	Southern Oscillation Index
SST	Sea Surface Temperatures
WAP	Western Antarctic Peninsula

Chapter 1 Introduction

The Earth's climate experiences natural variability and we see evidence of this in ice and sediment core records (Alley, 2000; Zachos et al. 2001). Natural temperature variability can occur as a result of volcanic activity, variation in the Earth's orbit and in solar irradiance (Ahmed et al. 2013). However, since the 1960's, ocean temperatures have risen at a median rate of 0.07°C per decade (Burrows et al. 2011) due to an increase in green-house gas (GHG) emissions that emerged as a consequence of the industrial revolution (Myrvoll-Nilsen et al. 2019). There has since been a sustained and statistically significant warming of the earth's overall climate (Abram et al. 2016) with conservative estimates detecting positive temperature trends for 84% of the earth's surface (Myrvoll-Nilsen et al. 2019).

From 1960 - 2018, the oceans have compensated for ~89% of the additional energy from GHG's (Johnson et al. 2020). This heat is drawn down into the deep ocean, which causes ocean heat content to rise and acts to provisionally buffer the extent of global climate warming (Abram et al. 2016; Johnson et al. 2020; Levitus et al. 2012a). However, even if GHG emissions were stabilised today, the oceans would continue to warm due to time lag effects, and hence, most of the impacts of recent GHG emissions are yet to be reflected in the temperature of both the atmosphere and oceans (Frölicher & Paynter, 2015; Levitus et al. 2012b; Wetherald et al. 2001).

The rate of warming across the World's oceans is not ubiquitous, but instead ocean and atmospheric circulation and the coupled ocean-atmospheric system influences the intensity of warming experienced across different regions (Ahmed et al. 2013; Deser et al. 2012). For example, changes in regional atmospheric circulation subjected the Western Antarctic Peninsula (WAP) and surrounding ocean to rapid regional warming during the second half of the 20th century (Meredith & King, 2005), followed by a period of cooling in the 21st century (Turner et al. 2016). This extreme natural variability at a regional level masks the long term temperature trend caused by anthropogenic signals, making detection of region-specific warming against a backdrop of extreme variability, challenging (Clem et al. 2020; Turner et al. 2016).

The mechanisms generating extreme temperature variability can usually be attributed to an interaction of local processes that affect ocean mixing (e.g. ocean advection), teleconnection processes from remote sources (e.g. Jet stream position), as well as large-scale climate modes (e.g. El Niño-Southern Oscillation) (Holbrook et al. 2019). For example, strengthening of the Leeuwin Current during a La Niña period, combined with anomalously high air-sea heat flux was responsible for the marine heat wave (MHW) event occurring off Western Australia in summer 2011 (Caputi et al. 2014). Extreme

temperature anomalies in the South Pacific and Western Antarctic in 2009/2010 were associated with atmospheric circulation changes during an El Niño event (Lee et al. 2010). In addition, high sea level pressure and suppression of the air-sea heat flux led to warming anomalies in the North Eastern Pacific in 2014 (Nicholas et al. 2015). There is also growing consensus that the occurrence of extreme and prolonged warming events such as MHW events has, and will continue to increase as a result of the overall warming trend in the global climate (Frölicher et al. 2018).

Previous studies have used a range of metrics to define MHW events, with little consensus between studies and often ambiguity in the parameters that are used to define a MHW (e.g. Pearce & Feng, 2013, Smale & Wernberg, 2013). However, the approach described by Hobday et al. (2016) is now often used in research to define temperature thresholds that mark MHW events. By this definition, warming events can be considered as a MHW when temperatures exceed the 90th percentile of seasonally varying baseline temperatures, for five consecutive days or more. By this definition, the temperature thresholds of a MHW are variable depending on the region studied as well as the season in which it occurs.

Already, the number of MHW days has doubled between 1982 and 2016, and as the climate warms by a predicted 2^{o}C (Allen et al. 2018), the number of MHW days is expected to increase further by a factor of 23, relative to pre-industrial levels (Frölicher et al. 2018). By the late 21st century, much of our oceans are predicted to enter a state of 'permanent MHW status' (Frölicher et al. 2018; Oliver et al. 2019) where daily sea surface temperatures (SST) will largely fall within the 90th percentile of those currently experienced. These predictions pose a significant risk to the marine environment since there is already evidence that MHW events can have significant ecological consequences, with many species experiencing mass mortalities as temperatures exceed thermal capacities (Garrabou et al. 2009). Declines in habitats such as seagrass and kelp forests as well as increased prevalence of toxic algae have had subsequent implications for community dynamics where food and habitat resources are compromised (Caputi et al. 2014; Nowicki et al. 2019; Santora et al. 2020).

The mechanisms underlying a species capacity to tolerate thermal stress can be reflected in the thermal history of the animal. For example, ectotherms inhabiting environments with variable temperatures have been shown to have a larger thermal tolerance range compared to temperature stable environments (Magozzi & Calosi, 2015; Sandoval-Castillo et al. 2020). This effect of thermal history is alluded to in the 'Climate Variability Hypothesis' conceived by Stevens (1989), where the hypothesis states that a larger climatic variability gives rise to larger thermal ranges.

In addition to an animal's thermal range, generation time will likely be a factor determining a species resilience to change, since shorter life-spans allow for transgenerational

plasticity and 'evolutionary rescue' (*sensu* Bell, 2017), to rapidly changing environmental conditions (Morley et al. 2017; Somero, 2010). There are other factors that have been shown to help and also hinder an animal's ability to tolerate temperature change, such as population size and the genetic variation within the population (Peck, 2011; Somero, 2010), as well as individual body size and activity levels (Peck et al. 2009; Rohr et al. 2018). For this reason, there will likely be 'winners' and 'losers' in a warming climate scenario, with consequences for ecosystem structure and services.

Species often considered to be 'losers' in a warming climate, are Antarctic ectotherms. These species are typically exposed to cold temperatures averaging about 0^{o}C with very little seasonal variability, where temperatures range ± 2^{o}C (Clarke et al. 2008). Within this characteristically cold marine environment, many endemic species persist, adapted to cope with not only freezing temperatures, but also to a light regime that drives highly seasonal productivity (Peck, 2005; Peck et al. 2014). Slow growth rates are reported for many Antarctic species (Fraser et al. 2007), for example, maximum growth rates of encrusting bryozoans have been recorded as 5 – 10 times slower in Antarctica compared to their tropical and temperate counterparts (Barnes et al. 2007; Bowden et al. 2006) and the Antarctic limpet, *Nacella concinna,* has the slowest growth rate reported for any limpet ranging between 0.059 and 0.323 year^{-1}(Clarke et al. 2004) compared to growth rates ranging from 0.400 to 1.661 year^{-1} for the limpet genus *Cellana*, which inhabits temperate and tropical regions (Henriques et al. 2017). The likely cause of these slow growth rates is debated, however it is thought be a combination of low temperature and sporadic food supply (Baird & Stark, 2013; Thomas Brey & Clarke, 1993; Peck, 2018). There is also an increased cost of growth at cold temperatures due to a reduced efficiency of protein synthesis, with large amounts of energy used to make the protein required for growth (Peck, 2016, 2018; Rastrick & Whiteley, 2013). In addition to slow growth rates, delayed sexual maturity, longevity and low metabolic rates are also features of many Antarctic ectotherms (Arntz et al. 1992; Baird & Stark, 2013; Bigatti et al. 2001; Clarke, 1983; Peck, 2018). These adaptations could have evolved either to limit energy expenditure or else been forced as a result of limitations in food supply.

Antarctica and the Southern Ocean are made unique by their geographic and oceanographic isolation (Convey et al. 2009). It is the only continent not linked by its continental shelf to another continent, which is drove the formation of the oceanic Polar Front 25-35 million years ago (Peck, 2018). This front limits the free exchange of warmer waters with the cold waters of the Southern Ocean and it is this distinct temperature divide that serves as an important mechanism in delivering nutrient rich waters by the Antarctic Circumpolar Current (ACC) around the global ocean (Aronson et al. 2007; Turner et al. 2014). Cold ocean temperatures around Antarctica enable the Southern Ocean to draw in excess heat and carbon dioxide from the atmosphere, leading to a poleward shift of ocean

fronts and an overall increase in SST with consequences for sea ice cover and changes in physical and chemical properties of the water column (Constable et al. 2014; Rozema et al. 2017). These changes have cascading effects on sea level, ocean circulation and nutrient upwelling across the globe (Convey et al. 2009). The vulnerability of the Antarctic to anthropogenic climate change is therefore of global significance.

Our knowledge of the species that inhabit the unique Antarctic marine environment is limited by the inaccessibility of the region (Griffiths, 2010). Investigating community dynamics, ecosystem structure and functioning as well as species life-histories is key to understanding how the environment is regulated and balanced (Kaiser et al. 2013). Since most species identified in Antarctica are endemic, there is an urgent need to establish a baseline of knowledge for assessing future changes to habitats and species (Convey & Peck, 2019).

Research continues to focus on temperature thresholds and the effects of thermal stress on the allocation of energy in different species, whether that be responses to gradual change or short-term extreme events. However, it is important to first understand how energy is inherently allocated to functions and the seasonal and interannual variability of these allocations in the natural environment. From this baseline, we can better identify and understand the changes in energy allocation and functioning attributed to environmental change. Reproduction is one of the key biological functions as it determines the persistence of species and populations. Determining the drivers of reproductive periodicities in marine species has been the focus of much research, with variables such as photoperiod, temperature change, food availability and lunar cycles all shown to regulate gametogenesis and spawning (Emilio et al. 2018; Grange et al. 2004; Kelly, 2001; Muthiga & Kawaka, 2008; St.Gelais et al. 2016; Zhadan et al. 2017, 2018). However, despite evidence that these environmental factors often act as cues, there is still unexplained interannual variability in the reproductive effort of the Antarctic sea urchin *Sterechinus neumayeri* (Brockington et al. 2007), the brittle star *Ophionotus victoriae* (Grange et al. 2004), the brachiopod *Liothyrella uva* (Meidlinger et al. 1998), and the scallop, *Adamussium colbecki* (Tyler et al. 2003). The underlying drivers of interannual variability in these species remain largely unresolved due to the lack of multiyear studies observing the relationships between reproductive effort environmental conditions. This type of data is especially challenging to collect in a region such as Antarctica due to its remoteness and inhospitable environment. Studies across several years would be needed to find significant correlations or capture variability of large scale climate metrics such as the El Niño Southern Ocean Oscillation (ENSO) or Southern Annular Mode (SAM) (Grange et al. 2004).

Functions can be split into immediately critical for the maintenance of the individual, and long-term critical for population continuity. Immediately critical functions play important

roles in energetic consumption and delivery, as well as defence from predation (Bailey, 2001; M. S. Clark et al. 2008; Morley et al. 2009). These functions enable immediate persistence and survival of the individual (Peck, 2011). Critical functions for population continuity are rooted in reproductive success, where energy is directed to gamete development, fecundity, and spawning (Brown et al. 2004). Reproductive effort is therefore an important measure of fitness and can be used as a barometer to identify changes to energetic demands and allocation (Burger et al. 2019; Charnov et al. 2007). Since reproduction is not immediately critical for life, the energy allocated to gamete development under stress situations induced by environmental change may be redirected to other functions critical for the individual's survival (van der Meer, 2006). As such, reduced reproductive effort could lead to significant consequences for long-term population continuity as a result of environmental stress.

Functions immediately critical for maintenance and survival, such as oxygen consumption and delivery, feeding and food absorption efficiency, play an important role when coping with short-term stress or extreme climate events such as MHWs (Fitzgibbon et al. 2017; Pörtner et al. 2017). Failure of these functions relating to the acquisition and allocation of energy will define a long-term limit to survival where once these functions fail, an animal will not be able to sustain life (Peck et al. 2002). By assessing the effect of environmental change on biological functioning that is critical for individual survival, in addition to population health such as reproductive effort, we can better understand how animals respond to stress, allocate energy, and ultimately adapt or recover from stress.

1.1 Thesis aims and objectives

This thesis aims to inform our understanding of the effect of environmental change on energy demand and allocation in marine ectotherms, using functions including feeding and oxygen consumption as indicators of change in energetic demands, and variability in reproductive effort as an indicator for change in energy allocation. For this purpose, I focus on temperature as an environmental driver and explore the characteristics of warming that cause changes to species functioning. I use the Antarctic sea urchin, *S. neumayeri,* as a study species due to its inherent sensitivity as a polar organism to temperature. The key focus points of this thesis are as follows:

1) If we are to understand how the temperature interacts with fundamental biological functions such as reproduction, we first need to identify innate internal rhythms that may occur on multiyear to decadal scales, especially for slow-paced species such as Antarctic taxa. In Chapter 2 I aim to document the long-term reproductive ecology of *S. neumayeri*, characterising the seasonal and interannual variability observed and the key drivers that underpin energy allocation to reproduction.

2) Little is known about functional deterioration as a species approaches its thermal limit, and in the context of short-term warming like MHWs, animals are likely to experience temperatures that compromise functions critical for sustained survival of the individual, rather than immediate lethal effects. In Chapter 3 I aim to determine thermal limits to these critical functions and understand how these limits change under different onset rates of warming.

3) There is now strong evidence in climate models that predict summer ocean temperatures will increase by at least 2^{o}C by 2100, and with this shift there will be an associated increase in the intensity of MHW events. Experimental work detailed in Chapter 4 involves acclimation of *S. neumayeri* to predicted future climate conditions with subsequent exposure to short-term warming events such as those experienced previously during MHWs on the WAP. This chapter aims to understand the role of acclimation in the functional response of *S. neumayeri* to short-term warming and determine how energy demands change following long-term and short-term exposure.

Chapter 2 Multiyear trend in reproduction underpins interannual variation in gametogenic development of an Antarctic urchin

This chapter has been published as:

De Leij, R., Peck, L. S., & Grange, L. J. (2021). Multiyear trend in reproduction underpins interannual variation in gametogenic development of an Antarctic urchin. *Scientific Reports*, 11(1), 1–13. https://doi.org/10.1038/s41598-021-98444-4

Abstract

Ecosystems and their biota operate on cyclic rhythms, often entrained by predictable, small-scale changes in their natural environment. Recording and understanding these rhythms can detangle the effect of human induced shifts in the climate state from natural fluctuations. In this study, I assess long-term patterns of reproductive investment in the Antarctic sea urchin, *Sterechinus neumayeri*, in relation to changes in the environment to identify drivers of reproductive processes. Polar marine biota are sensitive to small changes in their environment and so serve as a barometer whose responses likely mirror effects that will be seen on a wider global scale in future climate change scenarios. My results indicate that seasonal reproductive periodicity in the urchin is underpinned by a multiyear trend in reproductive investment beyond and in addition to, the previously reported 18-24 month gametogenic cycle. The model provides evidence that annual reproductive investment could be regulated by an endogenous rhythm since environmental factors only accounted for a small proportion of the residual variation in gonad index. This research highlights a need for multiyear datasets and the combination of biological time series data with large-scale climate metrics that encapsulate multi-factorial climate state shifts, rather than using single explanatory variables to inform changes in biological processes.

2.1 Introduction

Reproduction is a fundamental process for all life. Reproductive periodicities are often intrinsic rhythms entrained by external cues that aid synchronicity in reproduction, as well as timing the arrival of vulnerable early life-stages with favourable conditions (Brockington & Clarke, 2001; Takemura et al. 2010). To understand environmental influences on

reproductive processes, innate reproductive periodicities must be detangled from environmental fluctuations, both for regular seasonal variation and isolated events.

Seasonal and annual reproductive periodicities have been well documented in marine invertebrates. Evidence suggests that local environmental cues including photoperiod (Kelly, 2001; Muthiga, 2006), water temperature (Emilio et al. 2018; St.Gelais et al. 2016), food availability (Grange et al. 2004; Zhadan et al. 2018), and lunar cycles (Balogh et al. 2019; St.Gelais et al. 2016; Zhadan et al. 2018), play roles in regulating gametogenesis. However, reproductive cycles and their drivers still remain challenging to interpret, since they are often regulated by the interplay of multiple climate variables (Stenseth et al. 2003).

Changes to the climate state can affect populations at local, regional and global scales (La et al. 2019; Turner, 2004; Wood et al. 2016). For example, the large-scale climate metric, Southern Oscillation Index (SOI), is most known for its regional impacts on the tropical Pacific (Wood et al. 2016; Xuebin & Mcphaden, 2008). However, strong links have been found between El Niño- Southern Oscillation (ENSO) and extreme events such a heat waves and storms, across the globe (Oliver et al. 2018). SOI and extreme events drive ecological processes (Conde & Prado, 2018; Ryan et al. 2017), and more specifically, reproductive processes (Santidrián Tomillo et al. 2020; Wilson et al. 2018), with some impacts reaching as far as Antarctica (Testa et al. 1991; Welhouse et al. 2016). Multi-factorial indices, rather than single variables, instead provide a context for large-scale oceanographic variation, and hence integrate both locally measured components of weather and rarer, infrequent, extreme events (Stenseth et al. 2003).

Although regulation of gametogenesis, reproductive cycles and synchronisation of spawning events are undoubtedly influenced by environmental factors, temporal patterns in some species are largely regulated by endogenous rhythms that govern not only reproduction, but other developmental and biological functions such as growth and seasonal activity (Brown et al. 2013; Román-González et al. 2017). These rhythms may be caused by an internal oscillator, allocating energy based on life history requirements on seasonal, annual or decadal cycles (Román-González et al. 2017).

To understand how climate interacts with fundamental biological processes such as reproduction, we first need to identify these innate internal rhythms (Ainley et al. 2013; Doney et al. 2012), especially for slow paced species, including many Antarctic taxa. Antarctic marine invertebrates have adapted *in situ* over millennia to unique conditions characterised by low and stable temperatures and extreme seasonality in light and food availability (Peck, 2018). Many species have adapted to control and minimise energy expenditure (Brockington & Clarke, 2001; Peck, 2016), and exhibit extended reproductive

cycles, where gametogenesis often takes 18-24 months to complete instead of the 6-12 months characteristic of their temperate counterparts (Brockington et al. 2007; Grange et al. 2007).

The Antarctic sea urchin, *Sterechinus neumayeri,* is one of the most functionally important Antarctic shallow marine species. It has a circumpolar distribution and is the most dominant echinoid in the near-shore benthic community, having recorded abundances up to 223 individuals m^{-2} (Brockington, 2001). *Sterechinus neumayeri* is an important predator and grazer. It is also a model research species due to its ease of husbandry, including laboratory spawning and larval culture (Bosch et al. 1987; Stanwell-Smith & Peck, 1998). The urchin also has an extended 18-24 month gametogenic cycle (Brockington et al. 2007).

This study aims to document the reproductive ecology of *S. neumayeri* across multiple years, characterising seasonal and interannual variability and the key factors underpinning reproductive allocation. To this purpose, I investigated the reproductive cycle of *S. neumayeri* over a seven-year period (2012-2018). Seasonal and interannual variations in reproductive condition were explored in relation to locally measured environmental variables (e.g., temperature, chlorophyll a, etc.) and the regional climate metrics SOI and SAM due to their influence in the Southern Ocean and connection with extreme events.

2.2 Methods

2.2.1 Study site and sampling

Sterechinus neumayeri were collected from Hangar Cove (67°33'54.2"S 68°07'13.1"W), located near the British Antarctic Survey's Rothera Research Station on the Western Antarctic Peninsula (Figure 2.1). Adult urchins (19-51 mm diameter; n=16) were collected monthly (weather permitting) from 2012 to 2018 by SCUBA divers (13-21 m depth), with the exception of a 6-month gap from August 2015 to January 2016, when thin ice prohibited access to the collection site. Specimens were preserved in 10% buffered formalin solution until analysis.

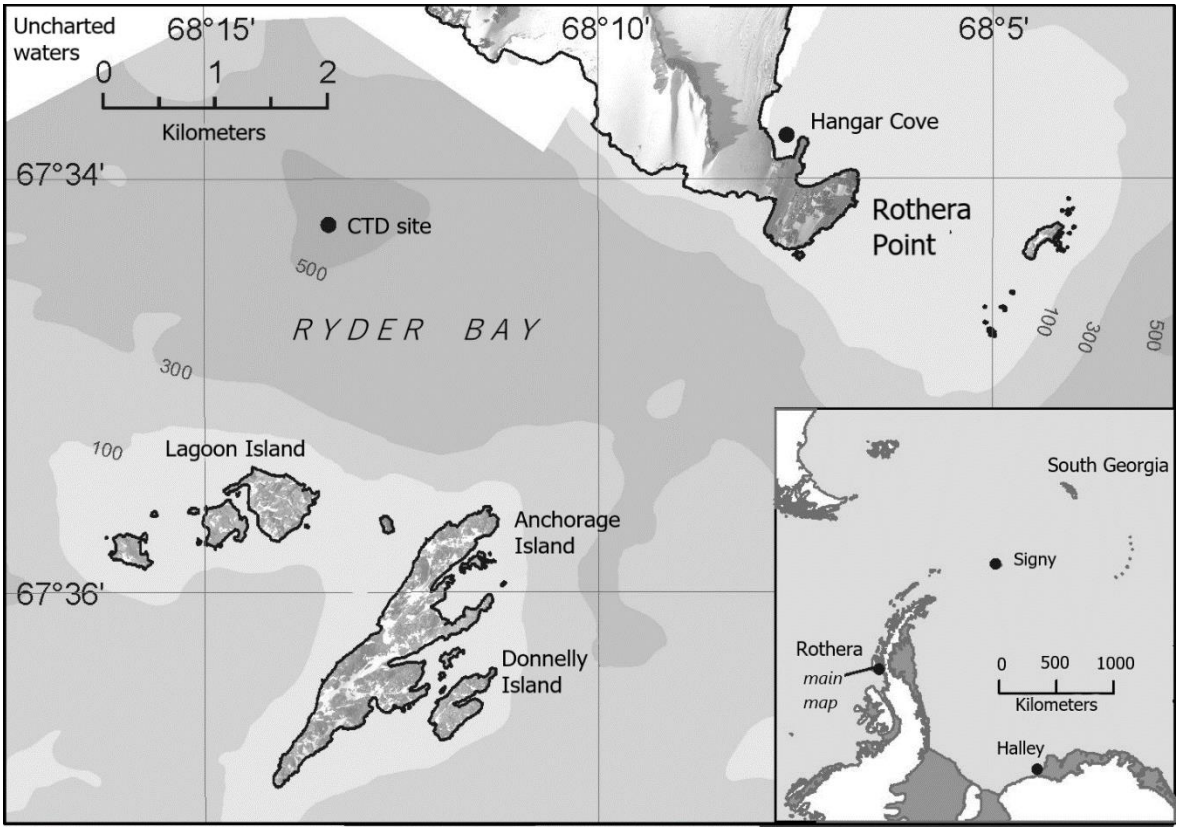

Figure 2.1: Location of Hangar Cove study site at Rothera Point, Adelaide Island, Antarctica (67°33'54.2"S 68°07'13.1"W) and insert map showing Rothera Point on Western Antarctic Peninsula. Marine environmental data are collected at the site south west of Rothera Point as part of the British Antarctic Survey Rothera Time Series monitoring programme (RaTS). Large-scale map indicates the position of Rothera Research Station on Adelaide Island, on the Western Antarctic Peninsula. Figure modified from Grange et al. (2011).

2.2.2 Measuring reproductive condition

Gonad Index (GI), oocyte size and tissue composition in females and maturity stage in males were used to describe urchin reproductive condition. Total gonad wet mass was measured, and water content and dry gonad mass obtained from subsamples of gonad tissue. GI was used instead of direct gonad mass to allow for differences in animal size, and was derived by calculating the gonad mass as a proportion of total body size according to equation (3), following Bronstein et al. (2016):

$$GI = \frac{\text{Total gonad dry mass (mg)}}{\text{Test diameter (mm)}} \quad (3)$$

A subsample of wet gonad tissue was examined for oocyte size and tissue composition for females, or maturity stage for males following standard wax histology procedures (Alturkistani et al. 2015). In brief, tissue was dehydrated in a graded isopropanol series,

cleared in XTF clearing agent, embedded in paraffin wax, sectioned at 7 µm and stained with haematoxylin and eosin.

Individuals were sexed and female tissue sections viewed under a light microscope (Olympus BHS (BH-2)) at x10 magnification and photographed using a Nikon D5000 camera (Appendix A, Figure A6). To obtain oocyte size data, outlines were drawn around representative oocytes in images using imaging software, Fiji (image-J v2) (Rueden et al. 2017; Schindelin et al. 2012). Only oocytes with a visible nucleus or nucleolus were measured to ensure oocytes were centrally sectioned and maximum circumferences measured. Where possible, at least 5 females were analysed each month and 100 oocytes measured at random per female. Subsamples of 100 oocytes were used to calculate an average oocyte size distribution (Brockington et al. 2007). Oocyte area (A) was used to calculate the Equivalent Circular Diameter (ECD) according to equation (4), used in previous studies (Lau et al. 2018; Reed et al. 2014) to determine the size of a spherical oocyte with an equivalent area.

$$ECD=\sqrt{\frac{4A}{\pi}} \quad (4)$$

Male tissue sections observed under light microscope at x10 magnification were staged for maturity based on the development of the testes. Testis maturity level (Appendix A, Figure A7) was categorised from representative images following Brockington et al. (2007):

Stage 1: Spent/Recovering: Lumen empty. Nutritive phagocyte (NP) tissue lining is of variable thickness and possibly a thin layer of spermatogonia on the germinal epithelium.

Stage 2: Growing: Spermatogonia visible on germinal epithelium; spermatozoa present at moderate density in lumen.

Stage 3: Mature: Lumen densely packed with mature spermatozoa in swirls. Lumen stains intense blue. Spermatid production may still be evident. Nutritive tissue generally highly reduced.

To visualise changes in male maturity as a continuous variable, both seasonally and across years, the occurrence of each stage was converted to a percentage frequency for each month ((number of individuals at given stage / number males sampled in month) x100). Percentage frequency of maturity stage was then modelled as a smoothed function for month, using the local regression smoother (LOESS) method (Cleveland, 1979).

2.2.3 Nutritive phagocytes (NPs)

Sea urchin gonad tissue serves two functions. Tissues contain both the developing gametes and NPs, a storage tissue. Variation in GI is thus a product of variation in both tissue types and not limited to maturing gametes. Understanding how the proportions of these tissues change seasonally is important to understanding gonad function and interpreting seasonal GI variation. Images taken for oocyte size were, therefore, used to quantify proportions of NPs to oocytes in female gonads. For this purpose, three females from each month were selected at random, where for each, three images of histological sections from different areas in the gonad were used to provide a representative assessment. The relative areas occupied by germ cells and NPs were calculated using Fiji (image-J v2) 'Area' tool. This process involved first selecting only NPs as defined by specific colour thresholds and converting these areas to a mask. The mask % area relative to the image was then calculated. This process was also applied to oocytes. Gonad tissue was almost exclusively formed from oocytes and NPs, hence % area of NPs and oocytes was calculated relative to the total gonad tissue area in each image.

To relate NP and oocyte % areas to gonad size and inform how these proportions contribute to seasonal GI variation, NP and oocyte proportions in the gonad were averaged across individuals for each month using images that were of highest quality from across the time-series. Following this, NP and oocyte percentages were scaled to represent relative proportions of the corresponding GI (averaged for all females for each month). Gonad oocyte and NP proportions were calculated based on % area tissue coverage estimates from image analysis according to equation (5).

$$\left(\frac{Ao}{Ao+Anp}\right)=AAo;\ \left(\frac{Anp}{Ao+Anp}\right)=AAnp \qquad (5)$$

$$\overline{AAo} \times \overline{GI}=\text{Oocyte proportion of the gonad}$$

$$\overline{AAnp} \times \overline{GI}=\text{Nutritive phagocyte proportion of the gonad}$$

Where Ao = Percentage area of oocytes; Anp = Percentage area of nutritive phagocytes; AAo = adjusted area of oocytes relative to gonad tissue total area; AAnp = adjusted area of nutritive phagocytes relative to gonad tissue total area; $\overline{AAo}$ = monthly mean of AAo; $\overline{AAnp}$ = monthly mean of AAnp; $\overline{GI}$= monthly mean of female GI.

2.2.4 Environmental covariates

Environmental data were collected weekly from Ryder Bay (67°34'12.0"S 68°13'30.0"W), ~ 4km west of Hangar Cove. This oceanographic sampling regime is an on-going part of the Rothera Oceanographic and Biological Time Series (RaTS) that has run continuously

since 1997 (Clarke et al. 2008; Venables et al. 2013). Data from March 2012 to March 2018 were obtained for physiological drivers including temperature and salinity (at 15m depth), as well as sea-ice extent and chlorophyll-a (Chl-a) concentration (a proxy for food availability). The regional climate metrics, Southern Oscillation Index (SOI) and Southern Annular Mode (SAM), were also considered as a covariate measure. SOI was represented as the standardised anomaly of the mean atmospheric sea level pressure (MSLP) difference between Tahiti and Darwin (Australian Bureau of Meteorology), calculated according to equation (6).

$$SOI = 10 \frac{Pdiff - Pdiffav}{SD(Pdiff)} \quad (6)$$

Where *Pdiff* = (average Tahiti MSLP for the month) - (average Darwin MSLP for the month); *Pdiffav* = long-term average of *Pdiff* for each month, *SD (Pdiff)* = long-term standard deviation of *Pdiff* for the month in question.

SAM was represented as the standardized 3-month running mean value of the Antarctic Oscillation index, reported by NOAA National Weather Service Climate Prediction Centre.

2.2.5 Data analysis

Data were initially tested for normality and homogeneity of variance, and identification of outliers and between-variable relationships, as per Zuur et al. (2007). A chi-squared test was used to assess whether sex ratios deviated from 1:1. A t-test was used to determine differences in size (i.e. test diameter and whole animal mass) and GI between males and females. An analysis of variance (ANOVA) was also used to determine differences in oocyte size between months of comparable gametogenic maturation/ stage across the time series (i.e., between years). Where significant difference were found ($p < 0.05$), the ANOVA was followed by a post-hoc Tukey pair-wise test.

An initial linear regression model of GI with time revealed patterns in the residuals, indicating an underlying non-linear relationship. Following this, a generalised additive model (GAM) was used to examine factors influencing reproductive state (Zuur et al. 2007). The response variable, GI, was used as a measure of reproductive state and modelled against smoothed ecological and environmental variables. Time, Chl-a, temperature, fast ice concentration, salinity, SAM and SOI were considered in the model as continuous predictors. Month and season were considered as factors accounting for seasonal periodicities and modelled as main effect predictors using cyclic cubic regression splines, and finally sex was considered both as an interactive and main effect predictor. To meet the assumptions of normality, GI was square root transformed.

An initial pair's plot was constructed to determine co-linearity between predictor variables before adding them to the model. Of the explanatory variables that correlated (threshold correlation for inclusion = 0.50), the most ecologically relevant variable was included in the initial model. If both variables were ecologically relevant, then the weakest predictor was removed. Penalised cubic regression splines were used to estimate the smooth function for each non-cyclic predictor variable and with knots limited to 5 which was deemed adequate to explain the data, without over-fitting (Burnham & Anderson, 2002). Using the "FSSgam" package in R (Fisher et al. 2018) a full-subsets information theoretical approach was used to compare a complete model set of all predictor variables from the environmental and ecological data available. Other relevant R packages for the model included the "MuMin" and "mgcv" packages (Wood, 2011) .

All candidate predictors were considered during the initial model exploration and ranked in order of conditional probability, calculated by the 'Akaike Information Criterion' (AIC). Variable weights were ranked by importance and predictors ranking low were excluded. Residuals from the 'best' model were checked for normality and homogeneity of variance using the "gam.check" function in the "mgcv" package.

Decomposition analysis was carried out on the gonad index time series data as an alternative method, to identify any overall trends and seasonal components. This analysis produced results very similar to the GAM model and did not provide any additional information. However, this additional analysis did substantiate the GAM model results (Appendix A, Figure A8). Decomposition of the environmental variables was also explored and trends, seasonal cycles and residual variations were observed in relation to the GI trend. Decomposition of the environmental variables allowed the trends observed for each factor to be regressed against SOI to determine how this large-scale climate metric might relate to single variables measured in the time series. Lag effects were also considered and incorporated where visualisation of the trends alluded to a delay in biological response. The R code for this analysis is given in the Supplementary information (Appendix A, Text A1).

2.3 Results

The total number of female urchins collected each year exceeded the number of males. Overall, the sex ratio was significantly skewed towards females at 1.32:1 (chi-squared = 13.38, $p < .001$, n = 718) (Appendix A, Table A1). The gonad index was significantly higher in females ($t_{(661)} = 2.26$, $p = 0.024$) however there was no significant difference in animal size between the sexes (Appendix A, Table A2).

2.3.1 Seasonal cycles

Males and females exhibited seasonal cycles in GI, oocyte size, nutritive phagocyte proportions and male maturity (Figure 2.2), where both males and females presented synchronous cycles, although there was considerable individual variability. GI peaked in June and September for both males (12.8 ± 1.97 SE and 9.54 ± 1.48 SE, respectively) and females (11.1 ± 1.05 SE and 12.6 ± 1.24 SE, respectively). In both cases, GI then decreased to a minimum in January (5.74 ± 0.59 SE for males, and 5.67 ± 0.40 SE for females, Figure 2.2A). For females, mean oocyte size, measured as ECD; µm, increased from January to peak in July (74.4 µm ± 0.57 µm SE), followed by a decline and a subsequent increase again in September (71.8 µm ± 0.68 µm SE). Mean ECD then decreased from September to a minimum in January (46.3 µm ± 0.31 µm SE, Figure 2.2B). The proportion of gonad area dedicated to NPs was inversely related to ECD (r^2 = 0.45, $p < .001$), where, as oocytes matured, relative proportions of NPs decreased (Figure 2.2C). However, as a proportion of GI, NPs increased in April to 60.8% ± 2.1% SE of GI, and then again in December to 79.6% ± 2.0% SE of GI. At its lowest, the proportion of GI accounted for by NPs declined to 49.5% ± 2.8% SE of GI in August (Figure 2.3). The overall GI pattern with 2 peaks resulted from the combined variation in oocyte and NPs.

The proportion of males in spent and recovering maturity stages peaked in January (52.0% ± 13.2% SE), followed by increasing proportions of individuals transitioning to growing stages of maturity, peaking in May (75.7% ± 7.0% SE, Figure 2.2D). Following this peak, proportions of mature males increased from May to October/November (peaking at 87.7% ± 10.3% SE of individuals), from which point the proportion of spent and recovering individuals increased again until January (Figure 2.2D).

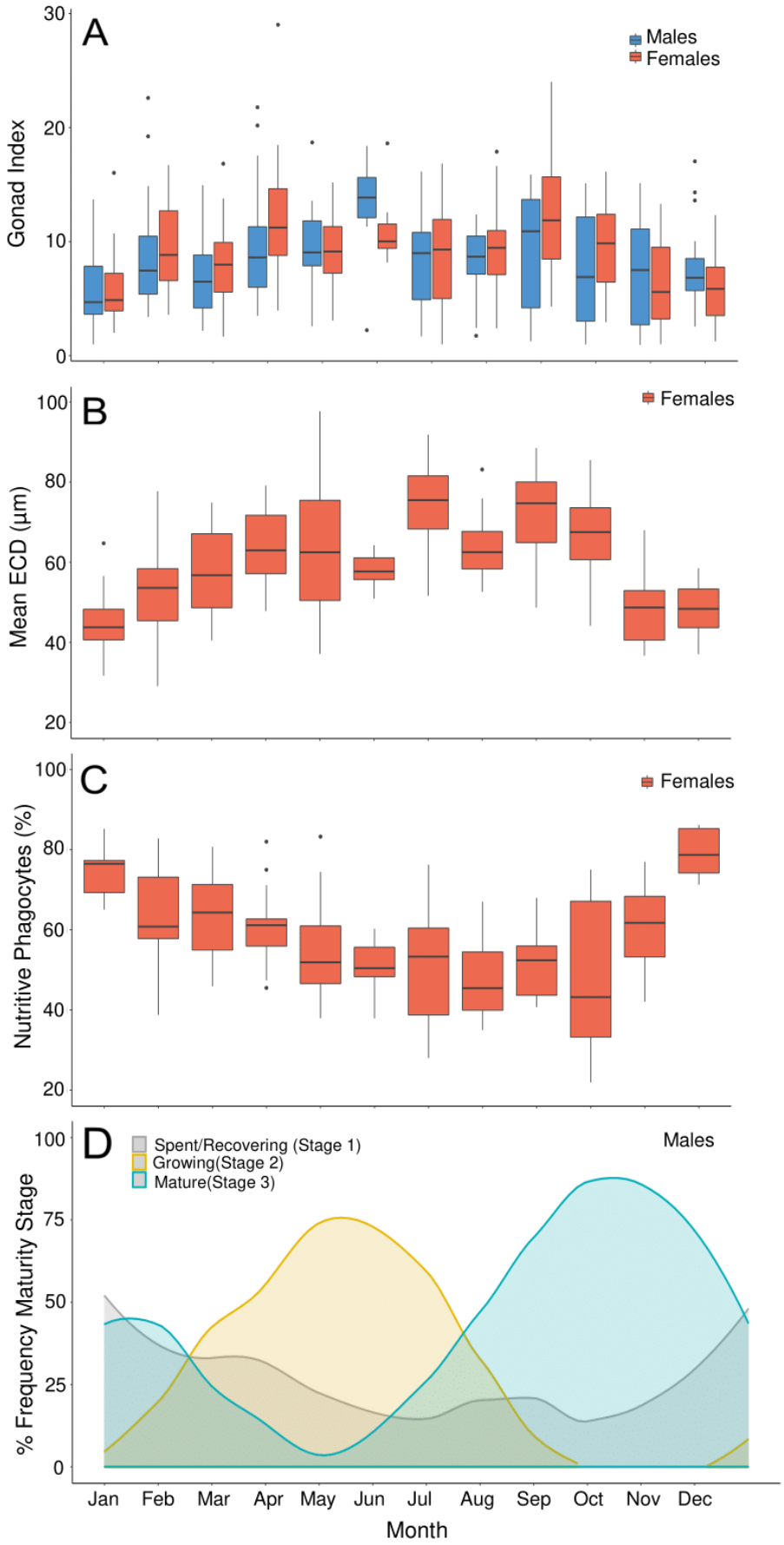

Figure 2.2 Monthly changes for *Sterechinus neumayeri* in a) gonad index for males (blue) and females (red); b) mean equivalent circular diameter (ECD) of oocytes present in female gonads; c) percentage (%) of gonad tissue in females composed of nutritive

phagocytes; d) percentage frequency (%) of male gonad maturity stages where frequencies are smoothed by the function y~x using the local regression smoother (LOESS) method. The smoothing span was chosen to reflect seasonal changes. Data as box plots are displayed with the central line in the boxes representing the median value, the upper and lower hinges representing the 25th and 75th percentiles, and the upper/lower whiskers representing the largest/smallest value, no further than 1.5 times the interquartile range from the hinge. All data outside these ranges are plotted as points.

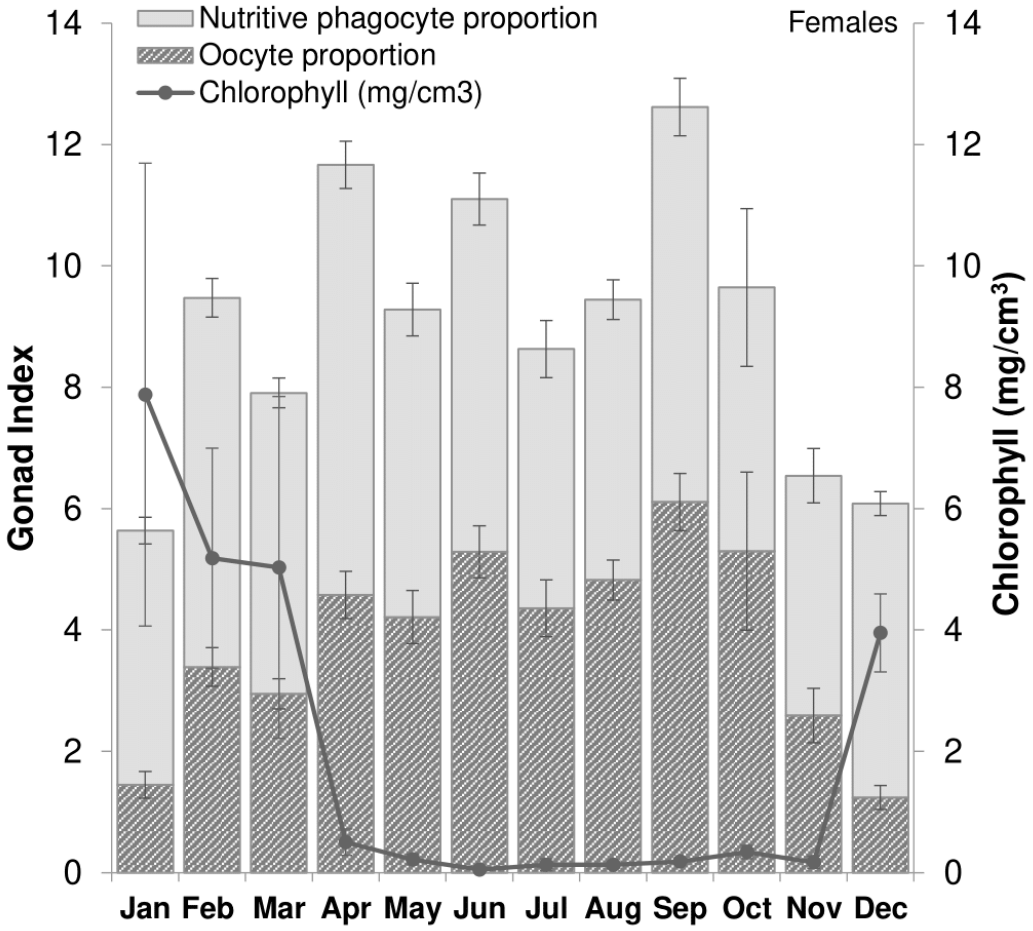

Figure 2.3: Monthly female gonad index as proportional area of nutritive phagocytes (NP) and oocytes. Monthly data for proportions are ± the standard error of the NP or oocyte equivalent GI based on replicate months. Chlorophyll data are represented on the secondary y-axis and have been averaged from the time series (2012 – 2018), ± standard error.

2.3.2 Changes in Gonad Index

The partials plot analysis revealed co-linearity between temperature and Chl-a (Pearson's r = 0.73) and between salinity and temperature (Pearson's r =0.54). Therefore, based on a weighted importance analysis, only Chl-a was included in the model. The starting model fit (null model) was as per equation (1).

$$\text{Gonad Index} = f(\text{Time}) + \varepsilon \quad (1)$$

Where f is the smoothing function. This model had an AIC of 1368. Initially, single environmental variables considered as potentially ecologically influential, were added to the model. Following automated comparisons of all possible model variations, Chl-a was identified as the main environmental predictor of GI variation, with sex as a factor and as an interaction with the smoothed functions of time and Chl-a. Since other single environmental variables were not considered significant, the large-scale climate metrics, SOI and SAM, were included as additional factors to Chl-a and sex. There is some evidence that SOI and the SAM can influence each other (Fogt et al. 2011). However, the partials plot in the time-series did not reveal co-linearity between SAM and SOI. Other studies have also reported weak relationships between these metrics (Kwok & Comiso, 2002; Santamaría-del-Ángel et al. 2021). As such, I included both metrics in the model since both were significant factors in explaining some of the remaining variance in GI and together, improved the model AIC. It should however be noted that the SAM had the lowest relative importance comparative to other variables in the model (Appendix A, Figure A1). The final model resulted as per equation (2).

$$\text{Gonad Index} = f(\text{Time, by} = \text{Sex}) + f(\text{Chlorophyll, by Sex}) + f(\text{SOI, by Sex}) + f(\text{SAM}) + \text{Sex} + \varepsilon \quad (2)$$

This model had an AIC of 1259, compared to the null model. This model was ranked highest with regards to AIC, and explained 41.4% of the variance in GI. Model predictions fitted well with the raw data and aside from the functions of time and sex, environmental covariates, Chl-a, SOI and SAM, were considered the best predictors of variance in GI, explaining 12.4% of the variance. The model met the assumptions of homogeneity of variance and model residuals were normally distributed. All Cooks distance values were < 0.034 and were not considered influential (Montgomery & Peck, 1992).

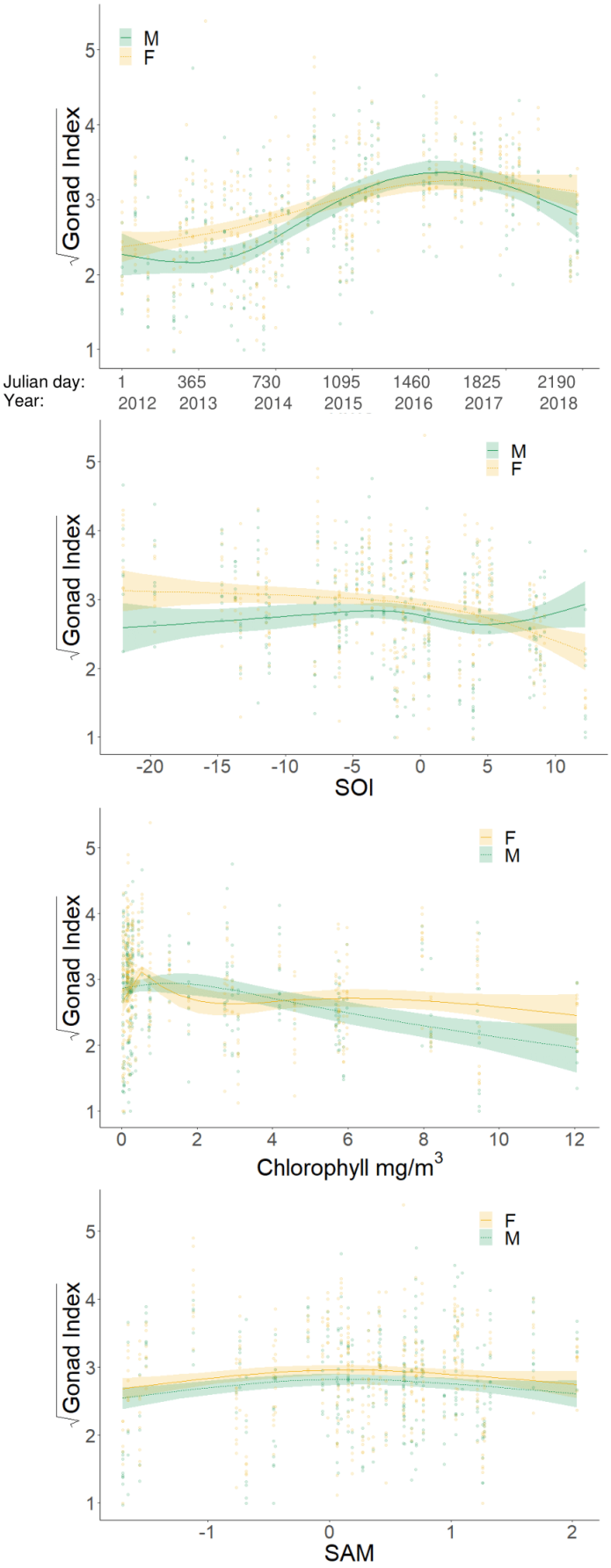

Figure 2.4: Smoothers of the effect of the four non-parametric terms: time, Southern Oscillation Index (SOI), chlorophyll and Southern Annular Mode (SAM), on the gonad index of *Sterechinus neumayeri,* from the optimal GAM model. Shaded area represents a

95% confidence interval and data points represent raw gonad index data. The magnitude of change in gonad index as a response to the change in the x-variable is represented on the y-axis as the square-root transformed gonad index. For the axis ‘time’, year intervals are plotted on every 1st January. Green represents males and yellow represents females.

The estimated covariate smoothers (Figure 2.4) show there was a positive relationship for the smooth function of time, where both male and female GI increased from mid-2013 to mid-2016. Male GI then declined until the end of the time series suggesting a multiyear trend. The variation in GI explained by the model was limited by the individual GI variability within each month sampled. However, the model captures the overall increasing and decreasing trend observed over time.

For the covariate SOI, there were limited data for extreme negative SOI values of < -15, and so over-interpretation of the model predictions at this tail end was avoided. In comparison, data collected for SOI values > -5 were comprehensive and showed a negative association between GI and SOI for females when SOI was positive. This was not the case for males, where the relationship was not significant. For the covariate SAM, there was evidence of a bell-shaped curve in the relationship, with GI values peaking at SAM values of 0. Negative and positive SAM values resulted in lower GI. There was less certainty in the negative association between GI and positive SAM values due to the increase in the 95% confidence interval (CI) and the poor fit between the data points and the model prediction. As such, over-interpretation of this association was avoided.

There was good data coverage at low Chl-a concentration because of the highly seasonal productivity. However, the association of GI with Chl-a concentration was negative for males from concentrations exceeding 1.5 mg m^{-3}. This downward trend followed an initial increase in GI for both males and females at low Chl-a concentrations. This inverse relationship was also evident from the decomposition analysis, where seasonal cycles were extracted from both GI and Chl-a (Figure 2.5).

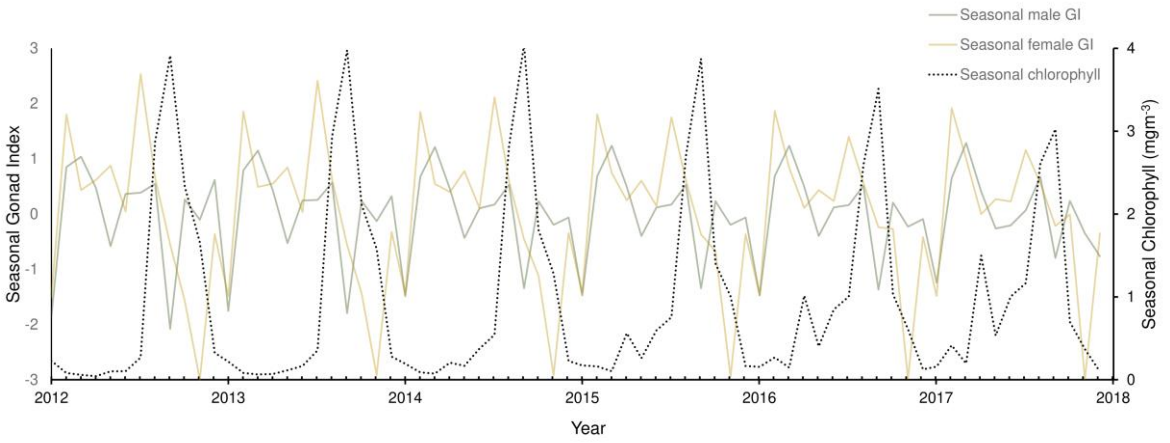

Figure 2.5: Seasonal cycle of gonad index for males (solid green line) and females (solid yellow line), extracted from decomposition analysis, overlaid on seasonal cycle of chlorophyll (dotted black line) extracted from decomposition analysis.

Chlorophyll and temperature trends, extracted by decomposition analysis, showed positive linear relationships with SOI, where positive values of SOI (La Niña) correlated with high temperature ($R^2 = 0.207$, $p < .001$) and Chl-a concentrations ($R^2 = 0.226$, $p < .001$) (Appendix A, Figure A2 and A3). Other variables lacked significant linear relationships, lagged or unlagged, with the SOI trend.

2.3.3 Oocyte growth and maturation

Oocyte mean diameters varied significantly between years for the months March-August and also for November and December, with March having the most interannual variability. For all other months, the mean ECD was not significantly different between years (Appendix A, Table A3).

Size distributions of developing oocytes within individual females were bimodal for most months of the year (i.e., from February/March, through to October). In December oocyte sizes were mostly 6–80 µm. The oocyte distribution then broadened, with bimodal peaks appearing from January to February/March, and oocyte sizes ranging from 12-122 µm. In July, the frequency of large oocytes (80-135 µm), peaked at 51.1 % ± 4.9 % SE, and steadily decreased until November, when they almost disappeared from the distribution accounting for 9.6 % ± 2.5 % SE of the distribution. Over this period, a cohort of small oocytes (12-80 µm) increased in frequency from 49.0 % ± 4.9 % SE in July, through to 90.4 % ± 2.5 % SE in December (Appendix A, Figure A4).

2.3.4 Male maturity

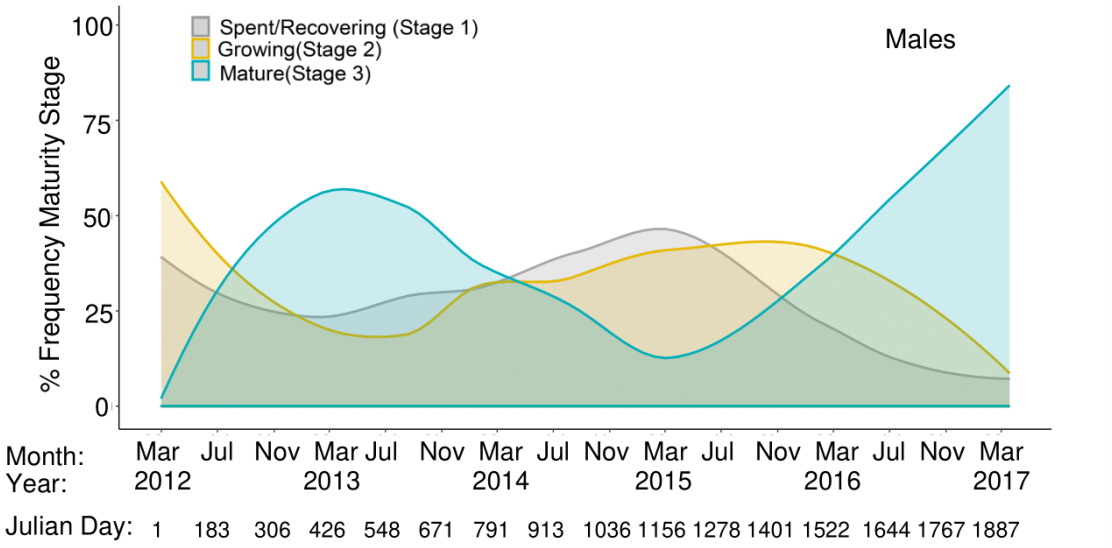

Figure 2.6: Long-term changes in the percentage frequency (%), represented as a density plot, of maturity stages in the male sample population from March 2012 - March 2017. Frequency densities derived from (LOESS) method. The smoothing span was chosen to reflect long-term changes rather than seasonal variability.

Males varied in reproductive maturity on both seasonal and interannual scales. Substantial individual variation was evident since the maturity categorisation was broad, with 105 ± 20 S.D. individuals in each category emphasising the large variation. Across the time-series, from March 2012-2017, there were periodicities in the proportion of maturity stages present (Figure 2.6). A distinct bell curve in the proportion of mature males occurred from March 2012-2015, peaking in March 2013. This distribution overlapped almost simultaneous bell curves in spent/recovering and growing stages, which peaked in March 2015 and November 2015, respectively.

2.4 Discussion

Data presented here comprise the longest reproductive time series of an Antarctic benthic marine invertebrate to date and are the first to provide evidence that reproductive allocation may be accumulated across a multiyear scale with no evidence for an environmental link. Where multiyear studies have been conducted, evidence is building that some marine invertebrates have endogenously driven growth and reproductive cycles, in which environmental variation is independent, or interacts with this internal rhythm to regulate reproductive investment and growth over time (Román-González et al. 2017; Takemura et al. 2010). The model outcomes suggest a multiyear trend in reproductive investment which could suggest an innate endogenous rhythm. Owed to the

number of years comprising the time series, repetition of this trend has not been captured in my dataset and therefore it is necessary to interpret these results with caution. However, several studies have recorded multiyear cycles of similar periodicities in a range of Antarctic species. For the crab-eater seal around the Antarctic Peninsula, the juvenile leopard seal at Macquarie Island, and the Weddell seal in McMurdo Sound, 4-5 year intervals for both reproduction and population peaks have been identified (Testa et al. 1991). Other Antarctic research has shown that some bivalves exhibit endogenous growth cycles, with a 9.06 year cycle present for *Aequiyoldia eightsi*, and two endogenous cycles of 5 and 6.6-years reported for *Laternula elliptica* (Román-González et al. 2017). There is therefore evidence for a temporal mediator of growth and reproductive investment in Antarctica, possibly because of low temperature effects on biological rates and extreme seasonality, where it may take multiple years to build reserves, with seasonal spawning and growth taking place against a backdrop of long-term investment over several years.

The very small number of multiyear investigations suggests endogenous cycles in growth and reproduction may be more common than previously identified. A similar trend to that identified in GI was also evident in the male maturity data, where I observed a single peak in each maturity stage across a 5 year period, with the 'growing' phase of maturity, matching the shape of the curve for variation in male GI. Extreme interannual variation in reproductive condition and a circaseptennial rhythm (7-year cycle) has been previously proposed for *S. neumayeri* (Brockington et al. 2007) based on studies of the Pacific purple sea urchin, *Strongylocentrotus purpuratus* (Halberg et al. 1987).

Alongside the temporal signal in GI, my data also indicate that there is environmental entrainment of this periodicity as the whole population builds gonad and spawns synchronously across the cycle. This entrainment likely arises from a combination of factors. However, my analysis identified a negative relationship in female GI when the SOI signal is positive (La Niña) and negative relationship in both male and female GI when the SAM signal is negative. Climate coupled atmospheric-oceanic-sea-ice processes, like SOI and SAM, are known to impact ecosystem variability in Antarctica, especially for the Antarctic Peninsula (Loeb et al. 2009; Saba et al. 2014; White et al. 2002). These effects could result from direct links caused by changes in physical factors including ocean temperature, or else indirect links resulting from altered primary productivity and food web dynamics (Cavanagh et al. 2017; Santamaría-del-Ángel et al. 2021; Vergani et al. 2008). Effects could also result from a combination of, or synergistic interactions between, factors. Isolating a single cause and effect of these large-scale climate indices is challenging, when many environmental factors are closely linked and the consequences of change in one variable cascades through multiple physical and biological pathways (Clark et al. 2013).

Relationships between SOI and climate parameters in Antarctica are non-linear, but there is strong evidence that El Niño and La Niña signals are translated widely across the southern hemisphere (Schneider et al. 2012; Turner, 2004). Here La Niña episodes have been correlated with warm SST anomalies and decreased sea-ice extent, while El Niño episodes produce opposite effects (Welhouse et al. 2016; Yuan, 2004). The time series encapsulates El Niño years up to values of -20, and La Niña values of +10. The model predictions indicate a negative association with reproductive investment for females when SOI is positive (La Niña), and a positive association when SOI is negative (El Niño). Reasons for this are unclear, however the regression analysis of Chl-a and temperature against SOI, suggest that positive SOI correlated with higher temperatures and higher chlorophyll concentrations, outside the usual seasonal variation. These relationships would likely have implications for sea-ice cover and water column stratification (Conde & Prado, 2018; Loeb & Santora, 2012). Because of this interaction of factors, the SOI can be used to highlight extremes in the environment and multifactorial shifts, rather than that of a single mechanism driving an ecological response.

The drop in GI at positive SOI (La Niña) is only present in females. Reasons for this could be owed to a higher energy requirement for oocyte development (Gómez-Robles & Saucedo, 2009; Moran et al. 2013). Therefore, reproductive costs for females may be higher and trade-offs in energy allocation to reproduction may be necessary during periods of environmental change (Gómez-Valdez et al. 2021). Possible changes in environmental variables as a result of La Niña events may then result in a reduction of GI indices for females only.

Impacts of large-scale climate metrics on Antarctic biodiversity have been identified across a range of taxa. Mammals including Weddell seals and Elephant seals have reproductive rates in phase with the SOI (Testa et al. 1991; Vergani et al. 2008). Other studies have shown strong links with plankton population abundance and krill reproductive recruitment success (Loeb et al. 2009), and seasonal vertical migration behaviour (La et al. 2019). Abundance of the planktonic tunicate, *Salpa thompsoni* has also been correlated with SOI (Loeb & Santora, 2012), as well as 5-year cycles in abundance peaks for krill, *Euphausia superba,* where high abundance was associated with greater sea-ice extent (Steinberg et al. 2015). The authors are unaware of any studies that demonstrate such correlations for Antarctic benthic species or SOI effects on species or ecosystems this far south.

Interestingly, studies have shown that the SAM is more closely linked to interannual sea surface temperature variability around the WAP, compared to SOI (Santamaría-del-Ángel et al. 2021). The model exploration shows that the SOI accounts for more of the variability in the GI of *S. neumayeri* than the SAM, and both temperature and SAM had low relative

importance in predicting GI. These results further suggest that temperature is likely not the most important or only driver of reproductive processes in these thermally sensitive species, and instead there is more complexity underlying the interaction between large-scale climate metrics, local environmental drivers, and biological functioning.

Temperature and Chl-a variation can be seasonal drivers of reproductive cycles (Grange et al. 2004; Zhadan et al. 2018). My results show that Chl-a concentration co-varies with reproductive condition in *S.neumayeri*, where the negative relationship between GI and Chl-a alludes to spawning being correlated with Southern Ocean summer phytoplankton characteristics (Rozema et al. 2017; Starr et al. 1990). Model predictions show that when Chl-a concentrations increase, GI declined, which is indicative of spawning. The relationship between GI and Chl-a may be indirect, whereby spawning is initiated prior to the bloom either by a trigger associated with early phytoplankton increase to facilitate feeding of planktonic larval stages (Bosch et al. 1987) or another environmental factor co-varying with Chl-a. This hypothesis would also result in a negative association between trends in GI and Chl-a. Again, we see different responses for males and females to high Chl-a concentrations. Since the GI relationship with Chl-a is likely a result of spawning, it may be that we observe a smaller reduction in GI in females following spawning due to the presence of nutritive phagocytes (NPs). I provide evidence that NPs are still present in the gonad following spawning, and hence will contribute to the higher post-spawning GI. Although I do not have NP data for males in this study, for the temperate sea urchin, *Strongylocentrotus droebachiensis*, the volume of NP in males was lower than in females throughout the gametogenic cycle (Harrington et al. 2007). If NPs contribute less to the GI in males, it is reasonable that we would see a larger decline in GI following spawning.

Seasonal patterns in *S. neumayeri* reproduction were evident in GI, male maturity and oocyte size distributions, all of which exhibited periods of maturation and growth, followed by phases that implied spawning across several months (e.g., decreasing GI, decreasing mean oocyte size for females, or increasing spent/recovering stages for males). Monthly changes in GI during the year highlight this reproductive seasonality. However, for urchins, gonad tissue comprises both germ cells (gametes) and NPs (Magniez, 1983; Pérez et al. 2008). My data demonstrate that fluctuations in female GI are caused by both the maturation of gametes and changes in gonad proportions dedicated to NPs. These changes are clearest in April, where GI increases significantly from March. However, this GI increase is due primarily to larger NP increases, rather than oocytes. The April GI peak for females follows the end of the summer phytoplankton bloom and suggests the resultant phytodetrital pulse to the seafloor is the primary nutritional source for this species. This explanation is further supported by fluctuations in *S. neumayeri* gut mass during the season. Gut mass decreases during the first half of the austral winter, when feeding activity ceases, followed by stabilisation until the onset of feeding in November

(Brockington, 2001). Gut index data for *S. neumayeri* in 2017/18 also supports this finding (Appendix A, Figure A5). NPs accumulate in late summer and early winter. During the period of cessation of feeding in winter NPs transfer nutrients to developing gametes. NP stores are also used to meet the urchin's energy requirements for metabolic maintenance during this time (Hernandez et al. 2020). My results suggest these nutrient stores are important reproductive reserves in *S. neumayeri* as proportions vary inversely with mean oocyte size and NPs are depleted as reserves are mobilised to maturing gametes.

This research demonstrates the need for long-term multiyear studies that encapsulate endogenous and environmentally driven reproductive investment against a backdrop of seasonal change. Relationships between reproductive cycles and single environmental variables are well reported, where spawning often coincides with seasonal changes (e.g., in temperature and chlorophyll). However, gradual environmental shifts over several years are rarely encompassed by single variable studies. Furthermore, it is more likely that such change occurs from alterations in multiple interacting variables. Large-scale climate metrics (e.g., SOI and SAM), can capture shifts in multifactorial environmental states and highlight how environmental alterations translate into ecological processes.

Identifying endogenous rhythms for growth and reproduction enables the partitioning of these processes from the effects of small-scale environmental change and large-scale environmental cycles on marine biodiversity. I have identified a potential multiyear trend in reproduction in a polar sea-urchin, *Sterechinus neumayeri,* from a seven-year dataset. There may be even longer cycles, and cycles like these may be cumulative across decades or multi-decadal timescales. To identify such long-term trends requires very long sampling and monitoring programmes, but these would be invaluable when assessing the impacts of the current environmental change that is occurring over decadal to centennial scales

Chapter 3 Functional thermal limits are determined by rate of warming during simulated marine heatwaves

This chapter has been published as:

De Leij, R., Grange, L. J., & Peck, L. S. (2022). Functional thermal limits are determined by rate of warming during simulated marine heatwaves. *Marine Ecology Progress Series,* 685, 183-196. https://doi.org/https://doi.org/10.3354/meps13980

Abstract

Marine heatwaves (MHWs) are increasing in both intensity and frequency against a backdrop of gradual warming associated with climate change. In the context of MHWs, animals are likely to experience sub-lethal rather than lethal effects, defining long-term limits to survival and/or impacting individual and population fitness. We investigated how functional sub-lethal limits track critical thresholds and how this relationship changes with warming rate. To this end, we monitored basic functioning, specifically the ability to right, feed and assimilate energy, as well as oxygen consumption rate in the common Antarctic sea urchin *Sterechinus neumayeri*. Water temperature in experimental systems was increased at rates of 1, 0.5 and 0.3°C d^{-1}, in line with the characteristics of MHW events previously experienced at the site where the study urchins were collected on the Antarctica Peninsula. Functioning was assessed during the simulation of MHWs, and sub-lethal limits were determined when the rate of functional degradation changed as temperature increased. Results suggest that thermal sensitivity varies between the key bio - logical functions measured, with the ability to right having the highest thermal threshold. Functions deteriorated at lower temperatures when warming was more rapid (1°C d^{-1}), contrary to lethal critical thresholds, which were reached at lower temperatures when warming was slower (0.3°C d^{-1}). MHWs and their impacts extend far beyond Antarctica, and in this context, my analyses indicate that the onset rate of MHWs is critical in determining the ability of an organism to tolerate short-term elevated temperatures.

3.1 Introduction

Historical temperature records have revealed positive temperature trends for the majority of the Earth's surface (Myrvoll-Nilsen et al. 2019), with the oceans being key to the regulation and capture of much of the excess heat present in the atmosphere (Marshall et al. 2015). As a result, marine environments are changing both physically and biochemically (Bopp et al. 2013). Included in these changes is the occurrence of marine heat waves

(MHWs), which are increasing in duration, magnitude and frequency, with alarming ecological consequences (Garrabou et al. 2009, Rubio-Portillo et al. 2016, Oliver et al. 2018). Physiological flexibility of species is crucial to survival during MHW events (Peck 2011), and species at low latitudes may be able to acclimate and adapt across generations to altered environments (Donelson et al. 2012, Salinas & Munch 2012, Clark et al. 2019a). As a result, predicting effects of MHWs on lower latitude species may need to consider shifting thermal ranges as these species adapt to climate change. It is unlikely that the same will apply to Ant arctic species, since many are physiologically limited by their capacity to acclimate and adapt to new temperatures because of their long generation times and delayed reproductive maturity (Peck et al. 2014, Peck 2018). For example, several invertebrate species such as the Antarctic scallop *Adamussium colbecki*, the limpet *Nacella concinna* and the bivalves *Laternula elliptica* and *Adacnarca nitens* take 4−7 yr to mature. The Antarctic bivalve *Aequiyoldia eightsi* starts reproducing at around 12 yr (Peck & Bullough 1993), and the brachio pod *Liothyrella uva* can take up to 18 yr before brooding young (Peck 2005, 2018, Oliver et al. 2019).

Predicting species and ecosystem responses to MHWs is challenging, owing to the past infrequency and variability of each event (Oliver et al. 2018). However, if we can track the functional deterioration of organisms when temperatures exceed their typical thermal range, this can inform our understanding of the relationships between the sub-lethal and lethal limits likely to be encountered during MHW events.

For organisms with slow growth and development and long generation times, like many of those found in Antarctica, thermal stress caused by MHWs is likely to trigger other mechanisms for survival such as biochemical and cellular stress responses (e.g. Clark & Peck 2009, Payton et al. 2016). Biochemical and genetic mechanisms, including a range of chaperone proteins, provide a short-term buffer that allows functioning to continue temporarily at temperatures outside the thermal niche of an organism (Deschaseaux et al. 2010, Clark et al. 2019b). Once animals are no longer able to maintain basic functions by these mechanisms, the sub-lethal limit to survival is reached.

Data on the functional thermal limits of species and MHW characteristics (i.e. rate, magnitude and duration) at which these thresholds are reached are rare, especially in fluctuating environments (Janecki et al. 2010, Peck et al. 2014, Ardor Bellucci & Smith 2019). Little is known about functional deterioration as a species approaches its critical thermal limit, and in the context of MHWs, animals are likely to experience temperatures that cause sub-lethal rather than lethal effects, defining long-term limits to survival and/or inhibiting population health (Pörtner et al. 2007).

This study aims to understand how functional (sublethal) limits track critical (lethal) limits and how this relationship changes with warming rate during a simulated MHW. To this

purpose, we monitored the ability to right, feed and assimilate energy, as well as the oxygen consumption rate, in the common Antarctic sea urchin *Sterechinus neumayeri.*

3.2 Methods

3.2.1 Sample site and animal collections

Sterechinus neumayeri were sampled from South Cove, Rothera Point (67° 34' 09.1" S, 68° 07' 52.7" W), from sites near the British Antarctic Survey's Rothera Research Station on the Western Antarctic Peninsula (WAP) during December 2019 (Appendix B, Figure A1). Adult urchins (test diameter range: 28−49 mm; n = 120) were collected by SCUBA divers at depths of 10−20 m and returned to the Rothera aquarium facility within 2 h of collection.

Sterechinus neumayeri is one of the most common and locally abundant members of the Antarctic marine shallow benthos, forming a significant component of the benthic community (Brockington 2001, Pierrat et al. 2012), with reported densities up to 600 m^{-2} (Barnes & Brockington 2003). It is a major scavenger of dead organisms and occurs in iceberg scours on the shallow Antarctic seabed (Dunlop et al. 2014); it is also a significant grazer and bioturbator of sediments (Lenihan et al. 2018). Because of this, *S. neumayeri* is an important carbon transformer in Antarctic shallow seas. Moreover, because of its abundance and ease of maintenance in laboratory culture systems, *S. neumayeri* has been the subject of extensive study of its embryonic and larval development, which is highly extended, sometimes lasting >100 d (Bosch et al. 1987). This species has also been the subject of studies of the effects of temperature on embryonic and larval development (Stanwell-Smith & Peck 1998), and the impact of ocean acidification on reproduction (Suckling et al. 2014) and energy budgets (Morley et al. 2016). Furthermore, there are long-term cycles in its reproduction (De Leij et al. 2021). These factors all make *S. neumayeri* one of the most important members of the Antarctic shallow benthic ecosystem and key to investigating responses to MHWs.

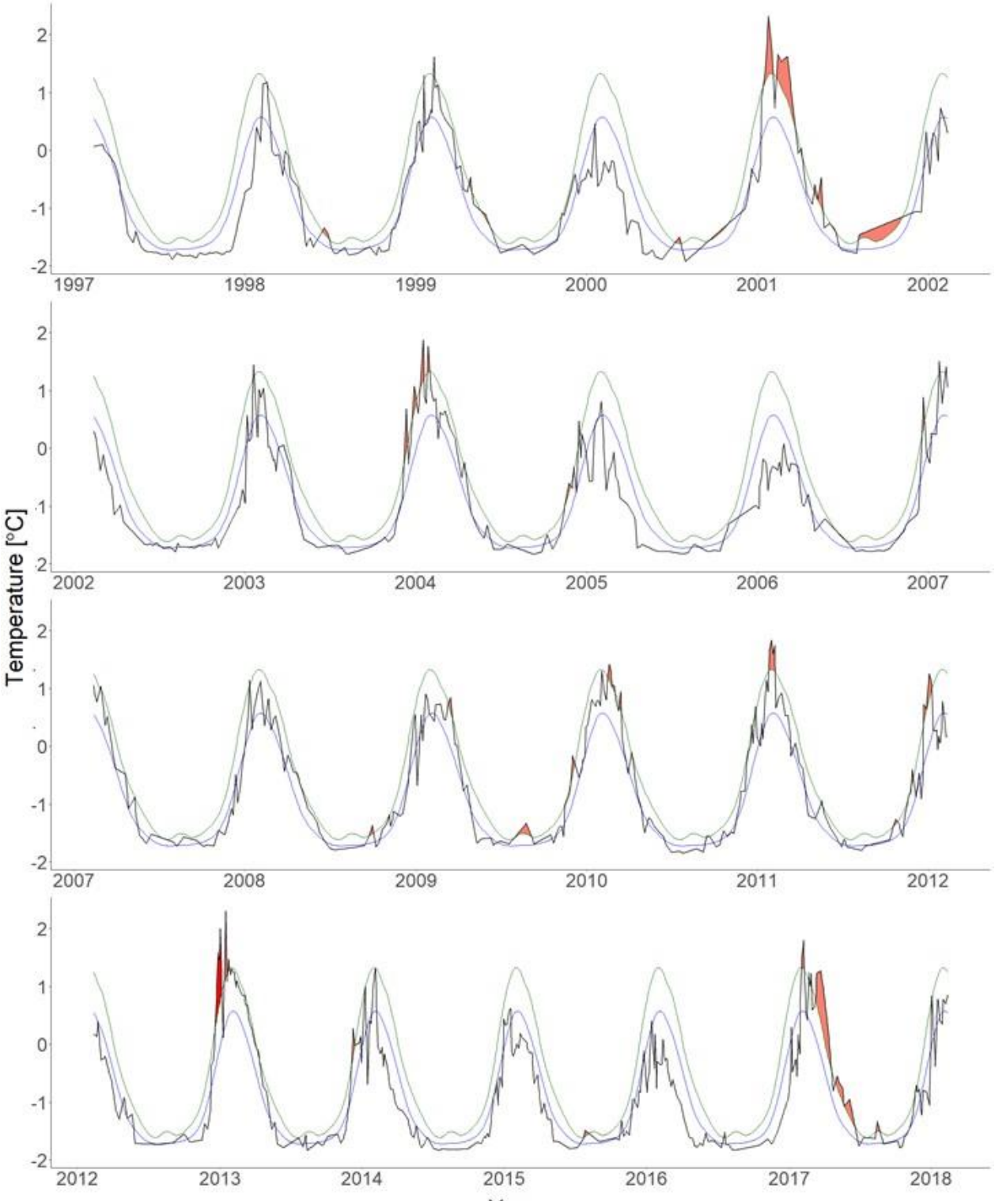

Figure 3.1: Times-series of temperatures (°C) experienced in Ryder Bay, Antarctica, at depths of 15 m, represented by the black lines. The data are split into panels to cover the entire span of the time-series, where the x-axis represents time in years. Blue lines represent the seasonal climatology of the region based on the full time-series of daily temperatures (1997 – 2018). Green lines represent the seasonally varying threshold for a marine heatwave (90th percentile). Temperatures exceeding the threshold for ≥ 5 days are highlighted in red and indicate the occurrence of a marine heatwave.

3.2.2 Experimental set-up and warming system

A decade of temperature data (1997-2017) from Ryder Bay on the WAP (sourced from the Rothera Time-Series (RaTS) environmental monitoring programme (Clarke et al. 2008, Venables et al. 2013)) was used in the R package "heatwaveR" (Schlegel & Smit, 2018), to detect past warming events (Figure 3.1) (see details of warming event analysis methodology and characteristics summary in the Appendix B, Text A1, Table A1, Figure A2). Studying the characteristics of these past warming events, including onset rate and magnitude, allowed me to set realistic warming rates for the experimental systems.

Urchins were held in flow-through aquaria (170 l) at ambient temperatures typical for December and January (−1.5 to +0.5°C) for 6 wk on a continuous light regime. During this time, animals were not fed to allow any ingested food to be processed and the production of faeces to cease. The cessation of faeces production is an indicator that metabolic rates have reached a 'standard' level at the start of the experiment. Previous research suggests that these urchins are able to sustain and experience natural periods of starvation for up 6 mo during winter (Brockington 2001), and hence 6 wk without feeding was unlikely to be detrimental to the physiological metrics measured in this study. Previous studies of oxygen consumption in Antarctic marine invertebrates has demonstrated that standard levels are reached in less, and often significantly less, than this time in the brachiopod *Liothyrella uva* and the limpet *Nacella concinna* (Peck 1989), in the amphipod *Waldeckia obesa* (Chapelle et al. 1994), in the isopod *Glyptonotus antarcticus* (Robertson et al. 2001) and in the sea star *Odontaster validus* (Peck et al. 2008).

After urchins were maintained in the flow-through aquarium (170 l) at ambient temperatures, 30 urchins were distributed to 4 main aquarium tanks to represent each warming treatment and the ambient control treatment. Ur chins were distributed at random. Replication within each of these treatments was achieved by floating 5 separate 6 l tanks, each containing 6 urchins in each main aquarium tank (170 l). Each main aquarium tank functioned as a temperature bath (Appendix B, Figure A3; 30 urchins per treatment, 5 replicates per treatment where data from urchins in the same replicate floating tank were pooled). Temperature treatments were not replicated due to space restrictions. The same treatment conditions (i.e. temperature) was translated to all replicate urchins, and as such, temperature was closely monitored to note and control variability (Appendix B, Figure A4).

The water in each floating tank was aerated using air stones and refreshed by 50% water change every other day. Water changes not only ensured that overall water quality was maintained, but also meant that any metabolic products, especially potentially toxic nitrogenous chemical species, were maintained at very low levels. Tank water samples were periodically analysed for pH (range: 7.5−8.0), NO_2 (0.05− 0.1 mg l^{-1}), NO_3 (0.5−1.0

mg l^{-1}) and NH_4 (stable at 0.1 mg l^{-1}) to ensure good water quality. Throughout the experiment, concentrations of the aforementioned compounds remained within the ranges stated. Urchins within each replicate tank were separated by aquaria egg crates and fine mesh partitions to ensure that individuals were produced was retained within compartments (Appendix B, Figure A3). During warming trials, experimental temperatures in the aquaria water baths were raised by 1, 0.5 or 0.3°C each evening, depending on treatment. Temperatures in the floating tanks increased more gradually than the water baths, allowing urchins to adjust slowly to each new temperature. Temperatures were checked every 30 min after each temperature change to ensure required temperatures were achieved and kept constant. Initially, temperatures fluctuated by up to ±0.3°C before stabilising after 1−2 h. Temperatures were subsequently monitored throughout the following day and held within ±0.1°C of the target experimental temperature (Appendix B, Figure A4). For ambient controls, urchins were held in the aquarium with the set-up and light conditions identical to the warming treatment conditions. Temperatures were maintained at those experienced in Ryder Bay, which naturally fluctuated between 0.9 and 1.9°C

3.2.3 Feeding trials

Urchins were fed pre-portioned amounts of food every 48 h. Previous studies fed *S. neumayeri* high protein diets, such as fish fillets (*Polachius virens*) (Suckling et al. 2014, Morley et al. 2016). In the current study, urchins were fed the foot of the common Antarctic limpet *N. concinna*, which has a comparable protein content to that of *P. virens* muscle. Based on feeding protocols of Morley et al. (2016), urchins were fed ~4% of their mean body mass every 3 wk, but this was spread across 48 h feeding increments in order to keep feeding activity constant and reduce the variability in daily metabolic activity.

Limpets were chosen as a food source since nutrient content could be controlled and pre-portioned. A more representative diet would be a varied one with algal biofilm, animal tissues and/or detritus (McClintock 1994). However, administering a varied diet would make it difficult to assess the amount of food consumed per urchin at the same time as standardising the nutritional content. There is evidence that diet, especially protein levels, can affect development and gonad growth (Liu et al. 2007, Zupo et al. 2019) as well as ingestion and assimilation rates in sea urchins (Azad et al. 2011). As such, by feeding a diet of limpets, it is possible that body condition may be altered and the ability to tolerate stress may be improved as a result.

Feeding was initiated 2 d before the beginning of the experiment to start the digestion process. Each urchin was allowed to feed for 48 h before any remaining food was removed and refreshed. After 48 h, each urchin was recorded as feeding or not feeding. Infrequently, urchins may have only partially consumed the food piece, which was recorded.

3.2.4 Faecal collection

Faecal production began 4 d into the experiment, 6 d after feeding was initiated. The presence of faeces was recorded for all urchins every 48 h. To measure faecal production, faeces were collected every 48 h by pipette and transferred to Falcon tubes from 10 urchins per treatment, where at least 1 sample was taken from each replicate tank within the treatment. The same urchins were targeted for faecal collection to minimise subconscious preferences towards urchins producing more faeces. This was not always possible since sometimes urchins did not produce any faeces or else the critical thermal limit (CT_{max}) was reached, and these urchins were removed. In these cases, a different urchin was chosen at random to sample from. For all other urchins, any remaining faecal matter was removed.

Collected faecal matter was centrifuged and the supernatant seawater decanted. Faeces were then rinsed with reverse osmosis purified water by agitating and centrifuging to remove any seawater salt. Washed faeces were pipetted into pre-ashed and pre-weighed foil boats and dried at 60°C for 24 h. Dry foil boats and faeces were placed in a desiccator to cool and then weighed (±1 mg). Dry faeces were subsequently combusted in a muffle furnace at 475°C for 6 h. Foil boats and ashed faeces were cooled in a desiccator and weighed (±1 mg). Dry mass and ash-free dry mass (AFDM) (i.e. organic content) were obtained by subtraction.

3.2.5 Respirometry

Oxygen consumption was recorded for 10 urchins per treatment, sampling 2 individuals from each replicate tank within each treatment. Oxygen consumption was recorded for the same urchins for every 2°C rise in temperature from ambient in each treatment. Methods for measuring oxygen consumption followed those described by Suckling et al. (2015), using 200−250 ml volume chambers. For each urchin, live wet mass (±0.01 g) was recorded where O_2 consumption was measured. AFDM was determined from live wet mass vs. AFDM regressions determined from a subsample of urchins (n = 40) collected from the same site. To obtain the ash mass of urchins, individuals were weighed live before freezing in liquid nitrogen and storing at −40°C. Frozen urchins were then placed in pre-ashed and pre-weighed ceramic crucibles and dried at 60°C until constant mass was obtained (±0.01 g). Once dried, urchins were combusted in a muffle furnace at 475°C for 6 h and subsequently weighed to obtain ash mass after cooling in a desiccator (±1 mg).

3.2.6 Righting

The time taken for urchins to right themselves was recorded for 10 urchins per treatment, sampling 2 urchins from each replicate tank within each treatment. The time taken to right was recorded for the same urchins every 2°C rise in temperature from ambient in each

treatment. Ten individuals were removed from their experimental tanks and placed in individual containers. These containers were previously filled and floated in water already at the experimental target temperature. Urchins were immediately inverted following transfer from experimental tanks to the floating containers and timed until the individual was fully upright. Urchins could not reach the sides of containers to aid in righting. Once righted, urchins were returned to their experimental tanks.

3.2.7 Critical temperature limits (CT_{max})

The CT_{max} was recorded for all experimental urchins in the warming treatments, where the limit was defined as the point at which the individual was unable to right itself within 12 hrs and had stopped eating and producing faeces. When an urchin began to show signs of reaching the CT_{max} (not feeding or producing faeces), it was inverted in the tank and left for 12 h. If the urchin had not righted itself after this period, it was removed and weighed suspended in water to obtain its live wet volume (± 0.01 mL).

3.2.8 Statistical Analysis

Where multiple urchins were sampled within the same floating tank, measurements of feeding, faecal production, righting and oxygen consumption were pooled so that n = 5, and the standard errors were calculated from these 5 replicate tanks.

To determine differences in functional responses between treatments, a 1-way repeat measures analysis of variance (ANOVA) was carried out in R (v. 4.0.5). This analysis was considered appropriate for this experiment due to the related and non-independent groups at each temperature timepoint. For this analysis, treatment group variances were compared when treatments reached the same temperature increments. For ambient controls, temperature timepoints were aligned with measurements taken at similar dates to treatment sampling. Variances were compared between groups and within timepoints for righting and oxygen consumption rates, and the resultant p-value was adjusted using the Bonferroni correction method. Significant differences ($p < 0.05$) were followed up with a paired t-test, and again, p-values were adjusted using the Bonferroni correction method. Data were initially log transformed to ensure that the assumptions of a normal distribution were met.

Segmented linear regression models were fitted in the R package ‘segmented’ (Muggeo 2008) to identify breakpoints in the linear relationships between functional process and temperature. Breakpoints were identified where the gradient of the relationship changed (McWhorter et al. 2018). The change in gradient was used to define the functional threshold of the process measured. It was especially important to use a method such as segmented regression to identify breakpoints in process rates. Segmented regressions were used to model these relationships not necessarily for the purpose of fitting the simplest model, but

rather to identify any change in the regressions gradient which then indicated that the functional response to temperature increase had changed. In some cases, a linear regression would be sufficient to explain the relationship; however, a linear model could mask the subtle change in the rate of degradation experienced when a species hits a thermal threshold. Alternatives would be to fit curves and identify changes in slope (e.g. Pörtner et al. 2006), but curves were not appropriate here. A Davies test was also conducted to determine significant ($p < 0.05$) differences in the gradients of the segmented slopes. Size effects on functional response were explored through scatter plots. Where relationships were observed, the effect of size (test diameter) and temperature on the functional response was assessed with a linear mixed effects model using the package 'lme4' and the function 'lmer' in R (v. 4.0.5). Test diameter and temperature were added as interacting fixed terms, and replicate tank ID was added as a random effect. Prior to any modelling, function responses were transformed to achieve normality in the distribution.

3.3 Results

3.3.1 Feeding and faecal egestion

On average (±SD), 80 ± 19% of animals fed in ambient conditions for the duration of the experiment. For the first 4 d of the experiment, in treatments where the temperature increase (T↑) was 1°C d^{-1}, the proportion of animals feeding exceeded all other treatments (97 ± 4%), including ambient conditions (87 ± 10%). Fifty percent of animals stopped feeding in treatments when temperatures exceeded 7.2, 8.2, and 9.2°C, where T↑ by 1, 0.5 and 0.3°C d^{-1}, respectively (Figure 3.2).

A breakpoint (where the slope of the regression changed) for the % individuals feeding was identified at 4.0 and 6.2°C in treatments where T↑ 1 and 0.5°C d^{-1}, respectively (Table 3.1). However, changes in the segmented slope gradients were not significantly different from linear regressions for these two treatments (Davies $p = 0.329$ and 0.301, respectively). A breakpoint for the % feeding in T↑ 0.3°C d^{-1} was identified at 8.2°C (Table 3.1), from which point the % individuals feeding declined rapidly and the relationship between temperature and the proportion of individuals feeding became significant ($p < 0.001$). The mean temperature breakpoint for the function of % feeding was 6.1 ± 1.2°C, averaged across all treatments.

The percentage of animals producing faeces tracked the proportion of animals feeding after the first 4 d (Figure 3.2). Following each breakpoint, the relationship between temperature and % individuals producing faeces became significant (Table 3.1). For the fastest rate of warming where T↑ 1°C d^{-1}, a breakpoint was identified at 5.2°C, above which the % individuals producing faeces rapidly declined from 100% to 10.3% within 6 days. Where

T↑ 0.3°C day^{-1} and 0.5°C day^{-1}, the regression breakpoint for faecal production was 8.3°C and 4.5°C respectively (Table 3.1). The mean temperature breakpoint for the function of % producing faeces was 6.0°C ± 2.0°C, averaged across all treatments.

Table 3.1: Summary statistics for linear regression relationships between the measured functions of *Sterechinus neumayeri* and temperature. β indicates the slope of the linear regression lines before the breakpoint (Slope_1) and after the breakpoint (Slope_2); SE_a indicates standard error for the intercept and slopes; df = degrees of freedom; bold p-values indicate significant relationships ($p < 0.05$) between temperature and the variable measured and bold Davies p-values represent a significant change ($p < 0.05$) in the gradient of the slope of segmented regressions. Values in the column BP indicate the localisation of the breakpoint or else NA indicates a single linear regression; SE_b (standard error) and R^2 refers to the goodness of fit for the entire model.

Function	β	SE_a	p-value	BP	SE_b	R^2	Davies p-value
Individuals feeding, 1°C day^{-1}			df=3				
(Intercept)	89.0	25.4	0.039	4.0	14.9	0.894	0.329
Slope_1	3.45	10.5	0.764				
Slope_2	-12.9	2.35	**0.012**				
Individuals feeding, 0.5°C day^{-1}			df=7				
(Intercept)	110.3	12.7	<0.001	6.2	6.78	0.964	0.301
Slope_1	-6.34	3.14	0.083				
Slope_2	-11.5	1.05	**<0.001**				
Individuals feeding, 0.3°C day^{-1}			df=12				
(Intercept)	95.3	7.53	<0.001	8.2	8.48	0.922	**0.001**
Slope_1	-2.73	1.38	0.071				
Slope_2	-20.3	2.92	**<0.001**				
Individuals producing faeces, 1°C day^{-1}			df=3				
(Intercept)	-29.0	23.1	0.298	5.2	13.5	0.881	**0.019**
Slope_1	24.1	9.54	0.085				
Slope_2	-13.3	2.13	**0.008**				
Individuals producing faeces, 0.5°C day^{-1}			df=7				
(Intercept)	34.0	28.6	0.274	4.5	12.1	0.844	**0.039**
Slope_1	13.3	8.54	0.162				
Slope_2	-10.3	8.68	**<0.001**				
Individuals producing faeces, 0.3°C day^{-1}			df=12				
(Intercept)	77.9	11.1	<0.001	8.3	12.5	0.762	**0.006**
Slope_1	-0.306	2.02	0.882				
Slope_2	-18.6	4.29	**<0.001**				
			df=14				
Faeces produced, 1°C day^{-1}	0.645	0.137	<0.001	NA	0.216	0.071	0.858
(Intercept)	-0.040	0.027	0.165				

Slope_1[1]							
Faeces produced, 0.5°C day^{-1}			df=31				
(Intercept)	1.52	0.214	**<0.001**	4.9	1.11	0.664	**0.043**
Slope_1	-0.23	0.072	**0.007**				
Slope_2	-0.06	0.025	**0.016**				
Faeces produced, 0.3°C day^{-1}			df=34				
(Intercept)	3.54	0.509	**<0.001**	3.3	0.294	0.729	**<0.001**
Slope_1	-0.718	0.202	**0.001**				
Slope_2	-0.051	0.020	**0.012**				
Time taken to right, 1°C day^{-1}			df=26				
(Intercept)	-8.60	9.04	0.350	NA	23.3	0.476	NA
Slope_1[1]	6.83	1.35	<0.001				
Time taken to right, 0.5°C day^{-1}			df=26				
(Intercept)	8.88	5.03	0.089	NA	13.1	0.302	NA
Slope_1[1]	2.61	0.731	**0.001**				
Time taken to right, 0.3°C day^{-1}			df=25				
(Intercept)	14.6	20.1	0.237	8.7	0.556	0.588	**<0.001**
Slope_1	0.384	3.66	0.459				
Slope_2	55.7	13.8	**<0.001**				
Oxygen consumption, 1°C day^{-1}			df=28				
(Intercept)	1.64	1.76	0.358	NA	4.64	0.551	NA
Slope_1[1]	1.50	0.248	**<0.001**				
Oxygen consumption, 0.5°C day^{-1}			df=33				
(Intercept)	4.29	1.10	<0.001	NA	3.17	0.368	NA
Slope_1[1]	0.611	0.134	<0.001				
Oxygen consumption, 0.3°C day^{-1}			df=28				
(Intercept)			**0.022**	NA	3.49	0.471	NA
Slope_1[1]	3.30	1.36	**<0.001**				
	0.957	0.185					

The mean mass of faeces produced in treatments where T↑ 0.3°C d^{-1}, was significantly greater than the faecal mass produced in ambient control conditions and treatments where T↑ 1° C d^{-1}, until temperatures exceeded 2.1°C ($t_{(4)}$ = 8.74, p = 0.006 and $t_{(4)}$ = 5.02, p = 0.044, respectively). Where T↑ 0.5°C d^{-1}, the mass of faeces produced was significantly greater than treatments where T↑ 1° C d^{-1}, until temperatures exceeded 2.1°C ($t_{(4)}$ = 5.31, p = 0.036). Despite this observation, no additional food was consumed in these treatments. There was no significant difference between the treatments or control as temperatures increased beyond 2.1°C (Appendix B, Figure A5).

Breakpoints in regressions were identified at 5.0 and 3.1°C for treatments where T↑ 0.5 and 0.3°C d^{-1}, respectively (Table 3.1). The breakpoints for these regressions marked a reduction in the gradient of the 2nd slope, whereby faeces produced d^{-1} mg^{-1} AFDM as a function of temperature decreased at a slower rate as temperatures increased. The mean

[1] Reporting only a single slope (Slope_1) indicates that no breakpoint was detected in the regression and therefore statistics for a single linear regression model is reported for the data.

temperature breakpoint for faeces produced was 4.1 ± 0.95°C, averaged across the slowest (T↑ 0.3°C d^{-1}) and intermediate (T↑ 0.5°C d^{-1}) rates of warming.

3.3.2 Righting

In treatments where T↑ 1°C d^{-1}, time taken to right became significantly longer than ambient controls when temperatures reached 9.2°C ($t_{(4)}$ = 6.06, p < 0.022). For treatments where T↑ 0.3°C d^{-1}, time taken to right only became significantly longer than ambient controls just before CT_{max} was reached, when temperatures reached 11.2°C ($t_{(4)}$ = 6.04, p < 0.023). For treatments where T↑ 0.5°C d^{-1}, time taken to right never exceeded ambient controls significantly, however mean righting times were consistently higher than control conditions throughout the warming period (Appendix B, Figure A6).

A breakpoint in the linear regression was identified at 8.7°C in treatments where temperature was raised at 0.3°C d^{-1} (Table 3.1). The relationship between temperature and the time taken to right became significant above this breakpoint temperature (p <0.001). For the other treatments righting time increased linearly without a breakpoint in the regression.

The interactive effect of urchin size and temperature on the time taken to right was significant ($t_{(204)}$ = 2.11, p = 0.034), where larger urchins took longer to right at higher temperatures (Appendix B, Figure A7, Table A3).

3.3.3 Oxygen consumption

Oxygen consumption rates were significantly higher in heatwave treatments compared to ambient controls when temperatures reached 7.2°C for all treatments. However, oxygen consumption rates were significantly higher than ambient controls from lower temperatures of 3.2°C in treatments where T↑ was 0.3°C d^{-1} ($t_{(4)}$ = 5.62, p = 0.030) and 5.2°C in treatments where T↑ was 1.0°C d^{-1} ($t_{(4)}$ = 4.98, p = 0.045). Overall, there was a positive linear trend between oxygen consumption and temperature for all treatments. However, at T↑ of 1°C d^{-1}, a drop in O_2 consumption occurred at 9.2°C, and at T↑ of 0.3°C d^{-1}, a drop occurred just before the CT_{max} at 11.2°C.

O_2 consumption increased at a faster rate per increase in temperature where warming rates were fastest at 1°C d^{-1} (slope gradient = 1.50) and increased at the slowest rate when warming rates were slowest at 0.3°C d^{-1} (slope gradient = 0.96) (Table 3.1). No breakpoint was identified in any treatment.

3.3.4 CT_{max}

The CT_{max} for urchins in treatments where T↑ was 0.3, 0.5 and 1°C d^{-1} ranged from 10.6 - 13.8, 11.2 - 13.7, and 12.2 - 14.2, respectively. The effect of warming rate on the CT_{max} was significant ($F_{(2, 12)} = 7.29$, $p = 0.008$), with post-hoc analysis identifying that for treatments where temperature increased at the fastest rate (1°C d^{-1}), the CT_{max} was significantly higher compared to treatments where temperature increased at a slower rate (0.3°C d^{-1}) ($t_{(8)} = -6.02$, $p = 0.001$).

Across all functions where breakpoints were identified, the slowest rate of warming (0.3°C d^{-1}) had a mean temperature breakpoint of 7.1 ± 1.3°C. In comparison, the mean temperature breakpoint was 5.2 ± 0.5°C, and 4.6 ± 0.6°C for intermediate (0.5°C d^{-1}) and fast (1°C d^{-1}) warming rates, respectively.

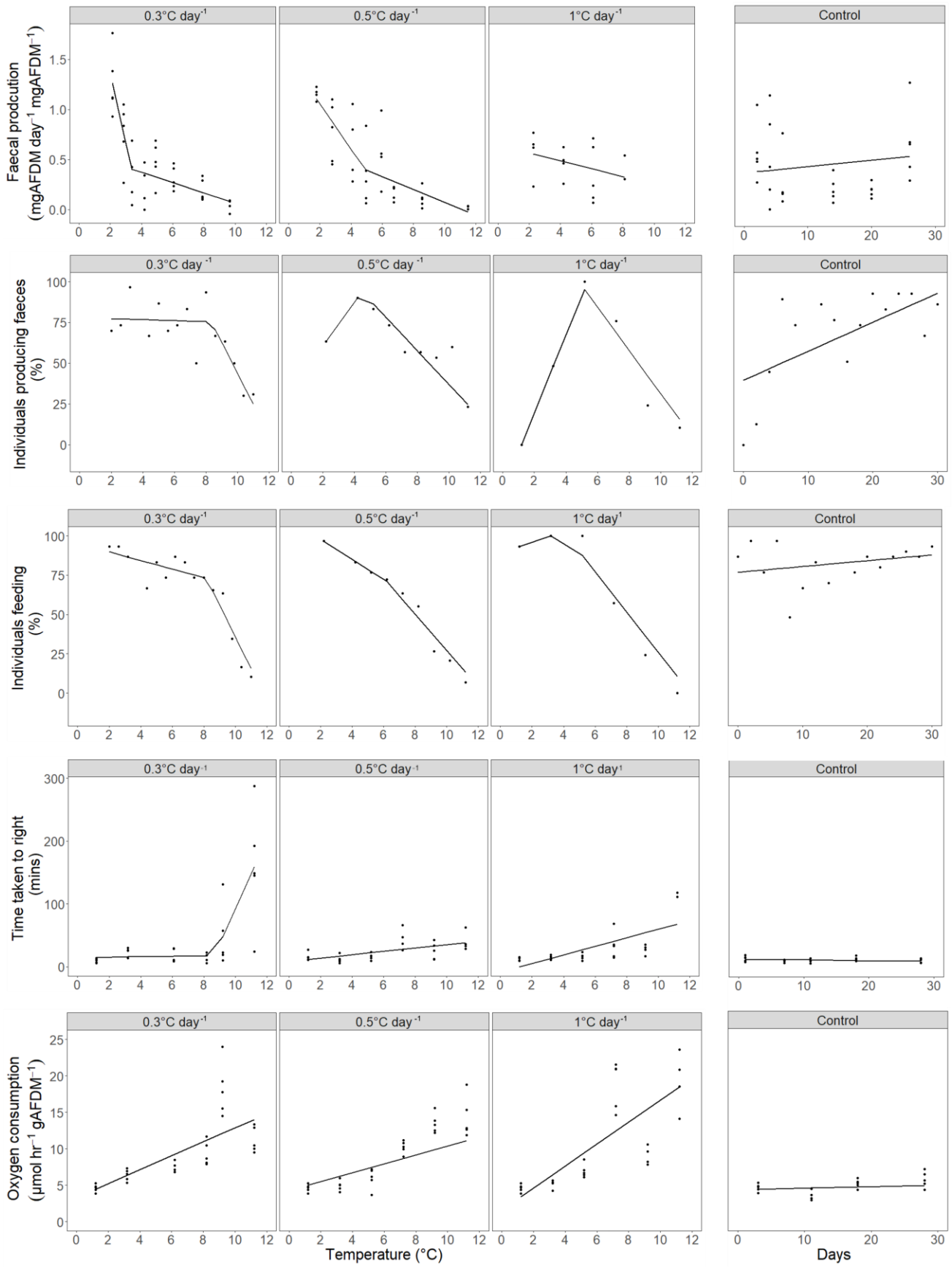

Figure 3.2: *Sterechinus neumayeri.* Biological functions measured in *Sterechinus neumayeri* in experimental conditions where temperatures were increased daily by 0.3ºC, 0.5ºC and 1ºC. Functions in warming conditions are plotted against increasing temperature and ambient control treatments are plotted against the number of days in the

experiment. Data points represent the pooled data within replicate floating tanks (n=5). Regressions are either segmented or linear depending on the optimum R^2.

3.4 Discussion

MHWs are predicted to increase in frequency, intensity and duration in the coming decades. Deterioration of basic animal functioning, critical for long-term survival, will likely be a more frequent consequence of the short-term warming (i.e. weeks to months) caused by MHWs, rather than mortality. However, little is known about functional impacts, especially thresholds and how these limits deteriorate with respect to CT_{max}. By understanding how key biological functions are affected by short-term temperature elevations and different warming rates, we can better understand how extreme climate events, typified by short-term warming, may impact individuals and populations, and hence communities.

In this study, we investigated the effect of warming rates typical of those expected during Antarctic MHW events on the functioning of the Antarctic sea urchin *Sterechinus neumayeri*. Functional thresholds were identified using segmented regressions, where a breakpoint indicated a gradient change in the response trend with temperature. The identification of regression breakpoints, or slope changes has been used previously to define ecological thresholds, and is considered a more flexible and realistic approach when interpreting complex, often non-linear, ecological relationships (Piepho & Ogutu 2003, Ferrarini 2011, Morley et al. 2014). Several studies have shown that faster warming rates result in higher CT_{max} in terrestrial (e.g. Terblanche et al. 2007, Allen et al. 2016) and marine (Peck et al. 2009) species. These observations, along with the CT_{max} data in this study, follow the failure rate model proposed by Kingsolver & Umbanhowar (2018), who showed that critical limits are reached at lower temperatures when warming accumulates over extended periods. However, the results for functional thermal limits follow the opposite trend to the CT_{max}, where functions are impacted negatively at lower temperatures when warming is rapid. Overall, in this study higher functional thresholds were reached when temperatures were raised slowly (thresholds averaging 8.3 ± 1.3°C). At the faster warming rates, functional thresholds were lower (5.4 ± 0.5°C or 4.6 ± 0.6°C). There was even evidence that some functions declined linearly, with significant deterioration from temperatures +2.8°C above ambient when warmed at the fastest rate. Thus, short-term exposure to more extreme temperatures has more impact on functioning than longer, chronic exposure to more slowly elevated temperature

Although metabolic acclimation is unlikely over such short time periods (apparent from the oxygen consumption data here, and also previous research on long-term acclimation of *S. neumayeri*; Peck et al. 2014, Suckling et al. 2015), short-term acclimation for some functions might be possible after an initial shock response when temperatures are

increased slowly. In my study, the shock response did not appear to subside at faster rates of warming, and instead mean functional thresholds were lower as warming rate increased. These results suggest that functional and lethal limits are likely driven and determined by different mechanisms. Previous studies have shown that lethal limits are likely set by one or both of physiological processes or cellular and biochemical mechanisms. At very rapid rates of warming, such as 1°C h^{-1} or 1°C d^{-1}, physiological mechanisms such as nervous and circulatory failure appear to be the limiting factors (Young et al. 2006, Pörtner et al. 2007, Bilyk & DeVries 2011). At slower rates of warming (1°C every 3 d to 1°C mo^{-1}), cellular and biochemical mechanisms such as accumulation of toxic products, e.g. protein carbonyls, enzyme tolerances or insufficiency of chaperone protein capacity appear to be limiting (Peck et al. 2009, Clark et al. 2017, 2018). The factors setting thermal limits and responses to warming were recently shown to be highly species specific (Clark et al. 2021, Collins et al. 2021).

The results also indicate that thermal sensitivity varies among key biological functions. For example, the function of righting in urchins was similar between treatments and ambient control conditions until temperatures reached 9.2°C for the fastest rates of warming, and the highest breakpoint of 8.7°C was identified for the slowest rates of warming. However, lower thresholds were identified for the other functions related to digestion such as % feeding or % producing faeces. Variation between functional thresholds could be related to function complexity, where a function involving multiple processes would be more likely to fail (Pörtner et al. 2007, Stevens et al. 2010, Peck 2011). Another explanation could be related to the extent to which functions limit survival and fitness, where the energy reserves of an organism allow for short periods of negative energy balance. In Antarctic marine species, such periods of negative energy balance can be very long, extending to months or even years of low food supply or starvation, because of the extreme environmental seasonality and the very low metabolic energy use characteristic of this fauna (Brockington et al. 2001, Harper & Peck 2003, Obermüller et al. 2010). However, being able to right provides immediate protection from predation, equivalent to mechanisms such as the ability to stay attached to the substratum in limpets (Morley et al. 2012b) or reburying in infaunal clams when disturbed and removed from the sediment by, for example, iceberg scour (Peck et al. 2004). Finally, where a function has a higher metabolic energy demand, it is more likely to be limited by food availability and energy delivery capacity (van der Meer 2006, Morley et al. 2012a, Peck 2018).

The breakpoints identified for the mass of faeces produced might not indicate a functional threshold. Instead, the initial high faecal production in the slowest and intermediate warming rates is likely a result of the initial increase in temperature causing food to move faster through the urchin, as also seen in the Antarctic plunderfish *Harpagifer antarcticus* (Boyce et al. 2000). This elevation in faecal production was only observed when

temperatures increased initially, after which faecal production reduced to rates similar to ambient control conditions. This effect was not observed in treatments with the fastest rates of warming since these slight increases in temperature of 1−2°C were likely not maintained long enough for gut passage rate to increase. Therefore, the results indicate that the breakpoints for faecal production may not have any direct implications on functionality and instead give evidence for the relationship between temperature and gut evacuation rate.

In thermally stressed environments, animals usually increase their oxygen uptake in order to meet increasing demands of functional processes (Gillooly et al. 2001). However, when oxygen uptake is increased, yet functioning deteriorates, it is hypothesised that this indicates a threshold where uptake, transport and delivery of oxygen can no longer meet the functional demands of the animal. This theory has been termed the oxygen and capacity limited thermal tolerance (OCLTT) hypothesis (Pörtner et al. 2017). This theory focusses on the limitations set by the physiology of an animal. However, as temperature increases, the concentration of oxygen diminishes, further reducing the availability of oxygen to the animal and potentially amplifying the effects of OCLTT. Reducing the concentration of oxygen in the water can limit functioning (Peck et al. 2007, Pörtner et al. 2007), and as such, the functional thresholds identified in this study may not only indicate thermal limits but may also be influenced by the reduced oxygen content as temperatures increased. If oxygen concentration was controlled and elevated throughout warming, the functional thresholds identified would likely be higher (Pörtner et al. 2006). However, warmer oceans will be accompanied by lower oxygen concentrations (Oschlies et al. 2018, Spicer et al. 2019) and the functional thresholds determined in this study will be more representative of a natural system than if oxygen were controlled.

Food availability and quality can also be a significant factor in determining functional scope (Welch et al. 1998, Lemoine & Burkepile 2012, Cheng et al. 2018), whereby the nutritional status and condition of the animal could affect energy delivery capacity similarly to OCLTT. For example, feeding and digestive capacity limited the thermal tolerance of juvenile spiny lobsters *Sagmariasus verreauxi* (Fitzgibbon et al. 2017), and the digestive capacity and food intake of individuals at high temperatures was related to depressed mitochondrial respiratory capacity in brown trout *Salmo trutta* (Salin et al. 2016). The capacity to assimilate energy would also play a role in determining energy delivery to tissues and is determined by physiological processes including consumption rate, absorption of food and gut evacuation rate (Boyce et al. 2000, Angilletta 2001). Hence, assimilation itself is energetically demanding and may limit functional thermal thresholds (Sandersfeld et al. 2015, Salin et al. 2016).

Thus, OCLTT may be a possible mechanism for determining functional limits observed in my experiments. However, there is no empirical support in the data for this theory. In both

experiments and in natural MHWs, other factors are likely to be involved, and obtaining sufficient energy from food may be necessary for successful functioning. Impacts on animal condition from warming may be especially important in highly seasonal polar environments where warming in winter, when food supplies are scarce, would increase energy use with little or no opportunity to mitigate the cost (Peck 2018). Species such as *S. neumayeri* that have been shown to spend periods in winter up to 7 mo without feeding (Brockington 2001) may be particularly vulnerable to such impacts.

My experiment included a period of 6 wk without feeding to allow metabolic activity to stabilise and be comparable between individuals. However, a caveat to this initial standardisation of conditions could influence the physiological response of the urchins to the warming in treatments. Nutritional status has been shown to affect the reproductive state of *S. neumayeri,* with a reduction in gonad index and maturation of gametes following 6 wk without food, compared to animals foraging naturally in the environment (De Leij 2021). Functional capacity has also been affected in other invertebrates under low food coupled with environmental stress; for example, blue mussels Mytilus edulis had a reduced ability to repair shells when high CO_2 was coupled with low food (Melzner et al. 2011), and green sea urchins *Strongylocentrotus droebachiensi* exhibited severe metabolic acidosis when exposed to elevated CO_2 with empty digestive tracts (Stumpp et al. 2012). Hence, we might consider that the elevated temperatures coupled with the suboptimal nutritional status at the start of the experiment may have impacted the thermal limits of certain functions. This would likely have resulted from a mismatch between a limited energy supply and stores, and an increased energy demand of the animal. However, the data in this study shows a reduction in the number of urchins feeding as temperatures increase, suggesting that food was not the limiting factor when this species approached its functional thermal limits.

From my analysis of the Rothera Time-Series environmental data, previous MHW events reached maximum temperatures of 2.3 ± 0.36°C, with onset rates of 0.3°C d−1. Days at heatwave status have extended up to 95 d, and cumulative intensities (a combination of temperature intensity and heatwave duration) have reached maxima of 54°C × day (Appendix B, Figure A2). Mean climate temperatures are predicted to shift by +2°C by 2100, and with that, climate extremes such as MHWs will increase in magnitude relative to this shift (IPCC 2014, 2019). My results suggest that functions such as feeding and faecal egestion are likely to be affected by MHW events occurring in 2100, if not before, and this will include increased metabolic demands with consequent impacts on annual energy budgets.

For a long-lived (>40 yr; Brey et al. 1995) and slow to mature (8−9 yr; Peck 2018) species such as *S. neumayeri*, there will be less scope for phenotypic and genotypic adaptations to a warming climate as might be possible for short-lived and rapidly maturing species

(Peck 2011, Donelson et al. 2012, Salinas & Munch 2012). However, there may still be opportunity for *S. neumayeri* to adapt to a warmer world. Within 80 yr (2020−2100), 8 generations of *S. neumayeri* will have succeeded the present population, and in the year 2100, the 5th, 6th and 7th generation could be present and reproducing in populations around Antarctica. If we consider the evidence of its capacity to acclimate, it may be possible for *S. neumayeri* to acclimate and adapt successfully to function in a +2°C warmer world (Morley et al. 2016). It is still uncertain, however, how this species will respond to acute warming, like that experienced during MHWs, in this warmer climate. The data in this study cannot be used to predict the implications of acclimation and adaptation on the subsequent tolerance to MHWs for *S. neumayeri.* Instead, the data provide insight into the effect of onset rate of acute warming, the thermal vulnerability of key biological functions and the difference between critical and functional thermal limits. Thus, according to my data, we could see reduced energy availability for *S. neumayeri* from changes in feeding and food processing rates during MHWs in warmer oceans, which would very likely reduce survival in marginal environments.

Following the results from this study, it would be important to explore recovery following MHW events. The data indicate reduced functioning as temperatures are raised across all rates of warming. However, the ability and rate of *S. neumayeri* to resume 'normal' functioning if returned to ambient temperatures is uncertain. The marine snail *Littorina littorea* loses motility under thermal stress, but when temperatures are lowered again, this function returns (Hamby 1975). To resume a single function may not indicate full recovery, and my study shows that different biological functions have varying thermal tolerances. As such, performance of all functions, including metabolic activity, would need to return to baseline levels for an animal to recover completely (Walter et al. 2013). Developing our understanding of recovery following acute warming and even the effects of repeat MHW events, could better predict the long-term implications of MHWs for this species. It is important to note that the functional and critical limits measured in this study are likely an example of a 'best case scenario'.

Experiments such as these can only predict the isolated effects of one variable. However, the additional energetic costs associated with physical factors such as salinity change and biological factors including varying food quality and quantity, species interactions, diseases and scavenging for food, need to be included before we can obtain dependable predictions for 'real world' scenarios that give information relevant to the variable conditions experienced across a species distribution range. What is limiting at the range margins for a species will differ from core areas (Kolzenburg et al. 2021). My data highlight that the deterioration of functioning when temperatures are raised, especially during MHWs, has implications for long-term survival and physiological functions. Therefore, functioning should be considered when determining organism thermal limits,

rather than traditional critical thermal limits. My findings show that fitness cannot be determined from a single function and instead functions vary in thermal sensitivity. A whole-organism approach to functional fitness is therefore necessary, considering functional complexity, importance and energetic demand. My results suggest that contrary to the relationship between critical thermal limits and onset rate, functional degradation occurs at lower temperatures when exposed to rapid warming (1°C d^{-1}). Therefore, when investigating the impact of MHWs on organisms and populations, it is important to consider the key features of the heatwave event, including the onset rate, exposure duration and how these characteristics act together to determine functional thresholds.

Chapter 4 Repeat marine heatwaves in a future climate: functional responses of the Antarctic sea urchin, *Sterechinus neumayeri*

Abstract

Against a backdrop of climate change, extreme events such as heatwaves are predicted to increase in duration, frequency, and magnitude over the next 80 years. Marine species will therefore experience acute changes superimposed on a chronic warming trend. The thermal thresholds of species will hence need to be broad enough to encompass these high temperatures or else alter optimal performance temperature ranges through processes such as acclimation to sustain functions and persist in the future. This study investigated the ability of the Antarctic sea urchin, *Sterechinus neumayeri*, a species that typically experiences a narrow temperature envelope of ±2°C, to acclimate to temperatures predicted for the end of the century in the marine environment. Following acclimation, the ability of *S. neumayeri* to function during simulated marine heatwaves (MHWs) (i.e., repeated acute warming cycles) was investigated. MHW simulations were of magnitudes, durations and frequencies previously experienced on the Western Antarctic Peninsula (WAP) over the past 20 years (1998 – 2018); and also aimed to be representative of future conditions. To investigate acclimation potential, experimental urchins were exposed to chronic warming of 2°C for 8 months prior to MHW simulations (i.e., warm-acclimated), whereas control urchins were unheated (i.e., cold-acclimated). Animal functioning in terms of oxygen consumption rate, righting response, feeding behaviour and energy assimilation were measured following acclimation and then during the MHW simulations. The results show that *S. neumayeri* can alter optimal performance temperatures through long-term acclimation. Oxygen consumption rates in *S. neumayeri* were overall elevated in warm-acclimation, however this was in line with what would be expected from a 2°C temperature increase with regards to Q_{10} values. In addition, the increase in oxygen consumption rate over baseline levels produced by acute warming was less in warm-acclimated compared to cold-acclimated urchins. Warm-acclimation appeared to enhance respiratory recovery following acute warming, however righting response times increased following acute warming, suggesting poorer recoverability. Despite warm-acclimation having some benefits for this species, there were still elevated oxygen consumption rates, lower energy assimilation rates and longer righting times following warm-acclimation, and acute warming from the MHWs caused significant and sustained increases in energy requirements. This research suggests that species, even those typically adapted to cold and narrow thermal regimes, may be able to cope with acute warming experienced during MHWs. Some may even enhance their thermal

resilience following acclimation to the gradual temperature increases predicted for 2100. However, the impact of acute thermal stress from repeat MHWs at both ambient and future temperatures will result in significant energetic trade-offs, with the potential for marked effects on functioning and hence distributions.

4.1 Introduction

Global climate records demonstrate a warming trend, with current research focussed on the potential impacts of regional change and mean rates of warming (Abram et al. 2016; Bilbao et al. 2019; Spence et al. 2017). Superimposed on this mean warming trend is an increase in the intensity and frequency of climate and weather extremes, with shifts in mean environmental temperature and more acute 'extreme' temperatures predicted (Frölicher & Laufkötter, 2018; Peck, 2005). Events such as marine heat waves (MHWs) have already been documented and are predicted to increase in magnitude, frequency, and duration under future environmental scenarios (Oliver et al. 2018). Under current national policies, the relative mean spatial extent of a MHW is predicted to become on average 21 times larger, ten times longer in duration (112 days), and six times more intense (max intensity 2.5°C) compared to preindustrial times (1861 - 1880), by the end of the 21st century (Frölicher et al. 2018).

Natural drivers of temperature variability in the oceans include large-scale climate modes and natural environmental cycles such as the El Niño-Southern Oscillation (ENSO), with both the frequency and intensity of MHWs strongly influenced by ENSO events, especially in the Southern Hemisphere (Oliver et al. 2018). In addition, variation in seawater temperature is influenced by changes in atmospheric circulation (Clem et al. 2020; Turner et al. 2016), solar output (Tett et al. 2002), and volcanic activity (Bilbao et al. 2019). However, currently 87% of MHWs are attributable to human-induced warming caused by greenhouse gases, sulphate aerosols, and ozone depletion (Stott et al. 2004). If global warming exceeds 2^{o}C, the percentage of MHWs attributed to human-induced warming is expected to rise to nearly 100% (Frölicher et al. 2018).

Acclimation capacity is one of the key factors that is likely to determine an organism's survival in a future climate (Calosi et al. 2008; Peck, 2011; Somero, 2010; Stillman, 2003) and can be defined as the ability of an organism to alter its optimal performance temperature and critical thermal limits with changing temperatures (Rohr et al. 2018). However, acclimation to warmer temperatures may have consequences to overall fitness, where maintenance costs and overall energetic demands may increase (van der Meer, 2006; Woodin et al. 2013).

Acclimation capacity is often determined by changes in acute C_{Tmax} following long-term exposure to altered conditions (Cheng et al. 2018; Morley et al. 2019; Peck et al. 2014; Sunday et al. 2019). Changes in functional metrics have also been investigated following acclimation, including cell stress responses (Clark et al. 2019b), proteomic changes (Garland et al. 2015), reproductive development (Foo & Byrne, 2017; Suckling et al. 2015), heart and circulatory function (Joyce et al. 2018), activity and locomotion (Azra et al. 2018), and oxygen consumption (Morley et al. 2016; Peck, 1989), as well as changes in population biomass and abundance (Pansch et al. 2018).

Factors determining an organism's acclimation capacity can be a combination of species traits, including activity levels and mobility (Peck, 2011; Peck et al. 2009), metabolic regulation ability (*sensu* Marshall & McQuaid, 2020), and then at the organism level, the thermal history, life history stage, and body size on an individual (Peck et al. 2007, 2009, Giomi et al. 2016, Cassidy et al. 2020, Ern et al. 2020, Gårdmark & Huss 2020).

Some marine ectotherms have shown a beneficial acclimation response (Collins et al. 2021; Deere & Chown, 2006). For example, the bivalve *Perna viridis* attained Arrhenius breakpoint temperatures 9^{o}C higher after warm acclimation (Cheng et al. 2018), and the gastropod mollusc, *Marseniopsis mollis,* increased CT_{max} by 2.3^{o}C after warm acclimation (Peck et al. 2010). However, this response is not universal, and as the number of species studied increases, there is growing evidence for significant interspecific variability in the thermal acclimation capacity of organisms, even within similar thermal environments (Clark et al. 2019a; Peck et al. 2010; Peck, 2018). For example, the Antarctic benthic gastropod mollusc *Marseniopsis mollis*, increased its acute upper temperature limit by 2.3^{o}C following acclimation to +3^{o}C for 60 days (Peck et al. 2010). In contrast, the bivalve mollusc, *Yoldia eightsii*, the brachiopod *Liothyrella uva* and the amphipod *Paraceradocus gibber*, all collected from the same location, experienced no change in temperature limits following the same acclimation (Peck et al. 2010). However, it was later reported that some Antarctic species require very long times to complete temperature acclimation, with some species such as the sea urchin *Sterechinus neumayeri* requiring between 6-8 months to acclimate to 2^{o}C (Suckling et al. 2015) and the limpet *Nacella concinna* requiring at least 9 months to acclimate to 2.9^{o}C (Morley et al. 2011).

Ecological stress memory is the mechanism whereby an organism's response to future thermal stress events is modified by its previous experience (*sensu* Walter et al. 2013). This response can be either manifest as a cumulative negative effect, or a positive effect due to acclimation or 'heat hardening' (Bilyk et al. 2012a; Bowler, 2005). There is evidence of both these responses in the marine environment (Bard & Kieffer, 2019; Bilyk et al. 2012a; Pansch et al. 2018; Peck et al. 2014; Suckling et al. 2015).

The aim of this study was to determine: 1) if there is evidence of successful acclimation in the urchin, *S. neumayeri,* following long-term exposure to temperatures predicted for the end of the century; 2) if acclimation to near-future temperatures affect the physiological response of *S. neumayeri* to MHW events; and 3) the effect of repeated MHW events on the physiology of both cold and warm-acclimated *S. neumayeri*. To address these aims, I exposed two groups of *S. neumayeri* for 8 months to a cold-acclimation temperature of 0^{o}C and a warm-acclimation temperature of 2^{o}C. Following acclimation, urchins were exposed to repeat heatwave simulations with frequency, magnitudes, and onset rates similar to those expected under an environmental-future scenario predicted by the IPCC (IPCC, 2014), climate models (Oliver et al. 2019), and from data on warming events previously experienced on the WAP. Physiological responses including oxygen consumption, righting response and feeding metrics were measured during MHW events and in the recovery periods between events to assess the effects of warming acclimation and repeat heatwaves on physiological status.

4.2 Methods

4.2.1 Animal collections and experimental conditions

Urchins were collected from Hangar Cove, Rothera Point (67°33'54.2"S 68°07'13.1"W), located on the WAP in the austral summer 2019. 300 urchins were SCUBA-diver collected at depths of 10-20 m and returned to the Rothera aquarium facility within 40 minutes of collection. Urchins were subsequently transported back to the UK via a temperature-controlled transport aquarium and held at the British Antarctic Survey (BAS) aquarium facility for 18 months. For the first 7 months, urchins were held across two, 280 L tanks and temperatures were maintained at -0.2^{o}C. Once a week, animals were fed a diet of frozen krill.

Acclimation of urchins to experimental temperatures began in February 2020, whereby 150 urchins were acclimated to the average ambient austral summer temperature of 0^{o}C. The other 150 urchins were acclimated to a future summer temperature of 2^{o}C based on IPCC estimates for 2100 average global sea temperature rise (IPCC, 2014). To reach this value, temperatures were gradually raised by 0.5^{o}C increments across a two-week period.

Urchins were held at treatment temperatures for a further 8 months in line with the previously published period required for *S. neumayeri* to acclimate to a temperature increase of 2^{o}C (Suckling et al. 2015). Animals continued to be fed a weekly diet of frozen krill for the duration of the experimental acclimation period.

Following the 8-month acclimation period, urchins were evenly distributed across six tanks in total, three replicate tanks at ambient and three replicate tanks at future temperatures, resulting in 50 urchins per tank. Each tank system was separate and fitted with a protein skimmer (V2 skim Pro 450, TMC), a biofilter (ZB-300 Ziss Aqua Bubble Bio), and aerators. Since the tank systems were not flow-through, 50% water changes were performed three times a week, and concentrations of Nitrite (NO_2^-) and Ammonium (NH_4^+) were measured twice weekly (JBL ProAquaTest, Water Test Kit). Water changes not only ensured that overall water quality was maintained, but also meant any anaerobic by-products that had accumulated were removed. Throughout the experiment, concentrations of NO_2^- and NH_4 remained well within the test kit manufacturers advised ranges (NO_2^- <0.2 mgL^{-1}, NH_4 <1.2 mgL^{-1}) (Appendix C, Figure A1 and A2).

Urchins were transferred to an artificial diet two weeks prior to the MHW simulations to mimic the nutrient availability of their natural environment. The diet (Vitalis© Marine Grazer) constituted 31% protein derived from fish, algae, molluscs, crustaceans and minerals. Based on feeding protocols in Morley et al. (2016), urchins were fed ~4% of their mean body mass every three weeks, but this was spread across weekly feeding increments in order to monitor feeding activity on a weekly basis, reduce the variability in metabolic activity, and reduce nutrient loading in the tanks following large food additions. Considering this, the diet was provided at 32 mg dry mass $urchin^{-1}$ $week^{-1}$. The amount was justified since it was within the typical average gut content of *S. neumayeri* (11 mg – 79 mg dry mass $urchin^{-1}$) previously observed in wild populations at South Cove, Rothera Point during the summer period, Nov – Jan (Brockington et al. 2001). Despite the experiment being conducted in Oct – Dec, it was thought that summer feeding levels would be required considering temperatures were similar to those experienced in summer. Within each tank, five urchins were isolated in small floating tanks and fed a greater portion of 64 mg mass $urchin^{-1}$ $week^{-1}$, directly to enable food to be given in excess and hence assess consumption rates when food was not limiting. Feeding was allowed for 48 hrs, after which all food was removed.

4.2.2 Marine heatwave simulations

The magnitude, length and frequency of MHWs during the experiment were based on the characteristics of past warming events in the WAP region. This information was derived from the Rothera Time Series (RaTS), a long-term environmental monitoring programme that measured sea surface temperatures weekly, from 1997 to 2017.

The R package “heatwaveR” (Schlegel & Smit 2018), was used to detect past MHWs, defining characteristics such as onset rate, duration, magnitude, and annual frequency (Appendix C, Figure A3). These values were used as a guide to design realistic warming

events. The median rather than mean was used for duration due to the large variability between events. The maximum magnitude experienced during a MHW (2.0°C) was used as the target peak for each MHW, and an onset rate of 0.5°C per day, slightly faster than that experienced in the environment, was implemented due to experimental time constraints. The frequency of events was set as three MHWs since the current average is two per year, and frequency of events are set to increase.

4.2.3 Physiological measurements

Oxygen consumption was recorded for 10 urchins per treatment, sampling 10 individuals randomly selected across the replicate tanks within each treatment, along with one control chamber (no animal) placed in each of the replicate tanks. Oxygen consumption was measured one week before warming began, at the peak of each MHW, and then again one week following the peak. Methods for measuring oxygen consumption followed those described by Suckling et al. (2015), with chambers ranging from 190 cm^3 – 300 cm^3 volume. For each urchin, where O_2 consumption was measured, volume (± 1 cm^3) was recorded and the respirometer volume was adjusted for this. Ash free dry mass (AFDM) (i.e., organic content), was determined from volume vs AFDM regressions derived from a subsample of urchins (n = 48). For the purpose of obtaining the AFDM of urchins, individuals were weighed live before freezing at -80°C. Test diameter (± 0.1 mm) of frozen urchins was measured before they were placed in pre-ashed and pre-weighed foil boats and dried at 60°C until constant mass was obtained (± 0.01 g). Once dried, urchins were ignited at 475°C for 6 hrs and remaining material weighed to obtain ash mass once cooled (± 1 mg).

As mentioned before, five individuals were isolated for the duration of the experiment in floating tanks and fed pre-weighed diet. After 48 hours, any remaining food was collected and dried in pre-ashed and pre-weighed foil boats at 60°C for 24 hours. Foil boats and dried food were placed in a desiccator to cool and then weighed to obtain dry weight (± 1 mg) before being ignited at 475°C for 6 hrs. Foil boats and ignited faeces were then cooled in a desiccator and weighed (± 1 mg) to allow AFDM to be obtained by difference with dry mass. All faeces produced in the seven days following feeding were collected and centrifuged so the supernatant seawater could be decanted. Faeces were then twice rinsed with RO (Reverse Osmosis purified) water by agitating and centrifuging to remove any residual seawater salt. Washed faeces were pipetted into pre-ashed and pre-weighed foil boats. Dry and AFDM were obtained as previously.

The time taken for urchins to right themselves when turned upside down was recorded for 10 urchins per treatment, sampling 10 individuals randomly selected across the replicate tanks within each treatment. The time taken to right was recorded one week before the

initiation of MHW trials, at the peak of each MHW event and then 2 weeks following the peak, just prior to the next phase of warming. Righting was also measured 21 days following the final MHW event. To measure time taken to right, urchins were selected at random and isolated in floating containers. Urchins were immediately inverted following transfer from experimental tanks to the floating containers and placed in positions that did not allow tube feet to attach to the sides of containers. Time taken for the individual to fully right itself was recorded and once righted, urchins were returned to the main tank.

4.2.4 Data analysis

To translate mass measures of feeding and faecal production into energy, the mass of food consumed (AFDW g) was expressed as energy consumed (kJ $week^{-1}urchin^{-1}$), where energy content of the food was derived from conversion factors based on the nutritional content of the diet (Table S1). The energy content of the faeces was assumed to be the same composition in the diet based on studies which have shown that in urchins the overall calorific content of faeces is not significantly different to that of the diet consumed (Dethier et al. 2019). As such, energy assimilation efficiency (%) was calculated from the difference between the energy content of the food consumed, and the energy content of the faeces produced using the following equation:

$$\text{Energy assimilation efficiency (\%)} = \frac{\text{Energy content of food consumed (kJ)} - \text{Energy content of faeces (kJ)}}{\text{Energy content of food consumed (kJ)}} \times 100$$

The Conover ratio, representing the proportion of organic matter lost from the food during passage through the digestive tract (Conover, 1966), was calculated using the following equation:

$$\text{Conover ratio (\%)} = \frac{\text{AFDM food} - \text{AFDM faeces}}{(1\text{-AFDM faeces}) \times (\text{AFDM food})} \times 100$$

The relationship between the feeding data (Conover ratio and energy consumption) and experimental duration was expressed as a segmented regression to identify changes in feeding behaviour where a change in the slope of the linear regression occurred (a breakpoint) (McWhorter et al. 2018). Segmented linear regression models were fitted through the R (v. 4.0.5) package ‘segmented’ (Muggeo, 2008) and a Davies test was conducted to determine significant (<0.05) differences in the gradients of the segmented slopes. For the scatter plots of feeding metrics, data were first pooled across urchins within tanks (n = 5), and then the average and standard error of the pooled urchin data was calculated across replicate tanks (n = 3).

Changes to oxygen consumption rates in each treatment were compared by calculating thermal dependence coefficient (Q_{10}) values, where Q_{10} is defined as the factor by which a physiological rate increases for every 10^{o}C rise in temperature (Hochachka & Somero, 2002; Peck, 2018).

Data are presented as kernel density histograms to visualise the distribution of response variable, comparing pre-, peak- and post-MHWs for each treatment, as well as differences between the MHW peaks and differences in the recovery periods following each MHW (post-MHWs). Prior to plotting or statistical testing, to ensure data were normally distributed, oxygen consumption was first square root transformed, righting time was log transformed and a log of the proportions (logit) transformation was used for both energy assimilation efficiency and Conover ratio. The distributions of the functions measured within each treatment were considered normally distributed following transformation and the assumption of homogeneity of variances was tested and satisfied via the Levene's *F* test. Differences in the functional response between the cold- and warm-acclimated treatments were assessed with a linear mixed effects model fit with a restricted maximum likelihood method. Treatment was added as a fixed term and replicate tank ID was added as a random effect. A two-sample t-test was conducted on the model to identify significant differences between treatments. Differences were also assessed between functional responses at temperatures of 2^{o}C in each treatment, i.e., when 0^{o}C acclimated animals were at +2^{o}C in a heat wave and +2^{o}C acclimated animals were outside a heatwave. Differences in the functional response between MHW periods (i.e., pre- post- and peak-MHWs) within each treatment were assessed, as well as differences in the functional response between both the peak and post MHW repeats (MHW1, 2 or 3), both with a linear mixed effects model fit with a restricted maximum likelihood method. MHW period or MHW repeats was added as a fixed term and replicate tank ID was added as a random effect. An ANOVA of the model was conducted to identify significant differences. Where significant differences were identified, post hoc Tukey pair-wise tests were conducted.

4.3 Results

4.3.1 Mortality and spawning

During the experimental period, there were two mortalities (<1% of entire experimental population); one in cold-acclimated conditions (control) and one in warm-acclimated conditions. Mortality was, therefore, very low, consistent between the experimental and control treatments, and not related to warming.

Before the start of the experiment, urchins in cold-acclimated conditions spawned in all three replicate tanks. This occurrence delayed the start of the warming trials by one week

to ensure residual effects from spawning had subsided and water quality in the tanks had returned to normal. Several other isolated spawning events occurred in cold-acclimated conditions on the 08/10/20 (three days into the first MHW) and 20/10/20 (5 days following the first MHW) in one of the three replicate tanks. Spawning individuals on these occasions were isolated to prevent initiating mass spawning of the other animals.

All results from the ANOVA and t-tests comparing differences between treatments and MHW phases are reported in Appendix C, A2 & A3.

4.3.2 Oxygen consumption

After acclimation and before the MHW simulations, the oxygen consumption in cold-acclimated conditions was lower (1.18 ± SE 0.12 O_2 µmolhr^{-1}gAFDM^{-1}) than warm-acclimated conditions (1.76 ± SE 0.13 O_2 µmolhr^{-1}gAFDM^{-1}), however this difference was not significant ($t_{(4)}$ = 2.4, p = 0.074) (Figure 4.1a). Oxygen consumption during the peak of the MHWs was significantly higher in warm-acclimated conditions (2.93 ± SE 0.15 O_2 µmolhr^{-1}gAFDM^{-1}) compared to cold-acclimated conditions (2.30 ± SE 0.14 O_2 µmolhr^{-1}gAFDM^{-1}) ($t_{(57)}$ = 3.6, p < 0.001) (Figure 4.1b), and there was a significant difference in the oxygen consumption between treatments post-MHWs ($t_{(58)}$ = 2.2, p = 0.034), with consumption being higher in warm-acclimated conditions (2.74 ± SE 0.13 O_2 µmolhr^{-1}gAFDM^{-1}) compared to cold-acclimated conditions (2.21 ± SE 0.17 O_2 µmolhr^{-1}gAFDM^{-1}) (Figure 4.1c). Oxygen consumption rates at 2°C in warm-acclimated conditions, pre-MHW (1.76 ± SE 0.13 µmolhr^{-1}gAFDM^{-1}) were lower compared to acute warming of 2°C in cold-acclimated conditions, peak-MHW (2.23 ± SE 0.76 µmolhr^{-1}gAFDM^{-1}), i.e., when animals were both 2°C in both treatments. However, this difference was not significant ($t_{(74)}$ = -0.9, p = 0.355) (Figure 4.1d).

Oxygen consumption in cold-acclimated conditions during peak-MHW (2.30 ± SE 0.14 O_2 µmolhr^{-1}gAFDM^{-1}) conditions was significantly higher than pre-MHWs (1.18 ± SE 0.12 O_2 µmolhr^{-1}gAFDM^{-1}) and post-MHWs (2.21 ± SE 0.17 O_2 µmolhr^{-1}gAFDM^{-1}) ($F_{(2, 65)}$ = 9.70, p < 0.001 and p = 0.008, respectively) (Figure 4.2 a). However, there was no significant difference between pre-MHW conditions and post-MHW ($F_{(2,65)}$ = 9.70, p = 0.156). In warm-acclimated conditions, oxygen consumption during peak-MHW was significantly higher than pre-MHWs and post-MHWs ($F_{(2,63)}$ = 21.6, p < 0.001 for both). As for the cold acclimated treatment, there was no significant difference between pre-MHW conditions and post-MHW conditions ($F_{(2,63)}$ = 21.6, p = 0.163) (Figure 4.2 d). In both cold- and warm-acclimated conditions, there was no significant difference in oxygen consumption of individuals during the peak of the first, second or third MHW ($F_{(2,25)}$ = 0.764, p = 0.477 and $F_{(2,24)}$ = 0.115, p = 0.892, respectively) (Figure 4.2 b, e). This was also the case for post-MHWs assessments, with no significant difference between oxygen consumption in

recovery periods (post-MHWs) after the first, second and third MHW ($F_{(2,25)}$ = 0.356, p = 0.704 and $F_{(2,25)}$ = 0.042, p = 0.959, respectively) (Figure 4.2 c,f).

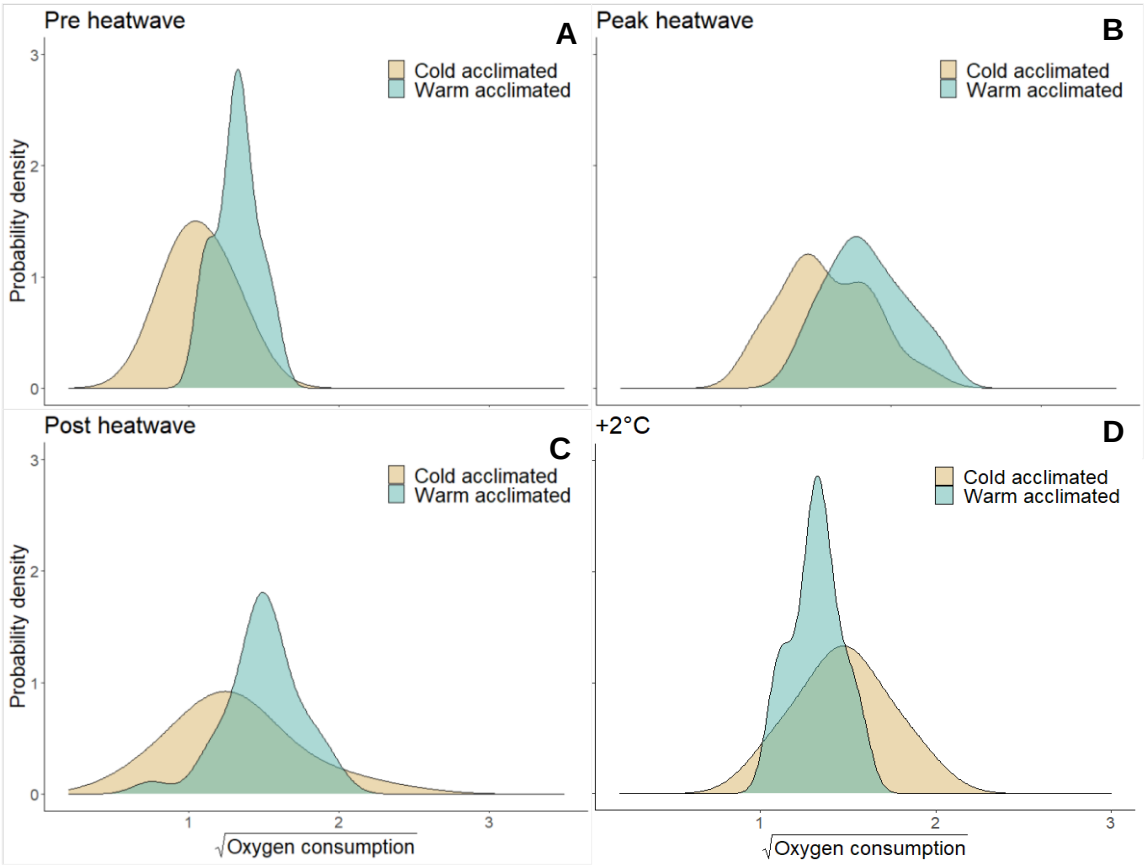

Figure 4.1 Kernel density histograms comparing distribution of square-root transformed oxygen consumption data for cold- and warm-acclimated *Sterechinus neumayeri* in A) pre-heatwaves, B) peak heatwaves C) post heatwaves and D) temperatures of 2ºC pre-MHW in warm-acclimated conditions, and peak-MHW1 in cold-acclimated conditions.

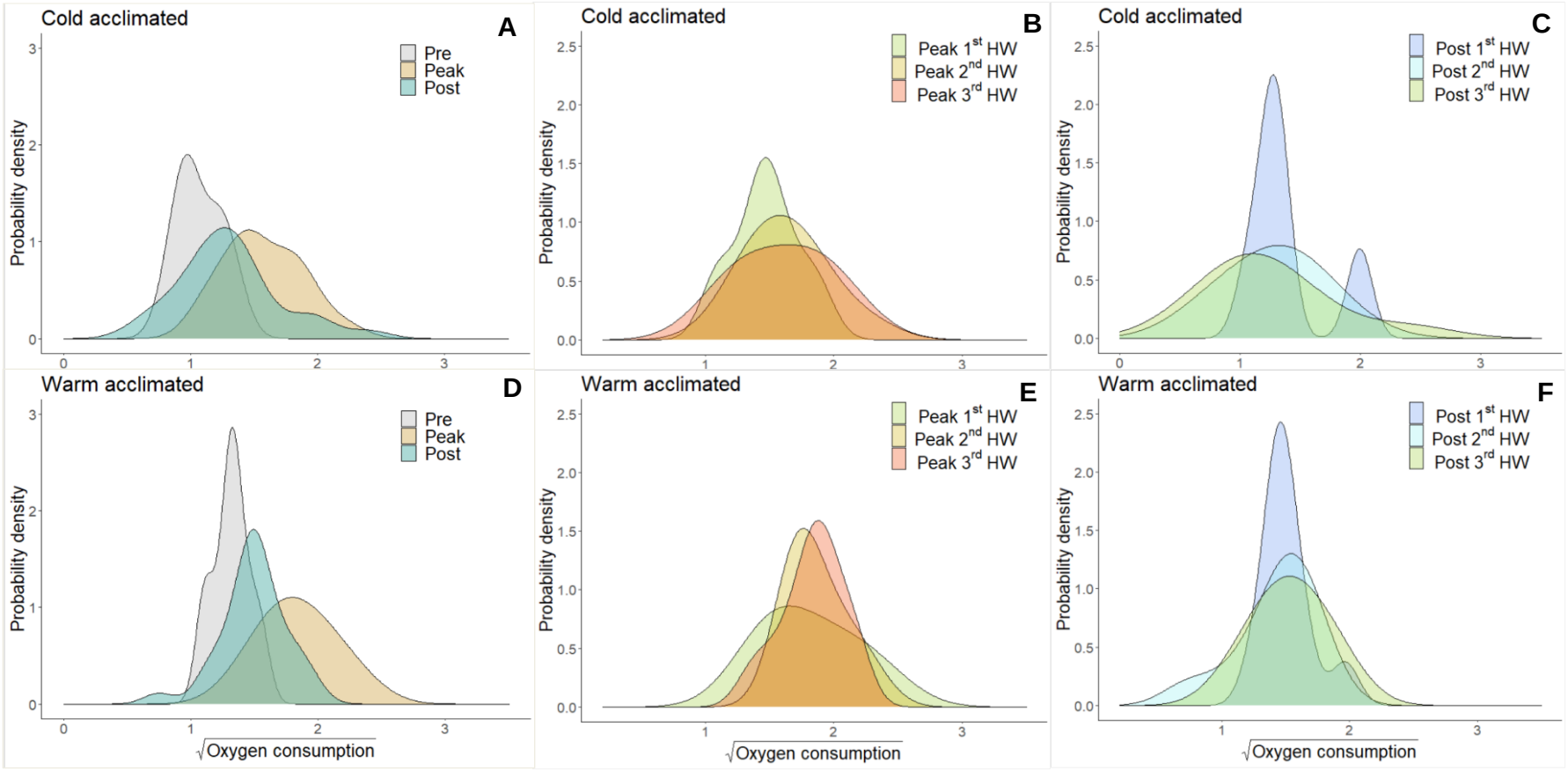

Figure 4.2: Kernel density histograms comparing distribution of square-root transformed oxygen consumption data for *Sterechinus neumayeri* in A) cold-acclimated conditions, peak and post heatwaves, B) cold-acclimated conditions, peak heatwaves C) cold-acclimated, post heatwaves, D) warm-acclimated conditions, peak and post heatwaves, E) warm-acclimated conditions, peak heatwaves F) warm-acclimated, post heatwaves.

Oxygen consumption rates in both cold- and warm-acclimated conditions increased during MHW at the same magnitude, relative to starting baseline consumption (Figure 4.3). Following the first MHW (post-MHW1), oxygen consumption rates in warm-acclimated conditions returned closer to treatment baseline levels compared to cold-acclimated treatments. In the second and third MHW peak, oxygen consumption rates in cold-acclimated conditions were consistently higher relative to treatment baseline values, as was the case during recovery periods (post-MHWs), for all three MHWs, although these differences were not significant.

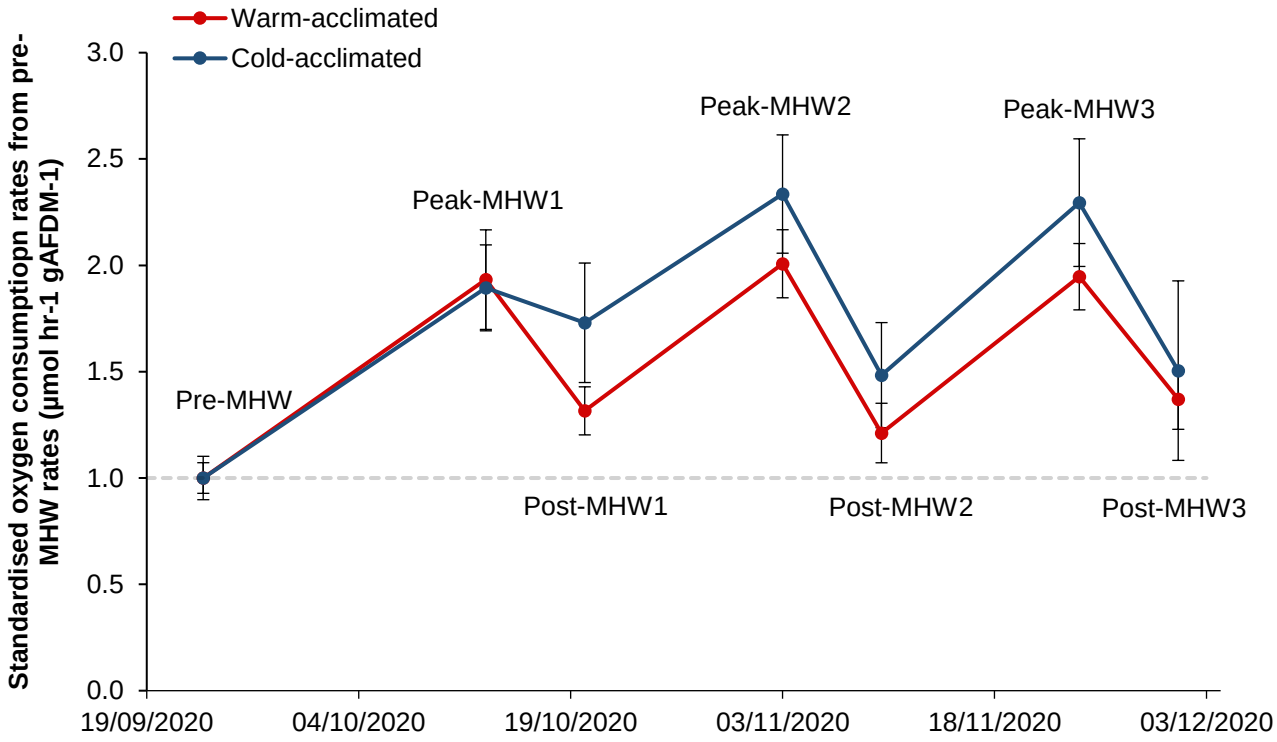

Figure 4.3: Mean oxygen consumption rates (± standard error) in each treatment, standardised to pre-MHW rates, where mean pre-MHW rates = 1 in both cold- and warm-acclimated treatments. Red circles and lines represent warm-acclimated data and blue circles and lines represent cold-acclimated data. The dotted grey line represents the pre-MHW standardised rate of 1. Where data is labelled as 'peak', temperatures were +2^{o}C in cold-acclimated and +4^{o}C in warm-acclimated. Where data is labelled as 'pre' or 'post', temperatures were 0^{o}C in cold-acclimated and +2^{o}C in warm-acclimated. MHW1, MHW2 and MHW3 represents the first, second and third marine heat wave, respectively. Q10 values for changes in oxygen consumption rates during exposure to the first (Peak-MHW1), second (Peak-MHW2) and third (Peak-MHW3) marine heatwave, relative to pre-MHW rates for cold- and warm-acclimated conditions shown above each peak MHW.

The Q_{10} value for the increase in oxygen consumption rates following warm-acclimation to 2ºC was 2.44 ± SE 0.54. For cold-acclimated conditions, the Q_{10} for oxygen consumption rates during the first peak-MHW was 4.47 ± SE 0.54. Similarly, the Q_{10} for oxygen consumption rates in warm-acclimated conditions during the first peak-MHW was 4.66 ± SE 0.80. Although not significantly different, Q_{10} values for oxygen consumption rates were higher when temperatures increased by 2ºC during peak-MHW2 and MHW3, in cold-acclimated conditions, compared to warm-acclimated conditions.

4.3.3 Time taken to right

There was no significant difference in the time taken to right between treatments, either in pre, post or during peak-MHWs (Figure 4.4 a, b, c). The mean time taken to right at 2ºC in warm-acclimated conditions, pre-MHW, was not significantly different to acute warming of 2ºC in cold-acclimated conditions (Figure 4.4 d).

There was no significant difference between treatments in the overall righting time during peak- or post-MHWs. However, after the third MHW, the righting time was significantly longer in cold–acclimated conditions during the recovery period (post-MHW3) ($t_{(17)} = -2.17$, $p = 0.045$). Following the MHW simulations, the righting times returned to pre-MHW conditions, with no significant difference between pre-MHW and post-MHW righting times (Figure 4.5 a,d).

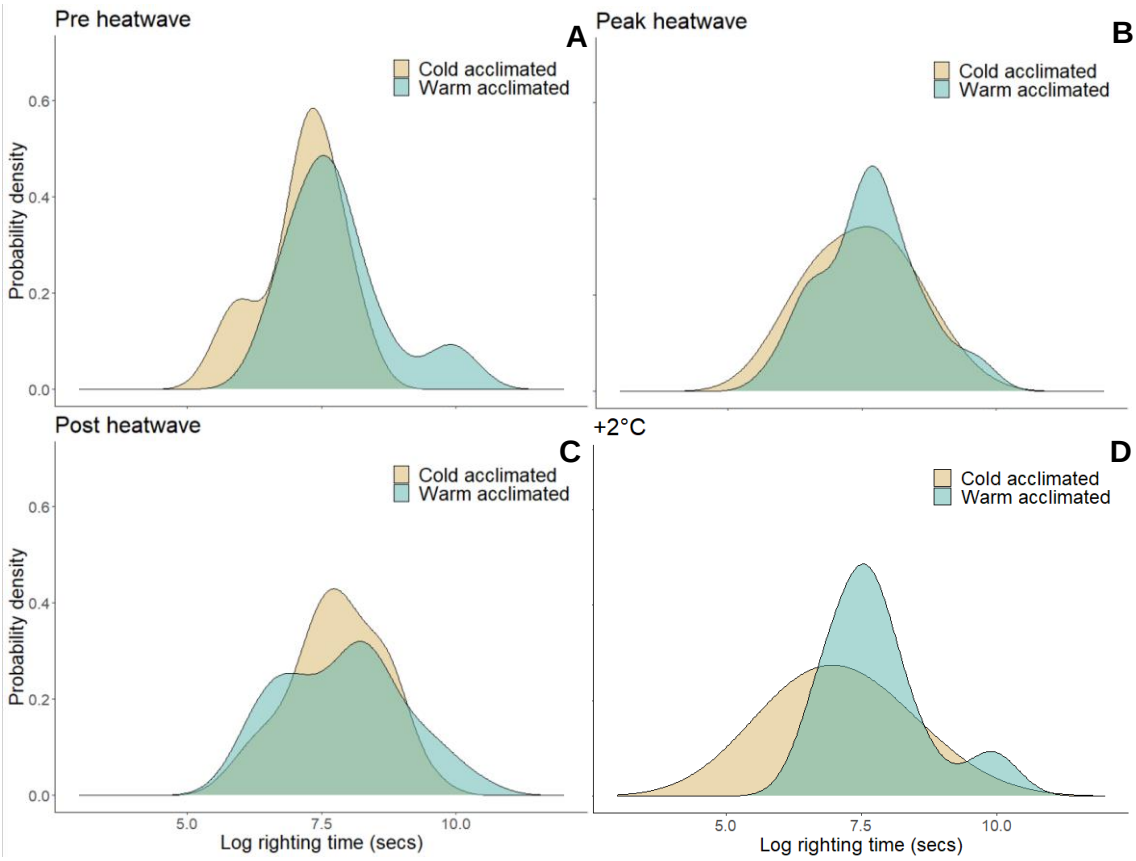

Figure 4.4: Kernel density histograms comparing distribution of log transformed righting time (seconds) data for cold- and warm-acclimated *Sterechinus neumayeri* in A) pre-heatwaves, B) peak heatwaves C) post heatwaves and D) temperatures of 2°C pre-MHW in warm-acclimated conditions, and peak-MHW1 in cold-acclimated conditions.

In cold-acclimated conditions (controls) the time taken to right in the third MHW peak was significantly longer compared to the first MHW peak ($F_{(2,25)} = 4.76$, $p = 0.031$) and the second MHW peak ($F_{(2,25)} = 4.76$, $p = 0.043$) (Figure 4.5 b). Thus there was an increasing trend in time taken to right from the first MHW to the third MHW. In warm-acclimated conditions, average righting times were similar in each MHW peak (Figure 4.5 e). This observation was also made for post-MHWs in both cold- and warm-acclimated conditions, with no significant difference between recovery periods (post-MHWs) after the first, second and third MHW.

There was a non-significant increase in the average time taken to right in cold-acclimated conditions post-MHWs, (MHW1: 2531 ± SE 712 seconds, MHW2: 3015 ± SE 628 seconds, MHW3: 4510 ± SE 1186 seconds) (Figure 4.5 c). Conversely, in warm acclimated conditions, there was a threefold decrease in average righting time between MHW1 and MHW3, although the differences were not significant, they were close ($F_{(2,22)} = 2.807$, $p = 0.082$) (MHW1: 5624 ± SE 1584 seconds, MHW2: 4240 ± SE 1440 seconds, MHW3: 1820 ± SE 423 seconds) (Figure 4.5 f). Mean righting times were slightly longer

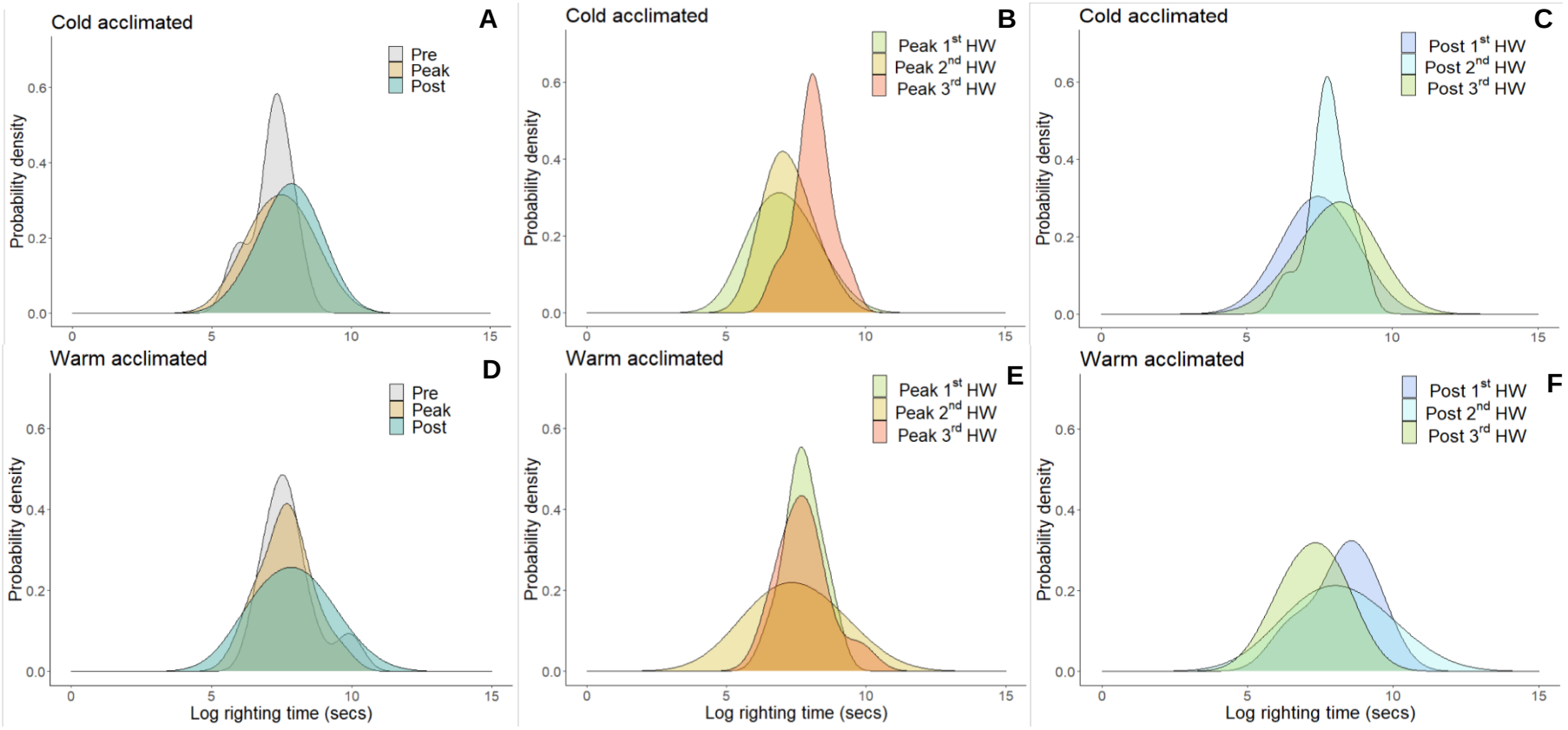

Figure 4.5: Kernel density histograms comparing distribution of log transformed righting time (seconds) data for *Sterechinus neumayeri* in A) cold-acclimated conditions, peak and post heatwaves, B) cold-acclimated conditions, peak heatwaves C) cold-acclimated, post heatwaves, D) warm-acclimated conditions, peak and post heatwaves, E) warm-acclimated conditions, peak heatwaves F) warm-acclimated, post heatwaves.

post-MHW compared to peak-MHWs, in cold- and warm-acclimated conditions, however these differences were also not significant

4.3.4 Energy demand

4.3.4.1 Energy consumption

There was a cumulative increase in energy consumption (kJ urchin^{-1} week^{-1}) in cold-acclimated conditions, following each MHW event (Figure 4.6 a). A segmented regression of these data identified a breakpoint during the peak of the third MHW, where the gradient of the slope flattened, however this change in gradient was not significant ($p = 0.153$) (Appendix C, Figure A4, Table A4).

Energy consumption (kJ urchin^{-1} week^{-1}) rose close to the maximum levels available to the urchins (defined by weekly food portions given) following the second MHW in warm-acclimated conditions and the third MHW in cold-acclimated conditions, after which this level of consumption was sustained for the duration of the experiment (Figure 4.6 b). In warm-acclimated conditions, energy consumption was significantly higher in the second and third MHWs than in the first MHW, both during the peak (peak-MHW) ($F_{(2,41)} = 8.08$, $p = 0.003$ and $p = 0.002$, respectively), and recovery periods (post-MHW) ($F_{(2,86)} = 10.2$, $p < 0.001$ for both differences). In cold-acclimated conditions, energy consumption was significantly higher in the final third MHW than in the first MHW during the peak ($F_{(2,41)} = 7.67$, $p = 0.001$), and energy consumption was significantly higher in the final third MHW, than in the first two MHW during the recovery periods ($F_{(2,86)} = 9.75$, $p < 0.001$ and $p = 0.050$, respectively).

A segmented regression of these data identified a breakpoint during the peak of the second MHW in warm-acclimated conditions, and the peak of the third MHW in cold-acclimated conditions, where the gradient of the slope flattened. This change in gradient was significant in warm-acclimated conditions ($p = 0.027$) (Appendix C, Figure A4, Table A4). There was no significant difference in average energy consumption between cold- and warm-acclimated treatments pre-, peak- or post-MHWs ($t_{(28)} = -0.035$, $p = 0.972$; $t_{(88)} = -0.52$, $p = 0.601$; $t_{(118)} = -0.26$, $p = 0.794$).

4.3.4.2 Energy assimilation

In cold-acclimated conditions, energy assimilation increased following each MHW event, peaking during the recovery phase and decreasing until the subsequent MHW (Figure 4.6 c). In warm-acclimated conditions, energy assimilation increased during each MHW and subsequently rose to a peak in the recovery phase before declining again (Figure 4.6 d). At the end of the acclimation period, pre-MHWs, the mean energy assimilation efficiency

(%) in cold-acclimated conditions (1.66 kJ ± SE 0.04 kJ, 93.9% ± SE 1.75%) was significantly higher than in warm-acclimated conditions (1.53 ± kJ SE 0.12 kJ, 86.5% ± SE 2.31%) ($t_{(28)}$ = -2.98, p = 0.006).

There was no significant difference between treatments in the energy assimilation efficiency during peak-MHWs. However, the difference was significant post-MHWs ($t_{(79)}$ = -3.89, p < 0.001), and energy assimilation efficiency was higher in cold-acclimated (0.42 kJ ± SE 0.01 kJ, 84.9% ± SE 1.48%) compared to warm-acclimated conditions (0.39 kJ ± SE 0.01 kJ, 76.7% ± SE 1.63%).

Assessing differences between MHWs in isolation indicated that post-MHW1 and post-MHW2, the mean energy assimilation efficiency (%) in cold-acclimated conditions was significantly higher than in warm-acclimated conditions ($t_{(4)}$ = -2.83, p = 0.047 and $t_{(28)}$ = -2.39, p = 0.024, respectively), however there was no significant difference post-MHW3. The mean energy assimilation efficiency (%) at 2^{o}C in warm-acclimated conditions, pre-MHW was significantly higher (1.53 kJ ± SE 0.12 kJ, 86.5% ± SE 2.31%) compared to acute warming of 2^{o}C in cold-acclimated conditions, peak-MHWs (0.75 kJ ± SE 0.06 kJ, 71.6% ± SE 2.48%) ($t_{(6)}$ = 2.52, p = 0.045).

4.3.4.3 Conover ratio

In cold-acclimated conditions, the Conover ratio increased rapidly following the first MHW event, and then increased at a steadier rate following the second MHW (Figure 4.6 e). A segmented regression of these data identified a breakpoint during the recovery phase after the first MHW (post MHW1), where the gradient of the slope reduced, this change in gradient was significant (p < 0.001) (Appendix C, Figure A4, Table A4). In comparison, in warm-acclimated conditions, the Conover ratio increased rapidly following the first MHW and then stabilised for the duration of the experiment at the onset of the second MHW (Figure 4.6 f).

There was a significant difference between treatments in the Conover ratio during peak-MHWs ($t_{(85)}$ = 2.46, p = 0.016), with warm-acclimated conditions having a higher Conover ratio (76.5 ± SE 1.38) than cold-acclimated conditions (71.2 ± SE 1.74). Assessing differences between MHWs in isolation showed that peak-MHW1 and peak-MHW2, mean energy assimilation efficiency (%) in warm-acclimated conditions was significantly higher than in cold-acclimated ($t_{(24.1)}$ = -3.0, p = 0.006, $t_{(23.8)}$ = -4.1, p < 0.001, respectively), however there was no significant difference during the peak-MHW3.

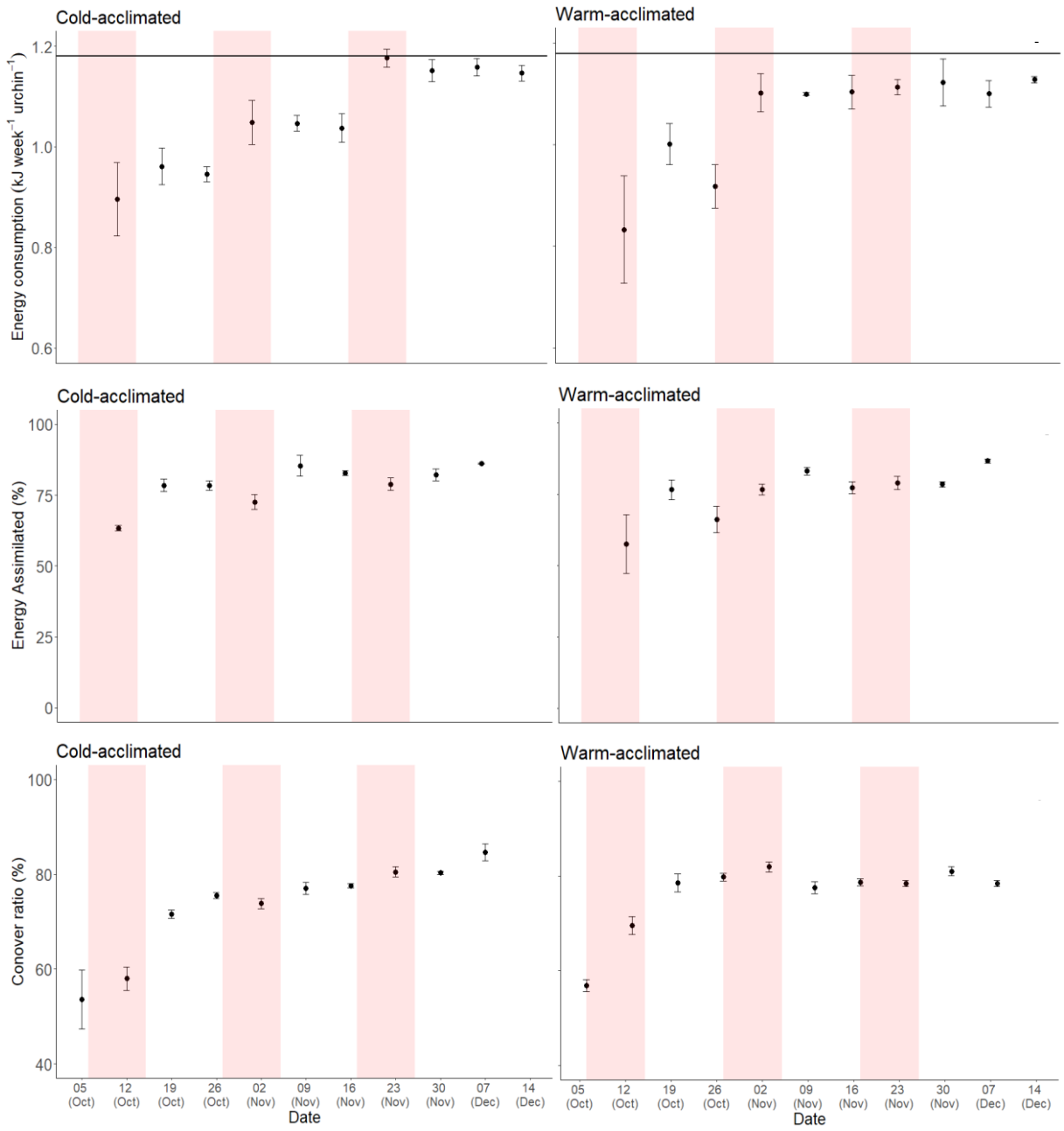

Figure 4.6: Time-series scatter plots of a) energy consumption in cold-acclimated conditions and b) warm-acclimated conditions, with the black, horizontal line representing mean energy content of AFDM of food fed, c) Energy assimilated (%) in cold-acclimated conditions and d) warm-acclimated conditions, e) Conover ratio (%) in cold-acclimated conditions and f) warm-acclimated conditions. Data are mean values, pooled within tanks and averaged across replicate tanks ± standard error. Pink shading represents peak-MHW periods.

4.4 Discussion

The response of species and communities to increases in the frequency, magnitude and duration of MHW events is poorly characterised, with no published experimental studies

on the effects of repeated MHWs across a single generation of polar species, and only three on temperate and tropical species (Pansch et al. 2018; Saha et al. 2020; Smale et al. 2015). Where data do exist they are variable and it is therefore expected that there will be 'winners' and 'losers' in the context of climate change (Somero, 2010). This study aimed to determine if acclimation to future temperatures (+2^{o}C) affects the physiological response of a polar ectotherm, the Antarctic urchin *Sterechinus neumayeri*, to warming experienced during MHW events. To this end, the study compared the functional response of cold and warm acclimated animals to multiple MHW simulations.

Studies on the ability of *S. neumayeri* to acclimate to warming have indicated that acclimation occurs when there is a sustained reduction in oxygen consumption rate following the initial temperature rise in the first month of exposure (Morley, Suckling, et al. 2016). My study indicates that *S. neumayeri* was able to acclimate after 8 months exposure to warming of +2.0^{o}C, whereby oxygen consumption rates at 2^{o}C in warm-acclimated conditions, pre-MHW, were lower (1.76 ± SE 0.13 µmolhr-1gAFDM-1) than those in acute warming of 2^{o}C in cold-acclimated conditions, peak-MHW1 (2.23 ± SE 0.76 µmolhr^{-1}gAFDM^{-1}). These results demonstrated a sustained reduction in oxygen consumption rates following warm-acclimation with animals exhibiting partial compensatory increases (*sensu* Precht et al. 1955) in oxygen consumption rates and Q_{10} values typical for those expected for this species (Brockington & Clarke, 2001; Peck, 2002).

Increases in oxygen consumption rates relative to pre-MHW rates showed that acclimation to 2^{o}C enables this species to recover rapidly following acute warming as well as reduce the Q_{10} in subsequent exposure to repeat MHWs compared to cold-acclimated conditions. There was also evidence of a positive effect of repeat MHWs on righting times in warm-acclimated conditions, compared to a negative effect on righting times following repeated warming during peak-MHWs for cold-acclimated urchins.

This study shows that acclimation of *S. neumayeri* to +2^{o}C is achieved after 8 months, but at a cost of higher compensatory oxygen consumption rates, lower energy assimilation rates, and longer righting times compared to cold-acclimated animals. Although these differences between cold- and warm-acclimated treatments were not always significant, the distribution of oxygen consumption rates and righting responses in warm-acclimated animals were higher overall compared to cold-acclimated conditions. The higher oxygen consumption and lower assimilation rates might suggest that in the long-term *S. neumayeri* may have less energy available for other requirements such as growth and reproduction, which would then have knock on effects on life histories and persistence in marginal feeding conditions (Cheng et al. 2018; Fitzgibbon et al. 2017; Kooijman et al. 2008; Salin et al. 2016).

Although oxygen consumption rates were higher and righting times were longer in warm-acclimated conditions, the observed shift in oxygen consumption was within the range of previous reports for this species. For example, previous studies on *S. neumayeri* show that oxygen consumption rates can reach 21.5 ± SE 5.0 O_2 µmolhr^{-1} gAFDM^{-1} when stressed to temperatures +10^{o}C above ambient, just before CT_{max} was reached (Chapter 3, De Leij et al. 2022) as well as maximum field rates of 5.9 O_2 µmolhr^{-1}gAFDM^{-1} during the austral summer being reported (Souster et al. 2018). Functions such as feeding activity, reproduction and growth that occur during summer have been shown to account for 80 – 85% of the increased metabolism, whereas seasonal temperature effects account for just 15 – 20% (Brockington & Clarke, 2001). These data would therefore suggest *S. neumayeri* may already have sufficient aerobic scope to cope in terms of energy provision under future warming conditions.

This study was conducted in the austral spring (Oct – Dec), although I exposed the cold-acclimated *S. neumayeri* to typical average summer temperatures for the collection site, Rothera Point for 8 months prior to applying MHWs. Regardless of temperature, oxygen consumption rates are lower in spring compared to summer since metabolic activity is largely governed by endogenous seasonal rhythms and physiological activity (Brockington, 2001; Brockington & Clarke, 2001; M. Brown et al. 2013). In summer, oxygen consumption rates for wild *S. neumayeri* are 39% higher than winter (Souster et al. 2018) and average metabolic rates for *S. neumayeri* of 4.66 ± SE 0.15 O_2 µmolhr^{-1}gAFDM^{-1} have been recorded in Jan – Feb, during constant feeding for animals with test diameters of ~35mm, similar to this study (Chapter 3, De Leij et al. 2022). If the difference in metabolic rates between spring and summer are allowed for, the increase in oxygen consumption in summer due to a MHW could result in maximum oxygen consumption rates of 7.45 ± SE 0.24 O_2 µmolhr^{-1}gAFDM^{-1}in the current climate, and 8.21 ± SE 0.26 O_2 µmolhr^{-1}gAFDM^{-1} in a future climate (according to average % increase derived across all MHWs, Appendix C, Table A5). These high rates would likely be caused by increased maintenance costs (Jager et al. 2016; Ndhlovu & Mcquaid, 2021), and although they are within the range of values previously reported for, and survived by *S. neumayeri,* there would be significant energetic trade-offs and potential effects on physiological functions, growth and reproduction (Cheng et al. 2018; Kooijman et al. 2008; Peck, 2005). If these maintenance costs were sustained throughout summer, it is likely that this would compromise long-term survival.

Evidence suggests that Antarctica will continue to experience cold winter temperatures of close to -2^{o}C, but with shorter periods of minimum temperatures, and there will be higher summer temperatures for longer periods (Peck, 2018). Therefore, Antarctic species will either need to adapt and broaden their thermal range, or else be in a lower overall annual energetic state.

Despite data from this study showing increased oxygen consumption rates during MHW events, there was no evidence of a cumulative effect following repeat MHWs. Oxygen consumption rates resumed to levels slightly above pre-MHW baseline conditions during recovery periods (post-MHWs) in cold- and warm-acclimated animals, however this increase was not significant for either treatment.

Energy consumption rates increased following each MHW, with levels not returning to treatment baseline rates during the recovery periods in either treatment. Recovery periods in this study (10 days) seemed to allow *S. neumayeri* to reset to normal functioning levels, but this appeared to be accompanied by an increase in energy consumption. These data suggest that although repeat events do not have a significant cumulative effect on oxygen consumption and hence maintenance costs, sustaining maintenance required increased energy acquisition with each MHW exposure, or there was a cost associated with MHWs that took longer than 10 days to repay, e.g. from the build-up of protein carbonyls (Abele et al. 2001; M. S. Clark et al. 2013). Previous studies have reported variable responses to repeat MHWs amongst species. For example, a study found negative accumulative effects in both biomass and abundance in the tellinid bivalve, *Limecola (Macoma) balthica* (Pansch et al. 2018) and in the growth of the seagrass, *Zostera marina* (Saha et al. 2020). Whereas the spionid polycheate, *Polydora cornuta*, exhibited buffering following a single MHW, where a significant reduction in abundance was observed after a single MHW, but higher abundance following three MHWs (Pansch et al. 2018). There was little to no effect following warming reported for some other species (Pansch et al. 2018; Saha et al. 2020; Smale et al. 2015).

Following acclimation in this study, warm-acclimated individuals had significantly lower energy assimilation rates compared to cold-acclimated conditions. This difference between treatments was also significant during the recovery periods following MHW1 and MHW2. This effect was also observed for *S. neumayeri* in another study, where after 40 months acclimation animals consumed less food, absorbed less energy, but exhibited elevated metabolism (Morley, Suckling, et al. 2016). A possible explanation for this may be a reduction in absorption capacity across the gut wall, or else attributed to gut evacuation rate (GER), essentially the speed at which food travels through the gut (Boyce et al. 2000). Evidence of reduced food assimilation capacity has also been shown in the temperate brown trout, *Salmo trutta,* following acclimation to warmer conditions (+9^{o}C) (Salin et al. 2016) as well as the Antarctic fish *Trematomus bernacchii*, following 9 weeks acclimation to 2^{o}C and 4^{o}C (Sandersfeld et al. 2015). Therefore, it might be that the higher oxygen consumption rates experienced in warm-acclimated conditions could be related to the increase in GER, ultimately reducing the energy assimilation capacity.

Consumption of food in this study increased cumulatively following MHW simulations in both acclimation conditions. The segmented regressions modelling energy consumption support this observation and show that there was a rapid increase and sustained requirement for more energy following the second MHW peak in warm-acclimated conditions, and following the third MHW in cold-acclimated conditions. The data also show that elevated energy consumption was sustained for at least 21 days following the third MHW peak in both treatments. Energy consumption was not measured beyond 21 days and therefore the duration that this would be sustained for is unknown. However, these results show that acute warming from the MHWs, but not chronic warming from the acclimation, causes prolonged and significant increases in food consumption requirements.

Despite no difference in the oxygen consumption among MHW events between treatments, both during peak-MHWs and post-MHWs, there was a significant increase in the time taken to right in cold-acclimated conditions, during the peak of the third MHW. During recovery periods, post-MHW, righting times were also progressively longer in both cold and warm-acclimated conditions. During peak-MHW, righting times were quicker compared to post-MHWs in cold-acclimated conditions until MHW3, and for all three MHWs in warm acclimated conditions. Increase in righting times in echinoderms has been recorded previously at raised temperatures (Ardor Bellucci & Smith, 2019), and is attributed to both raised metabolic rate and muscular contraction times. However, this effect is only apparent over a central range, beyond this, locomotor and muscular functions have been shown to decline (Ardor Bellucci & Smith, 2019; Brothers & McClintock, 2015; Morley, Martin, Day, et al. 2012). It is likely that acute warming may also increase rates of other physiological processes such as muscle contraction or water pumping in the urchin (Peck et al. 2008; Young et al. 2006a). However, since respiratory rates do not increase to match this and cellular energy processes, in particular protein synthesis, are not known to upregulate in response to warming (Fraser et al. 2007; Peck, 2016), energetic costs associated with acutely warmer temperatures may take longer to pay off.

The cumulative decrease in righting times during the recovery periods in warm-acclimated conditions might suggest that these animals, despite the rise in metabolic rate during MHW3, begin to experience positive effects from repeated acutely raised temperatures. These results evidence heat hardening (*sensu* Bilyk et al. 2012) in warm-acclimated animals, whereby a history of chronic warming stress improves the ability of an organism to adapt to acute warming stress (Bilyk et al. 2012a; Cheng et al. 2018; Giomi et al. 2016; Seebacher et al. 2015). For cold-acclimated animals, the results of the experiment show a cumulative negative effect of the MHWs on righting times, and suggest a reduced ability to recover following repeat acute warming stress. A similar response has been shown in

other species such as the temperate bivalve, *Limecola balthica*, where biomass and abundance was significantly reduced following exposure to multiple heatwaves comparative to a single heatwave (Pansch et al. 2018).

The data in this study suggest that warm-acclimated individuals were still functioning largely similarly to cold-acclimated individuals during repeat MHW events, despite being exposed to temperatures elevated by +2°C. This finding suggests that although baseline metabolic energy demands increased, the capacity to cope with stress was comparable if not improved after warm-acclimation, and that *S. neumayeri* likely has a strong capacity to cope, but not necessarily thrive, with predicted future warming to the end of the century on the Antarctic Peninsula.

4.5 Conclusions

- Q_{10} values for pre-MHW oxygen consumption rates after acclimation to +2°C suggest that animals have acclimated and are exhibiting partial metabolic compensation (*sensu* Precht et al. 1955).
- Oxygen consumption was higher in warm-acclimated conditions in pre-, peak-and post-MHW, however, relative to baseline rates for each treatment, oxygen consumption increased less in peak-MHWs and returned closer to baseline rates in warm-acclimated conditions, compared to cold-acclimated animals, suggesting an improved ability to cope with acute stress following warm-acclimation.
- Despite evidence of acclimation, energy assimilation was significantly lower in warm-acclimated conditions pre-MHWs, and although not significant, righting times were also longer. These results suggest that *S. neumayeri* could be functioning at a reduced capacity following acclimation. However, this reduced capacity in warm-acclimated conditions did not significantly increase righting times during MHWs compared to cold-acclimated conditions. Instead, there was a cumulative decrease in righting times in warm-acclimated conditions, and a cumulative increase in righting times in cold-acclimated conditions, providing further evidence that *S. neumayeri*'s ability to tolerate stress may be improved by warm-acclimation.
- Overall, despite *S. nuemayeri* experiencing reduced functional performance following long-term acclimation, it is likely that this species will be able to cope with both the gradual and acute warming predicted for the end of the century on the Antarctic Peninsula.

Chapter 5 General discussion and conclusions

The chapters in this thesis provide insight into how environmental change and associated extreme climate events affect marine animal functioning both in our present climate, and in an environmental-future scenario. I demonstrate for the first time that the large-scale climate metrics SOI and SAM are key environmental variables that account for the interannual variability observed in the reproductive investment of *Sterechinus neumayeri* (Chapter 2, De Leij et al. 2021). I also show that single environmental variables, in particular food (as chlorophyll), are important for seasonal investment and likely contribute to driving the mechanisms associated with annual spawning patterns (Chapter 2, Bosch et al. 1987, De Leij et al. 2021). However, I provide evidence that energetic investment into reproduction varies over several years in my study species, *S. neumayeri,* a process which is likely driven by an endogenous rhythm (Chapter 2, Brockington et al. 2007, De Leij et al. 2021). These results provide evidence that when environmental conditions remain within natural variability and are consistent with seasonal cycles, changes of a single environmental variable within this range may not affect long-term energetic investment or functional performance. However, as our global climate changes over the coming decades, we will see mean temperatures increase and because of this, the natural variability range of regional temperatures will shift (Peck 2005, IPCC 2019). With this shift, my data suggest there will be consequences for oxygen consumption and energy assimilation (Chapter 4), with subsequent effects on the functional response to extreme temperatures, specifically marine heatwaves (MHWs). I demonstrate that the functional response to extreme temperatures is dependent on a matrix of factors such as warming onset rate (Chapter 3, De Leij et al. 2022) and thermal history (Chapter 4).

Studying reproductive periodicities across multiple years has been the focus of several studies on Antarctic invertebrates (Grange et al. 2004, 2007, 2011, Brockington et al. 2007, Lau et al. 2018). In these studies, reproductive processes have been suggested to be driven in part by food supply, where variability, or lack thereof, in reproductive investment has been linked to sedimentation events (Grange et al. 2004), seasonal primary production (Lau et al. 2018) and feeding behaviour (Grange et al. 2007, 2011). This is also supported by the data presented in Chapter 2, where the GAM model suggests seasonal variability in chlorophyll was related to a reduction in gonad index, indicative of spawning events, for *S. neumayeri*. However, where multiyear variability in reproductive investment was observed, previous research has failed to confidently identify an environmental link with reproductive processes. Instead, two studies tentatively suggested that annual spawning was overlaid by a longer multiyear cycle driven by an innate, endogenous rhythm (Brockington et al. 2007, Lau et al. 2018).

The data presented in Chapter 2 are the first to provide evidence for *S. neumayeri* to support the hypothesis that multiyear variability of reproduction is driven innately as I identified a potential cyclic trend across a 5-year period. This chapter builds on previous research on *S. neumayeri* from Brockington et al. (2007), where common to both studies are the trends observed in annual patterns in gonad index and gamete maturity for both males and females. However, my research has specifically added to the weight of evidence for a longer reproductive cycle of several years, and enhanced understanding of the complex links between the environment and biological functioning. Overall, Chapter 2 suggests that energetic investment into reproduction for *S. neumayeri* has only minor association with interannual variation in environmental variables. This finding is surprising considering the seasonal influences of the environment on triggering spawning (for example food, lunar cycles, tides, photoperiod, temperature etc. (Emilio et al. 2018; Galley et al. 2008; Kelly, 2001; Muthiga, 2006; Smart et al. 2012; St.Gelais et al. 2016; Zhadan et al. 2018)). My research therefore emphasises the importance of endogenous rhythms in regulating gametogenic cycles for this species. In addition to this, my research in Chapter 2 is the first to demonstrate SOI influences this far south on Antarctic benthic species. This result demonstrates that the effect of environmental change on functional processes is likely multifactorial and teasing out single variable effects overlooks the interactive or synergistic nature of the effects of environmental variables.

Sterechinus neumayeri was used as the study species for the data chapters in this thesis. Antarctic benthic species have been reported to be inherently sensitive to thermal change due to their cold and thermally stable environment (Peck, 2005; Peck et al. 2004, 2010, 2014). However, *S. neumayeri* has recorded CT_{max} in excess of 5.7^{o}C higher than the maximum temperatures recorded at the sample site (Ryder Bay, Antarctic Peninsula) (Peck et al. 2009, 2010, 2014). Although populations at these locations typically only experience temperatures ± 2^{o}C, *S. neumayeri*'s geographical distribution ranges up to a latitude of 52°S (David et al. 2005; Pierrat et al. 2012). It is therefore likely that *S. neumayeri* has a higher thermal tolerance than would be expected for species found exclusively around the Antarctic Peninsula or further south (Calosi et al. 2010; Louthan et al. 2021; J. M. Sunday et al. 2011, 2012). When considering a species' thermal tolerance capability, geographical range may provide insight into whether a population has inherent mechanisms to cope with temperatures outside those experienced in its locality. For example, the Antarctic bivalve mollusc *Laternula elliptica*, and limpet *Nacella concinna* also have northern ranges extending up to the sub-Antarctic islands (Fuenzalida et al. 2014; Morley et al. 2009; Taylor et al. 2018). Interestingly, these species and *S. neumayeri* are the only three known Antarctic marine invertebrates that can produce heat shock proteins (HSP) that ultimately improves resilience to thermal stress (Clark & Peck 2009, González et al. 2016). Other marine organisms have lost the capacity to generate a

heat shock response, likely due to evolution at stable sub-zero temperatures (Hofmann et al. 2000). For example, the scallop *Adamussium colbecki,* and the crustacean *Paraceradocus gibber* both lack the ability to increase HSP production and are both constrained to higher latitudes (>60^{o}S) (Clark et al. 2008; David et al. 2005; De Broyer et al. 2007; Schiaparelli & Linse, 2006).

The concept that environmental variability leads to increased thermal tolerance range was originally proposed through the 'Climate variability hypothesis' (Stevens, 1989). This hypothesis largely focuses on terrestrial systems, however there is evidence that this concept also applies to marine systems (Sunday et al. 2011), where large climate variability is associated with higher thermal tolerance breadth. This finding demonstrates the role of thermal history in shaping an organism's response to temperature change and provides insight into the drivers of thermal sensitivity in organisms.

Chapter 3 adds to the growing consensus on the importance of warming characteristics on thermal limits (Peck et al. 2009; Terblanche et al. 2007). In addition to this, the data are the first to suggest that slower warming rates provide opportunity for *S. neumayeri* to temporarily adjust its physiology to acute extreme temperatures. I provide evidence in Chapter 3, that a slower warming rate increases the functional thermal limits, contrary to the relationship often observed with CT_{max} (Kingsolver & Umbanhowar, 2018; Morley, Bates, et al. 2016; Peck et al. 2009). Functional thermal sensitivity of Antarctic benthic species has been recorded for *L. elliptica*, *A. colbecki,* and *N. concinna*, whereby temperatures approaching 3^{o}C were detrimental to locomotor activities (Peck et al. 2004). These thresholds were determined from raising temperatures by 1^{o}C day^{-1}. Similarly, rates of 1^{o}C day^{-1} or higher up to 1^{o}C hr^{-1} have been used to determine CT_{max} and functional thresholds for several marine invertebrate ectotherms (Morley, Martin, Bates, et al. 2012; Morley, Bates, et al. 2016). We know from my data that this rate evoked rapid functional degradation. However, functional degradation was not observed after short-term acclimation when rates were slower (i.e., 0.3^{o}C day^{-1}) (Chapter 3, De Leij et al. 2022) or when warming was over several months in terms of long-term acclimation (Chapter 4). One study that considers warming rate measured CT_{max} at rates as slow as 1^{o}C month^{-1} for several Antarctic benthic invertebrates (Peck et al. 2009). However, most studies propose thresholds that overlook the importance of warming characteristics and draw conclusions on thermal sensitivity from unrealistic warming scenarios. My results also show there is a need to assess whole animal functioning when determining thermal limits. Previously, studies on temperature impacts on Antarctic marine ectotherms usually focus on one or two biological functions (i.e. locomotion (Janecki et al. 2010b; Kidawa et al. 2010; Peck et al. 2004), critical thermal maxima (Bilyk & DeVries, 2011; Morley et al. 2019; Peck et al. 2014), or respiratory functions (Joyce et al. 2018; Peck et al. 2002)) and draw conclusions from this for a species thermal thresholds. My results show that different

functions do not necessarily degrade at the same temperatures since the mechanisms behind them are very different (Chapter 3, De Leij et al. 2022) or else energy might be diverted to functions immediately critical for life. For example, locomotory functions such as time taken to right, started to degrade from 9^{o}C, whereas the function of feeding stopped from 4^{o}C (Chapter 3, De Leij et al. 2022). In these cases, I suggest that righting could be immediately critical for the protection from predation, whereas an organism's energy reserves allow for short periods of negative energy balance and therefore the function of feeding would not be immediately critical.

The data in chapters 2-4 in this thesis suggest that *S. neumayeri* can function well within a temperature range, even if temperature is variable within that range and we see evidence for this in the reproductive cycle of *S. neumayeri* (Chapter 2, De Leij et al. 2021) as well as in Chapter 3, where temperature change within a certain range causes little measurable difference in functioning capacity. Where we exceed the boundaries of this tolerance range, we observe degradation of functions (Pörtner et al. 2017). In Chapter 3, I use segmented regressions to highlight this non-linear relationship with temperature change. These segmented regressions identified 'tipping points' where the organism has a certain capacity to buffer the energetic demand associated with warming temperatures until it reaches a threshold (D'Amario et al. 2019; Jager et al. 2016; Morley, Martin, Bates, et al. 2012). Where tipping points have not been identified, warming rates havebeen rapid (>1^{o}C day^{-1}) (Azra et al. 2018; Morley et al. 2016; Peck et al. 2004) and similar to the results in Chapter 3, there is a linear relationship with temperature and functioning. Where warming rate is slower, we capture a window of buffering capacity for acute temperature change. In these cases, we see that even in the most thermally constrained species, such as those from the Antarctic, there is a potential for plasticity and acclimation to warmer temperature conditions (Bilyk et al. 2012b; Clusella-Trullas et al. 2013; Morley et al. 2016).

To determine how close an organism is to its functional tipping point, or else how much buffering capacity an organism has, we can look at its energetic status. Increasing oxygen consumption and energy derived directly from food or reserves (i.e., lipid stores in the gonad), can serve to buffer increased energetic demands associated with elevated temperatures (Epherra et al. 2015; Walker et al. 2013). In Chapter 3, oxygen consumption increased linearly as temperature increased and in Chapter 4, oxygen consumption increased and decreased in line with MHW simulations. In addition to this, food consumption was elevated following short-term exposure to acute warming (Chapter 4). Clearly, warming of a certain level increases the energetic cost of living, and to maintain 'normal' functional performance, energy supply must rise to meet demands (Cheng et al. 2018; Salin et al. 2016). However energetic supply cannot alleviate stress indefinitely, and there will still be a threshold which is approached as the supply of energy fails to meet demands (Pörtner et al. 2017).

As I discuss, an organism's response to warming is dependent on the characteristics of the warming event. In particular, I address onset rate in Chapter 3 as being a key feature that may determine functional degradation thresholds. Chapter 3 provides insight into the mechanisms behind vulnerability to temperature change. However, in the context of climate change, we are unlikely to see extreme events, such as MHWs, occur in isolation from the gradual warming predicted for the coming decades (Allen et al. 2018; Oliver et al. 2019). It was therefore important to explore the role of long-term acclimation in influencing *S. neumayeri*'s capacity to tolerate acute warming. Chapter 4 provided evidence to support previous reports on *S. neumayeri*'s acclimation capacity. In terms of oxygen consumption, *S. neumayeri* experienced a sustained reduction in consumption rate following 8 months acclimation and this supports previous reports on this species acclimation capacity (Suckling et al. 2015). Long-term acclimation studies on *S.neumayeri* report little or no effects of acclimation (Morley et al. 2016; Suckling et al. 2015). However, contrary to this, my results demonstrate acclimation to 2^{o}C increases mean time taken to right, oxygen consumption, and significantly reduces energy assimilation, compared to animals held at 0^{o}C, with additional effects on gamete maturation (Appendix D). Reporting on the effect of long-term warming on this array of functions is rare and I know of no other studies which have assessed and compared thermal vulnerability of this number of different physiological pathways. My study is therefore unusual, if not unique, in providing a more complete picture of how whole animal functioning might change with gradual warming.

Previous studies have acclimated *S. neumayeri* to 2^{o}C for up to 24 months and reported that oxygen consumption and somatic growth were not significantly different between warm-acclimated and control urchins (Suckling et al. 2015). However, one effect that was observed was an increase in egg size in spawned individuals, and in addition to this, other studies have documented changes in both fecundity and egg sizes following exposure to ocean stressors (Foo & Byrne, 2017). My data show a higher proportion of smaller oocytes present in females following warm acclimation (Appendix D), however, the spread of oocyte sizes present in the gonads was similar to cold-acclimated females, suggesting that maximum oocyte size had not changed. Instead, it is possible that the rate of gamete maturation or spawning time has changed following warm acclimation, rather than the ultimate size of mature oocytes. It must be acknowledged here that some, but not all, of the urchins in the cold-acclimated treatments spawned and this would have reduced the mean size of eggs remaining in their gonads.

Interestingly, the warm-acclimated individuals in my experiment did not spawn at any point from Sept – Dec, whereas the cold-acclimated urchins had spawning events in Sept and Oct, which is typical for this species (Brockington et al. 2007; De Leij et al. 2021). It might then be suggested that warm acclimation disturbs the natural rhythm of maturation and

spawning or even hinders the recognition of environmental triggers for spawning. These processes are essential for successful recruitment, larval survival and population continuity (Mercier & Hamel, 2009; 2010). Essentially, males and females must spawn in synchrony to allow for fertilisation to occur, and chlorophyll concentrations be optimal in the environment to sustain the larval phase of offspring development (Bosch et al. 1987). Animals also may need to spawn at set times in relation to annual productivity cycles to allow larvae to settle and metamorphose when suitable food supplies are available, the settlement timing hypothesis (Kuklinski et al. 2013; Stanwell-Smith et al. 1999; Todd & Doyle, 1981). My results suggest that adjusting to +2^{o}C may threaten seasonal and sex specific spawning times for *S. neumayeri.*

Despite evidence of negative effects on baseline functions following acclimation, my data are the first to provide evidence that an Antarctic invertebrate may have an improved capacity to tolerate extreme temperatures following long-term acclimation. This result shows that despite overall functioning diminishing following long-term acclimation, with reduced functioning and energetic capacity compared to animals at 0^{o}C (Chapter 4), there was an improved capacity to cope with acute warming. Similar outcomes have been observed in other studies, for example *Escherichia coli* bacterium grown at 32^{o}C outcompeted, in terms of growth, those grown at 42^{o}C, however those grown in warmer conditions survived longer at extreme temperatures (Leroi et al. 1994). In addition to this, there was an improved acute temperature or hypoxia tolerance following acclimation to warmer conditions in some marine species of fish and invertebrates (Collins et al. 2021; Seebacher et al. 2015). These results suggest that the effect of acclimation on thermal thresholds may not be a simple response where a threshold shifts or not, but it instead shows us that acclimation has generated a change in both functional capacity and energy allocation.

Previous studies have assumed a binary response following acclimation, where either an organism shifts its thermal range, or not, assessed by measuring the CT_{max} (Azra et al. 2018; Peck, 2005). My data suggests that the response of an organism is likely to be more complex than this and a change in the upper thermal limit (or CT_{max}) does not necessarily imply that all other functional capacity and performance will shift with it. Instead, results in Chapter 4 suggest that even if thermal limits shift and functional capacity at extreme temperatures shift, this does not mean that functioning between these temperatures will respond linearly. We know that CT_{max} does not represent the thermal capacity of physiological functions (Chapter 3, De Leij et al. 2022) and my data suggest that using CT_{max} as a measure of thermal adjustment overlooks the complexity of functional performance and other measures of fitness (Chapter 4).

When organisms are exposed to acutely stressful environments there are mechanism in place that allow for short term buffering, for example heat shock proteins (González-Aravena et al. 2018; Peck, 2011) or increasing energetic consumption (i.e. elevated oxygen consumption (Chapter 3, De Leij et al. 2022) or feeding (Agüera et al. 2017). These mechanisms are only suitable as temporary solutions and if the stress continues then there will be a long-term limit to survival (Peck et al. 2002). Climate models predict not only an increase in the magnitude of extreme warming events, but also an increase in frequency (Oliver et al. 2018). Already we are experiencing these predictions coming into effect across the globe. Some of the most publicised and well documented examples are the increase in hurricane activity in the Atlantic (IPCC, 2021) as well as the bleaching of coral reefs, where repeat exposure to warming with little recovery between events results in mass mortality events (Babcock et al. 2021). These events support the rationale behind Chapter 3 & 4, that effects of acute warming cannot be considered as isolated events, and we need to consider the environmental conditions proceeding the event and the characteristics of the event itself.

Chapter 4 explores the effect of repeated warming events on the physiology of *S.neumayeri.* Results suggested that the response to repeat events was dependant on acclimation temperature, giving further support to the hypothesis that thermal history influences an organism's response to acute warming (Seebacher et al. 2015; Sorte et al. 2011). My results demonstrate that *S. neumayeri* experiences diminishing resilience, in terms of time taken to right, after three sequential MHW events, increases in Q_{10} values for oxygen consumption following two sequential MHW events and linearly increasing food energy requirements that build following each MHW. These results suggest that in the current climate, repeat warming events would likely increase energy demands and decrease functional performance compared to a single warming event. However, my data also add to the evidence that warm acclimation may improve resilience to thermal stress (Leroi et al. 1994; Seebacher et al. 2015), where the data in Chapter 4 show decreases in time taken to right following each sequential MHW, lower Q_{10} values for oxygen consumption in warmed individuals compared to cold-acclimated urchins and improved capacity to recover to treatment relative baseline oxygen consumption levels following MHW events.

5.1 Future work and conclusion

Considering the research carried out for this thesis, it will be important to continue the collection of long-term time series data for reproduction. These data are needed to determine if there is a repeat in the extended cycle observed in the gonad index and capture a larger range of SOI/SAM variability. In addition to this, calculating changes in fecundity will give more information on changes in reproductive output associated with

fluctuations in the gonad index. I give evidence that nutritive phagocytes factor into the variability in gonad index and this should be explored further, for example in males as well as females.

Based on the reproductive data shown in Appendix D, further investigation into the implications of long-term acclimation on reproductive cycles should be carried out, with particular emphasis on whether spawning triggers are affected by a shift in temperature baselines. Given no evidence of spawning was observed in warm-acclimated conditions, despite sufficient gamete maturity, we might surmise that acute sensitivity to environmental variation in this species' current thermal range may be a critical feature that regulates reproductive periodicities. Changes to this sensitively could have negative implications for population persistence in a future climate and deserves further investigation.

The research in this thesis provides evidence that the future of marine species and communities is uncertain and likely dependant on species-specific capacities to buffer change. But what is clear is that the characteristics of thermal stress (onset rate, duration, repetition) have significant implications for organism responses. It is also clear that species have a certain buffering capacity for thermal stress over which functionality diminishes. This capacity will vary among species and for different environments. In essence, all individuals/species/populations will have an optimal thermal range and a threshold to environmental change. The ability to acclimate and evolve to new temperatures will undoubtedly benefit those who have this capacity, however there is always a cost to acclimation, and as the climate changes, it is inevitable that there will be tipping points or thresholds for all species, where endogenous rhythms may shift, and functionality deteriorate.

Appendices

Appendix A

Supplementary for Chapter 2

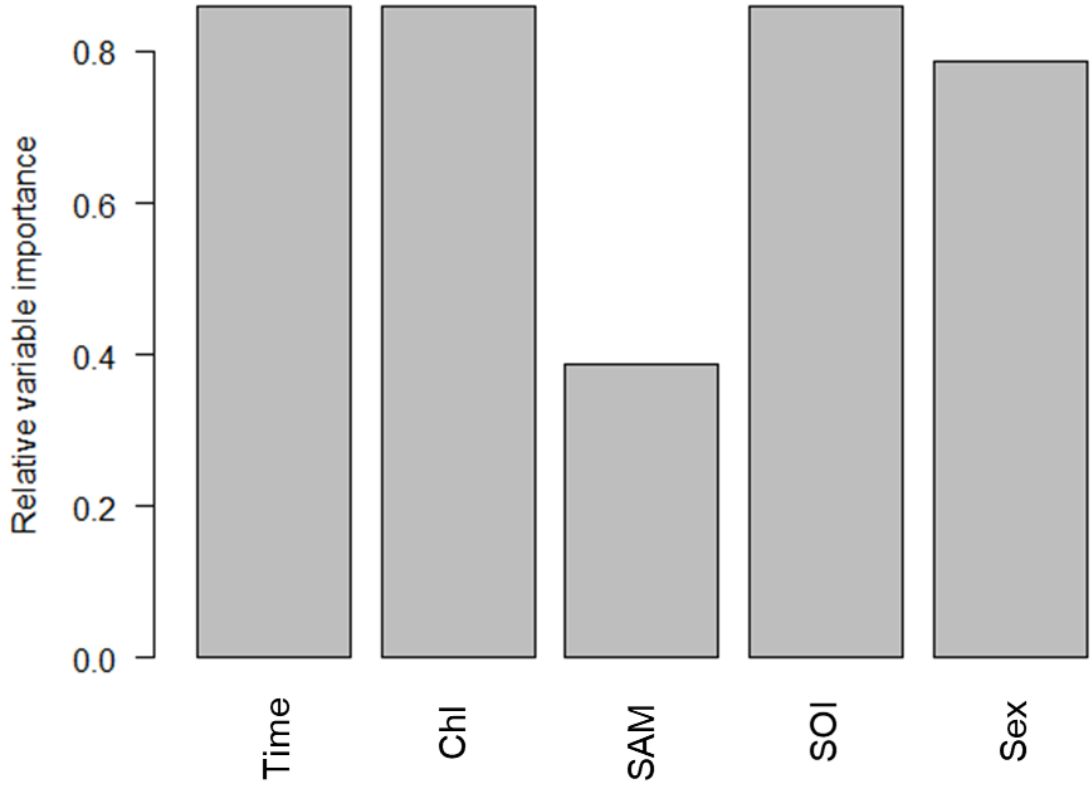

Figure A1: Relative variable importance of large-scale climate metrics and single variables in final general additive model exploration. Chl = Chlorophyll, SAM = Southern Annular Mode and SOI = Southern Oscillation Index.

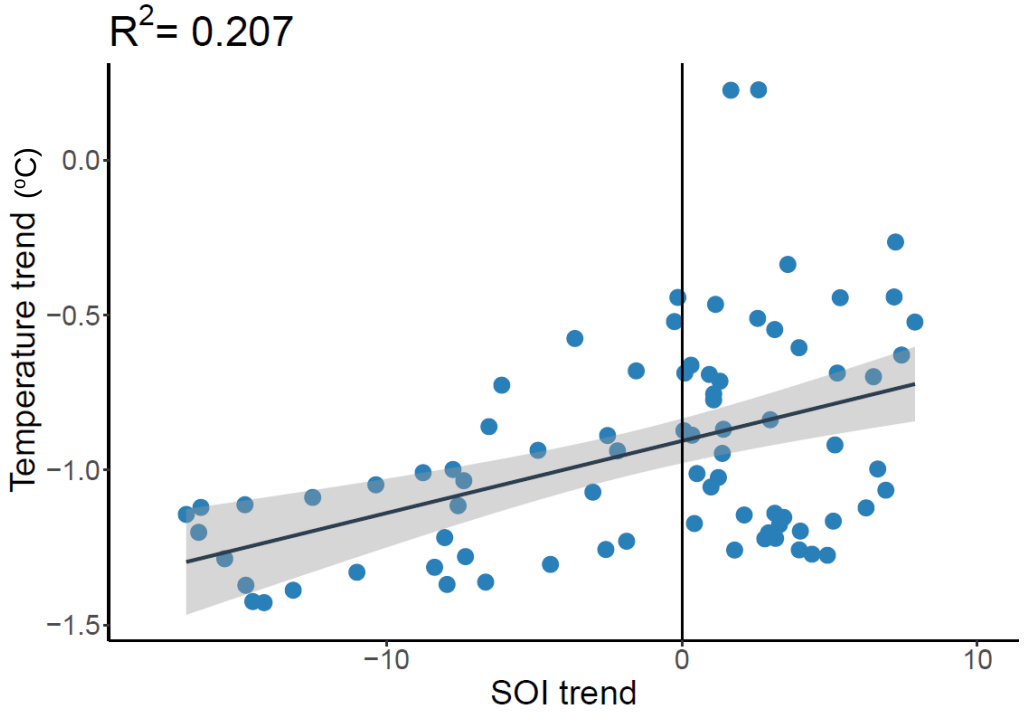

Figure A2: Linear relationship between the SOI trend data and the temperature trend data from 2012 – 2018, extracted from the decomposition analysis.

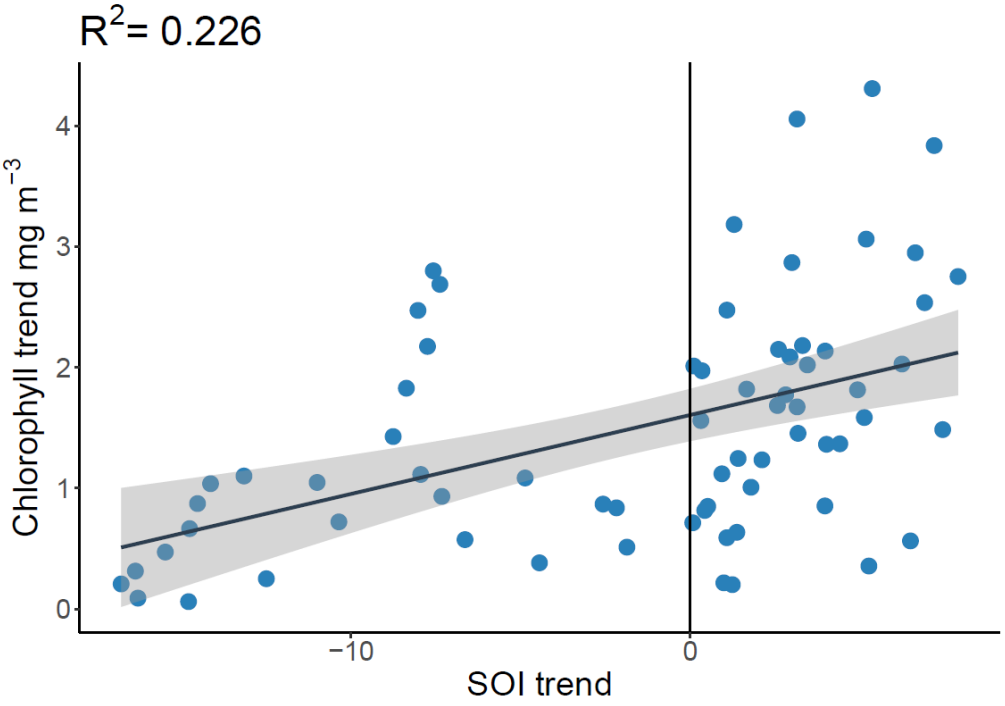

Figure A3: Linear relationship between the SOI trend data and the chlorophyll trend data from 2012 – 2018, extracted from the decomposition analysis.

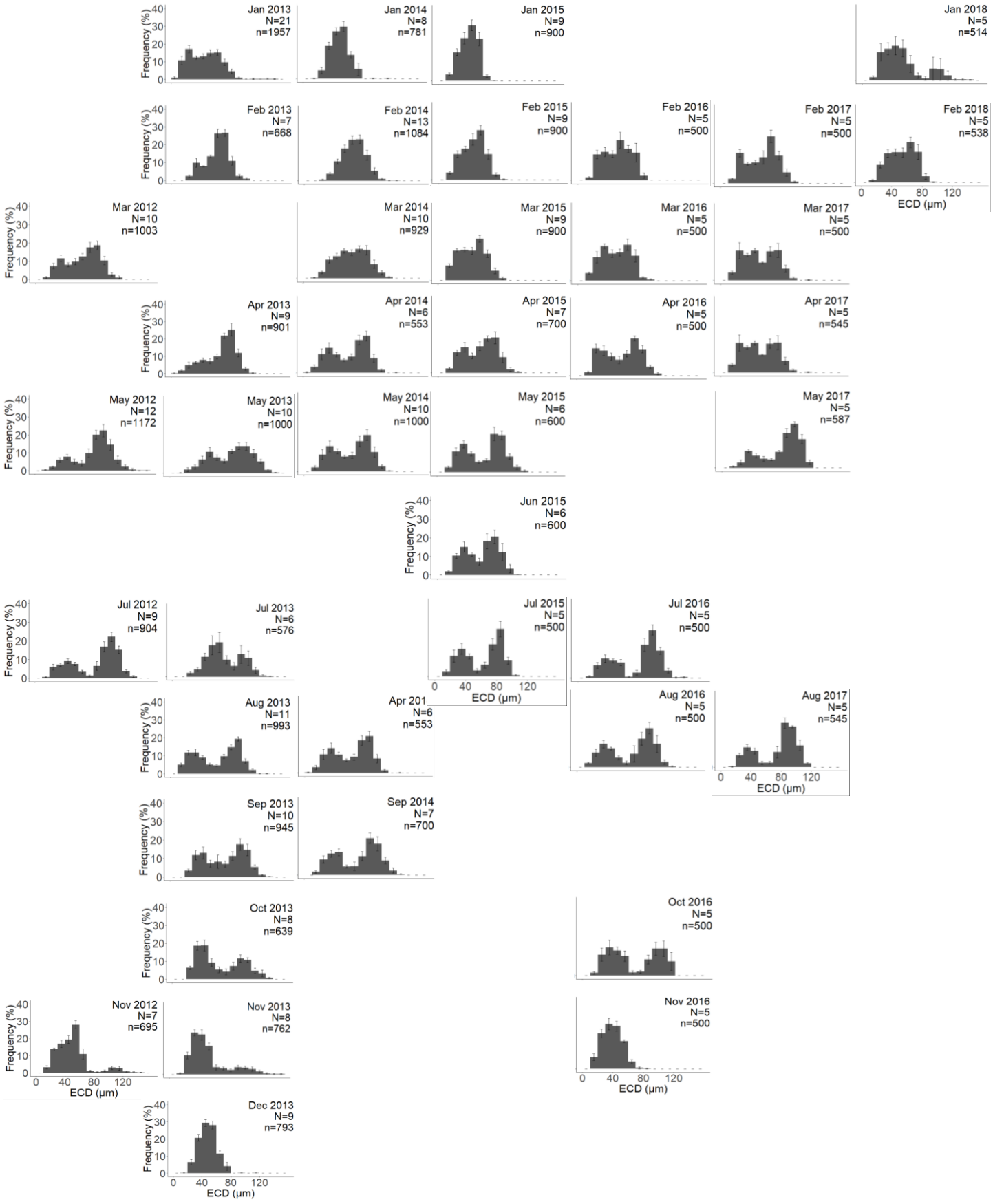

Figure A4: Oocyte size distributions (based on the calculation of Equivalent Circular

Diameter, µm) displayed as monthly histograms of female oocyte size percentage frequencies (%). From left to right, years are displayed from the time series from 2012 to 2018. From top to bottom, months are displayed from January to December. Error bars are ± standard error. N = total number of females included in the distribution, n = total number of oocytes measured in the distribution.

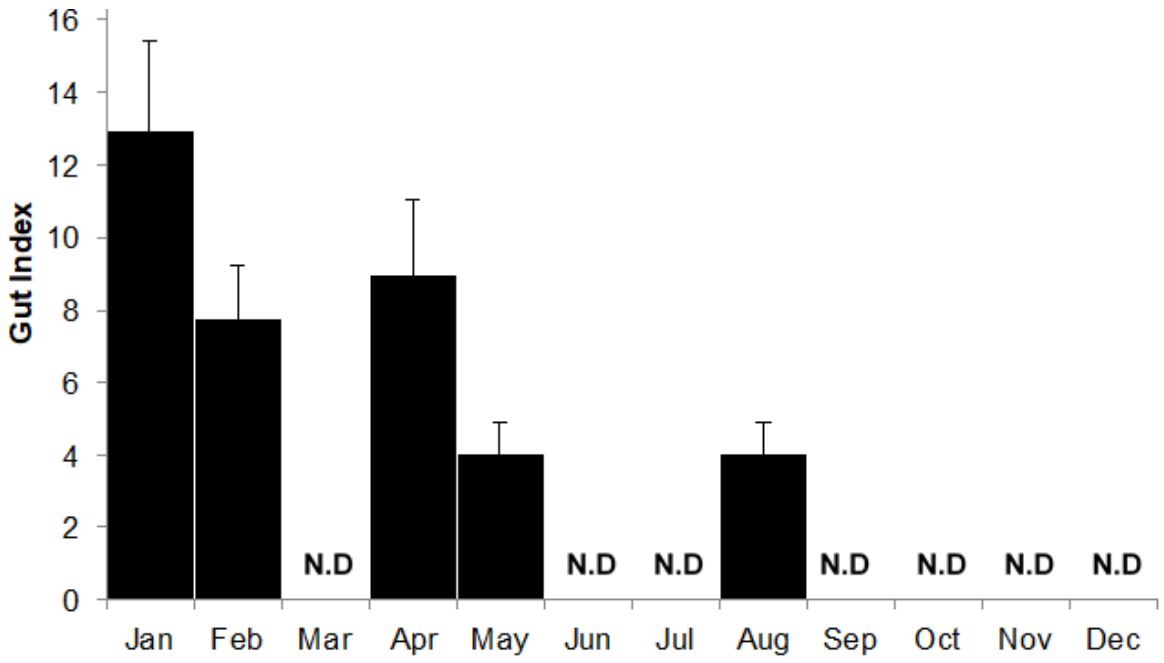

Figure A5: Gut index ((*gut mass/total animal mass) x 100*) of *Sterechinus neumayeri* from animals collected in April, May and August in 2017, and January and February in 2018. Error bars represent + standard error. N.D represents months where no data were available.

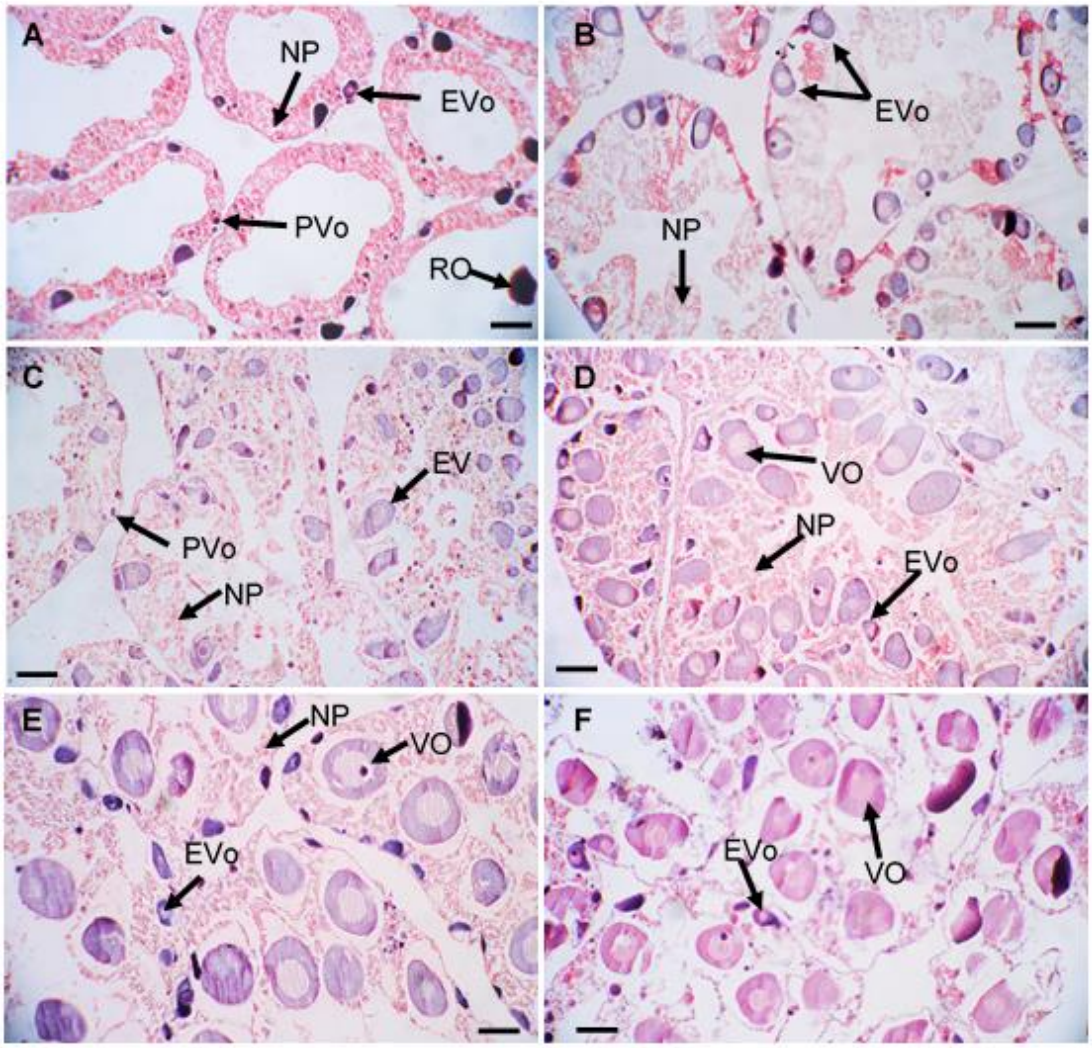

Figure A6: Histology sections of female *Sterechinus neumayeri* gonad tissue. A: Spent gonads with few pre-vitellogenic (PVo) and early-vitellogenic oocytes (EVo) beginning to appear around the edges of the gonad wall along with a lining of nutritive phagocytes (NP) and reabsorbing oocytes (RO) (November); B: Developing early-vitellogenic oocytes and thickening lining of nutritive phagocytes (February); C: Two cohorts of oocytes are present within the gonad, pre-vitellogenic and early-vitellogenic oocytes (March); D: Large, vitellogenic oocytes (VO) visible along with early-vitellogenic oocytes and further increase in nutritive phagocytes (April); E: Cohort of mature vitellogenic oocytes have reached maximal size and are ready to be released. Second cohort of early-vitellogenic oocytes present around the edges of the gonad wall (September); F: Mature vitellogenic oocytes and early-vitellogenic oocytes present in the gonad, reduction in nutrient phagocytes and increase in empty space as mature oocytes are spawned (October). Scale bars represent 100 µm.

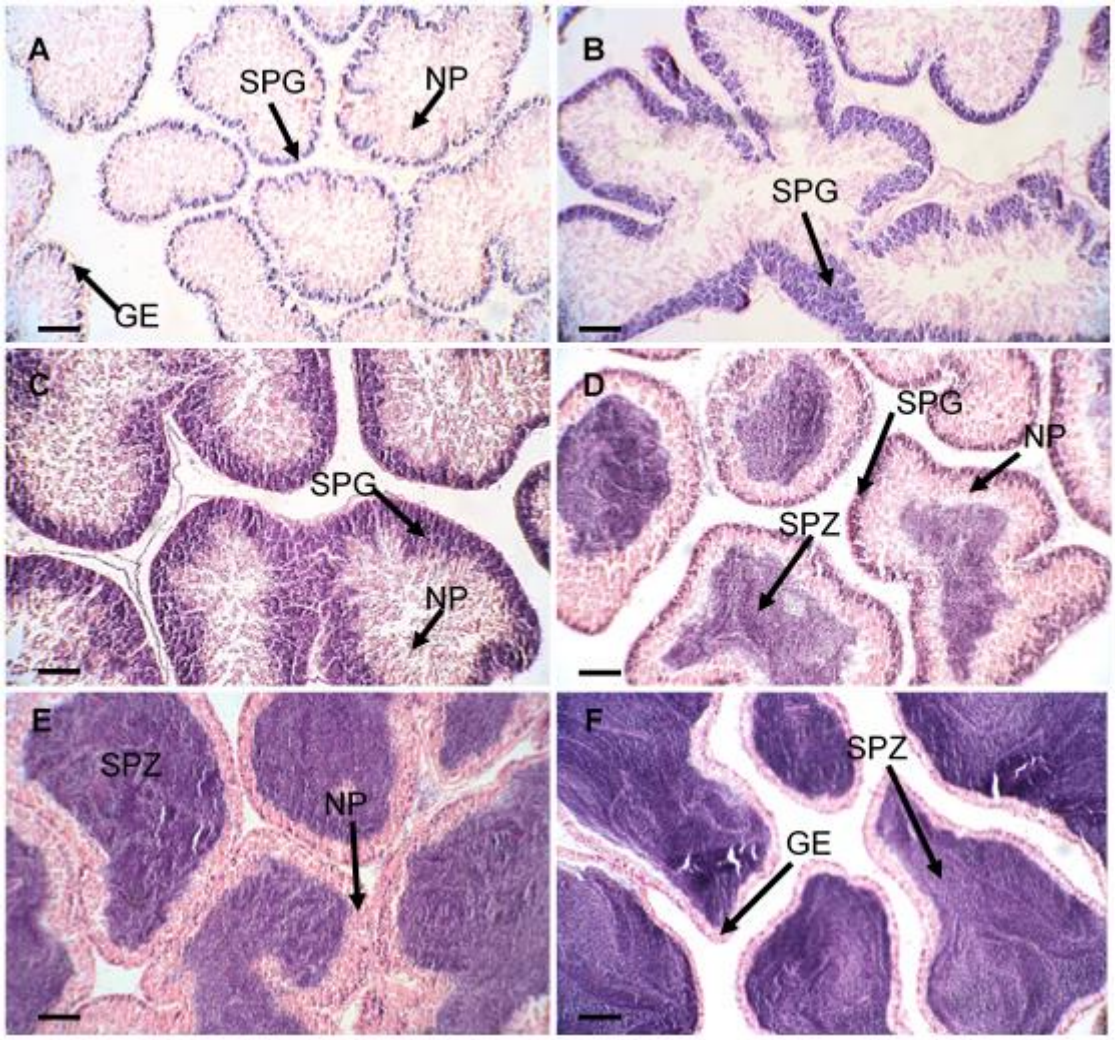

Figure A7: Histology sections of male *Sterechinus neumayeri* gonad tissue showing different stages of maturation. A: Spawned/recovering gonads with mainly nutritive phagocytes (NP) with a thin layer of spermatogonia (SPG) around the edge of the germinal epithelium (GE) (February); B: Thickening of spermatogonia layer (March); C: Further thickening of spermatogonia layer and nutritive phagocytes (NP) (April); D: First signs of mature spermatozoa (SPZ) in the central lumen (May); E: Increased production of spermatozoa in central lumen, surrounded by a thick layer of nutritive phagocytes and absence of maturing spermatogonia (September); F: Final stages of maturity with mature spermatozoa present in large volumes in the central lumen with only a thin layer of nutritive phagocytes around the wall of the germinal epithelium (October). Scale bars represent 100 µm.

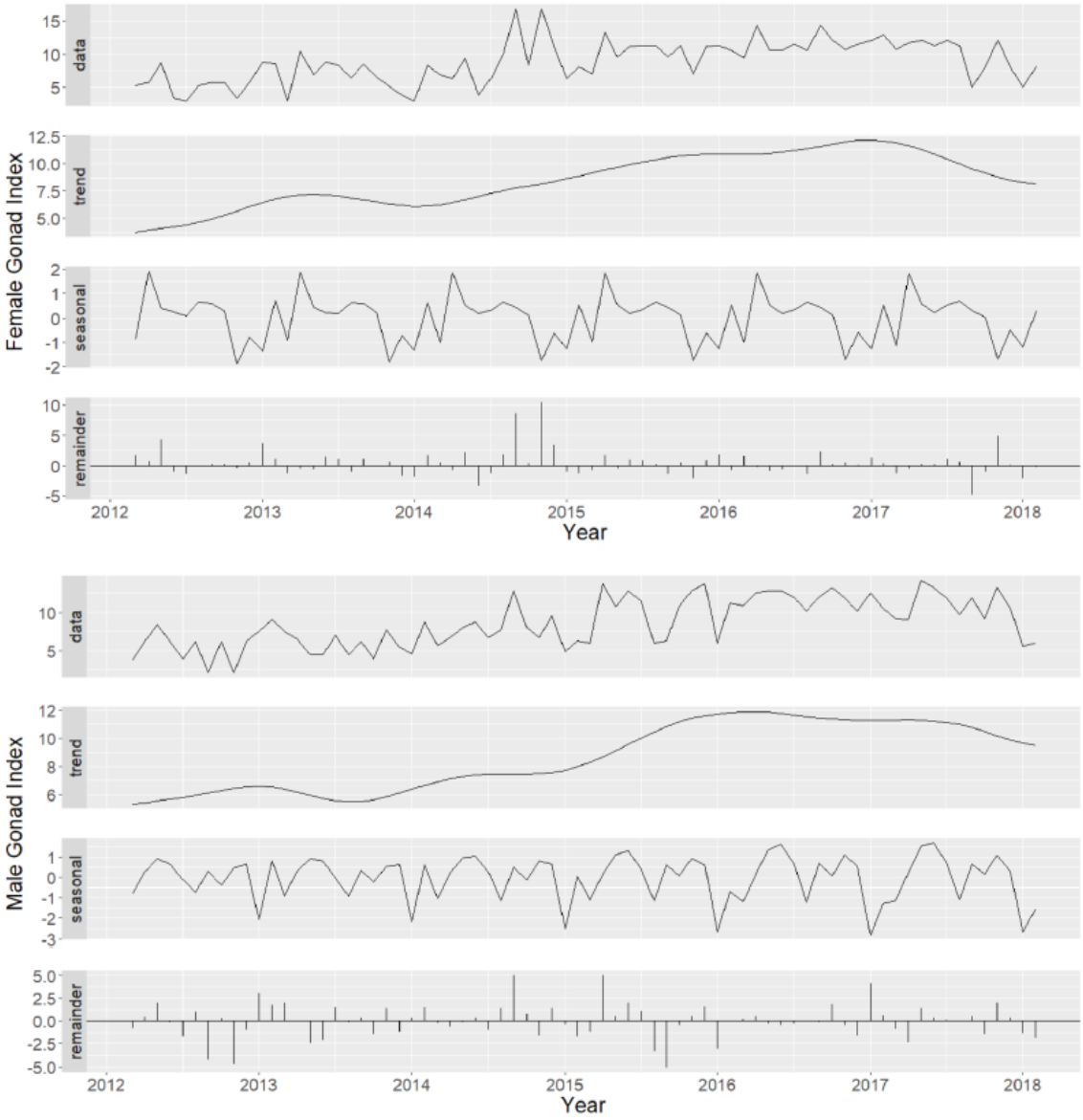

Figure A8: Decomposition analysis of female and male gonad index time-series, decomposed to the overall trend, seasonal cycle and remainder.

Table A1: Chi-squared analysis of sex ratio averaged within years and also overall from March 2012 - March 2018. F = Females, M = Males. p-values <0.05 are marked with an asterisk (*) to show significant differences.

Year	**F**	**M**	***Chi-squared test statistic***	***p-value***
2012	53	32	5.188	0.023*
2013	73	87	1.225	0.268
2014	70	58	1.125	0.289
2015	64	53	1.034	0.309
2016	66	47	3.195	0.074
2017	51	31	4.878	0.027*
2018	17	16	0.030	0.862
Total	408	310	13.376	0.000*

Table A2: T-test analysis of sex difference for variables of animal size: test diameter and wet weight, and gonad index. Mean values for males and females are shown under columns ‘F’ (female mean) and ‘M’ (male mean). p-values <0.05 are marked with an asterisk (*) to show significant differences.

Variable	**F**	**M**	***p-value***
Test diameter (mm)	31.4	31.5	0.590
Wet weight (g)	12.9	13.3	0.323
Gonad Index	8.90	8.19	0.024*

Table A3: ANOVA results for comparisons of oocyte Equivalent Circular Diameter between years for each month. June is exempt from the analysis as data were only collected in 2015. p-values < 0.05 were considered significant, F = F-statistic, df: degrees of freedom. Post-hoc Tukey pair-wise comparisons are listed where significant differences in the ANOVA were found with corresponding p value in adjacent column.

	January	**February**	**March**		**April**		**May**		**July**	
	p = 0.251 F = 1.452 df = 2, 28	p = 0.218 F = 1.522 df = 4, 34	p < 0.001 F = 19.32 df = 5, 40		p = 0.005 F = 5.541 df = 3, 22		p < 0.001 F = 24.65 df = 3, 34		p = 0.008 F = 5.146 df = 3, 21	
Tukey pair-wise test			2012 vs 2015 2016 2017	p < 0.001 p < 0.001 p = 0.001			2012 vs 2013 2014 2015	p < 0.001 p < 0.001 p = 0.001	2012 vs 2015	p = 0.005
			2013 vs 2015 2016 2017	p < 0.001 p = 0.002 p = 0.007	2013 vs 2015 2016	p = 0.009 p = 0.040	2013 vs 2014 2015	p = 0.003 p = 0.019		
			2014 vs 2015 2016 2017	p < 0.001 p < 0.001 p = 0.002						
	August		**September**	**October**	**November**		**December**			
	p < 0.001 F = 18.29 df = 2, 18		p = 0.609 F = 0.275 df = 1, 13	p = 0.940 F = 0.006 df = 1, 11	p = 0.004 F = 7.865 df = 2, 17		p = 0.037 F = 5.758 df = 1, 10			
Tukey pair-wise test					2012 vs 2016	p = 0.032				
	2013 vs 2014 2016	p < 0.001 p < 0.001			2013 vs 2016	p = 0.003	2013 vs 2014	p = 0.037		

Table A4: Model selection process including the variables of weighted importance, followed by a ranking of automated model generation. The models are ranked according to the lowest Akaike Information Criterion (AIC). (+) = Terms included in model, AICc = Akaike Information Criterion corrected for small sample size, BIC = Bayesian Information Criterion, R^2 = proportion of variance explained, d = difference in AICc relative to the top candidate model, w = Akaike weight.

Weighted importance	
Time	0.999
Chlorophyll	0.999
SOI	0.955
SAM	0.398
Sex	0.822

	Model 1	**Model 2**	**Model 3**	**Model 4**	**Model 5**	**Model 6**
Time		+	+		+	+
Chlorophyll			+		+	+
SOI			+			+
SAM	+	+				+
Sex	+	+	+	+	+	+
Time by Sex	+			+		
Chlorophyll by Sex	+	+		+		
SOI by Sex	+	+		+	+	
SAM by Sex			+	+	+	
AICc	1259.2	1263.7	1264.4	1264.5	1265.4	1266.0
BIC	1372.9	1353.6	1340.8	1376.8	1349.3	1333.3
R^2	0.414	0.403	0.397	0.412	0.399	0.392
d	0.000	2.647	3.349	3.420	4.326	4.941
w	0.470	0.125	0.088	0.085	0.054	0.040

Text A1: Decomposition analysis R code

```
#packages required
library(seasonal)
library(forecast)
library(magrittr)
library(mice)
library(tidyverse)
library(tidyr)

#gonad index for females
data <- gi_f
# OR gonad index for males
data <- gi_m

#average gi replicates by month
data_summary <- data %>%
  group_by(date) %>%
```

```
  summarize(mean = mean(gi))
#insert NAs in gaps
data <- data_summary %>% complete(date = seq.Date(min(date),
max(date), by="month"))

#Need time series with no gaps, so fill missing months with
predicted data using PMM (Predictive Mean Matching)
https://stefvanbuuren.name/fimd/sec-pmm.html
R Packages | Impute Missing Values In R (analyticsvidhya.com)
imputed_Data <- mice(data, m=5, maxit = 50, method = 'pmm')
summary(imputed_Data)
completeData <- complete(imputed_Data,2)
gidata <- subset(completeData, select = mean)# Selects collumns
from the aggregated data into a new dataframe

#create a time series object
timeseries_gi <- ts(gidata, start = c(2012, 3), end =c(2018, #2),
frequency = 12)
ts <- window(timeseries_gi, start=c(2012, 3), end=c(2018, 2))
plot(as.ts(ts))

#decomposition of data using X11 method. Based on classical
decomposition, but includes many extra steps and features in
order to overcome the drawbacks of classical decomposition.
fit <- seas(ts, x11 = "")
autoplot(fit)
```

Appendix B

Supplementary for Chapter 3

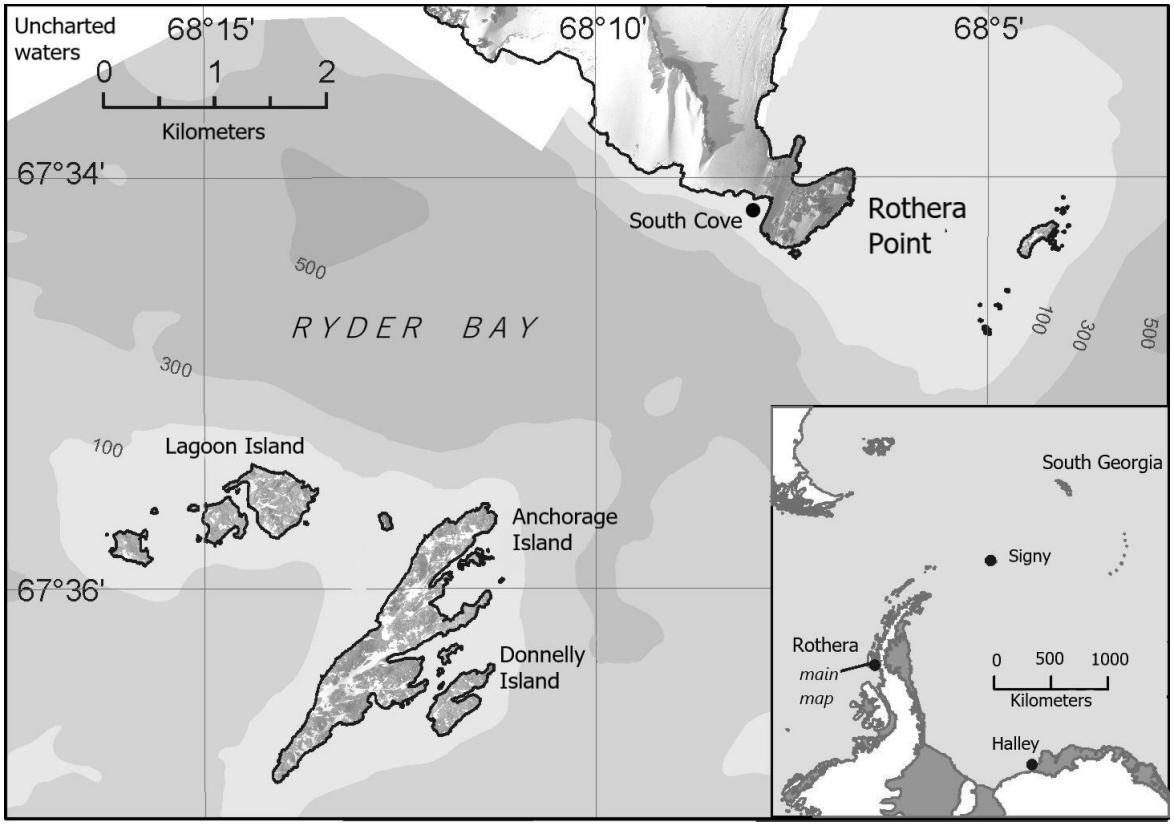

Figure A1: Location of Hangar Cove study site at Rothera Point, Adelaide Island, Antarctica (67°33'54.2"S 68°07'13.1"W) and insert map showing location of Rothera Point on Western Antarctic Peninsula. Marine environmental data are collected at the CTD site located south west of Rothera Point provide marine environmental data as part of the British Antarctic Survey Rothera Time Series environmental monitoring programme (RaTS). Large-scale map indicates the position of Rothera Research Station on Adelaide Island, on the Western Antarctic Peninsula. Figure modified from Grange et al. (2011)

Text A1: Marine heatwave analysis

The package 'heatwaveR' (Schlegel & Smit, 2018) was used to identify MHWs using the RaTS environmental data. I would like to acknowledge some limitations of the RaTs data for detecting MHWs using this package. Firstly, a period of 30 years is recommended to define baseline temperatures for the region of study (Hobday et al. 2016). However, owing to data acquisition in Antarctica being limited by remoteness, the RaTS data falls short of this recommendation, having 20 years of data (1997 – 2017). This limitation is acknowledged, and baseline temperature estimates are considered less robust as a result. In addition, the package also requires continuous daily temperature measurements,

whereas the RaTS data aims to collect four measurements per month, rather than daily data. In order to estimate daily temperature values, temperatures for dates occurring between measured time points were calculated by assuming that temperature increased/decreased linearly between time points. To this effect, the rate of temperature change between measured temperatures was estimated by calculating the difference in degrees celcius between the previous and subsequent measured temperatures, and then dividing by the number of days in between these two measured temperatures. This daily rate of change was then used to estimate daily temperatures in the RaTS data that were not directly measured.

Temperature thresholds for defining a marine heat wave event are outlined in Hobday et al. (2016). In summary, MHW temperatures were reached when temperatures exceeded the 90th percentile of the seasonal temperature range (calculated from baseline temperatures at Ryder Bay from 1997-2017). If this seasonal temperature threshold was exceeded for a period of >5 consecutive days, this was recorded as a MHW.

The analysis provided the date, duration (days), mean intensity (^{o}C), maximum intensity (^{o}C), cumulative intensity (^{o}C x days) and onset rate (^{o}C day^{-1}). These values were then used to inform the realistic and potential future temperatures and warming rates used in the experimental design.

Table A1: Summary of heat wave characteristics at Rothera, Antarctica from 1997 – 2017. Duration: number of days heatwaves lasted, mean magnitude: mean temperature across duration of heatwave expressed as ^{o}C above the seasonal average, maximum magnitude: peak temperature within each heatwave expressed as ^{o}C above the seasonal average, onset rate: ^{o}C per day increase until peak temperature, annual frequency: number of heat wave events per year. Averages represent the mean value ± standard deviation, except for the duration which is represented by the median. Maximums represent the maximum recording across all heat wave events 1997 – 2017.

	Duration (days)	Mean magnitude (^{o}C)	Max magnitude (^{o}C)	Onset rate (^{o}C day^{-1})	Annual frequency
Average	10 ± 17	0.7 ± 0.4	0.8 ± 0.5	0.1 ± 0.1	2 ± 2
Maximum	95	1.4	2.0	0.3	6

Table A2: Significant pair-wise comparison statistics of repeat measures ANOVA for oxygen consumption (µmol hr^{-1} $gAFDM^{-1}$), time taken to right (minutes) and faecal production (mgAFDM day^{-1} $mgAFDM^{-1}$). Mean ± standard error are listed below each treatment group in relation to the temperature timepoint measured. t = t statistic, df = degrees of freedom and adjusted p-values are Bonferroni corrected.

Function	Time point	Temperature (°C)	group1	group2	t	df	Adjusted p-value
Oxygen consumption	t1	3.2	0.3°C day^{-1} *6.41 ± 0.36*	1°C day^{-1} *5.20 ± 0.25*	5.62	4	0.030
	t2	5.2	0.3°C day^{-1} *7.47 ± 0.30*	Cntrl *3.73 ± 0.33*	5.87	4	0.025
			1°C day^{-1} *6.97 ± 0.42*	Cntrl *3.73 ± 0.33*	4.98	4	0.045
	t3	7.2	0.3°C day^{-1} *9.38 ± 0.74*	1°C day^{-1} *18.8 ± 1.47*	-11.68	4	0.002
			0.5°C day^{-1} *10.2 ± 0.39*	1°C day^{-1} *18.8 ± 1.47*	-8.46	4	0.006
			0.5°C day^{-1} *10.2 ± 0.39*	Cntrl *5.15 ± 0.26*	9.72	4	0.004
			1°C day^{-1} *18.8 ± 1.47*	Cntrl *5.15 ± 0.26*	10.97	4	0.002
	t4	9.2	0.3°C day^{-1} *18.2 ± 1.7*	1°C day^{-1} *9.38 ± 0.59*	14.59	4	0.001
			0.3°C day^{-1} *18.2 ± 1.7*	Cntrl *5.73 ± 0.50*	9.18	4	0.005
			0.5°C day^{-1} *13.5 ± 0.60*	Cntrl *5.73 ± 0.50*	17.53	4	0.000
			1°C day^{-1} *9.38 ± 0.59*	Cntrl *5.73 ± 0.50*	5.35	4	0.035
	t5	11.2	0.3°C day^{-1} *11.25 ± 0.79*	Cntrl *4.34 ± 0.16*	18.28	4	0.000
			0.5°C day^{-1} *14.3 ±1.27*	Cntrl *4.34 ± 0.16*	19.55	4	0.000

			1^{o}C day^{-1} *20.8 ± 2.15*	Cntrl *4.34 ± 0.16*	11.00	4	0.002
Time taken to right	t5	9.2	1^{o}C day^{-1} *28.5 ± 3.11*	Cntrl *10.6 ± 1.65*	6.06	4	0.022
	t6	11.2	0.3^{o}C day^{-1} *159.6 ± 42.5*	Cntrl *9.14 ± 1.19*	6.04	4	0.023
			1^{o}C day^{-1} *115.7 ± 2.33*	Cntrl *9.14 ± 1.19*	13.47	2	0.033
Faeces produced	t1	2.1	0.3^{o}C day^{-1} *1.26 ± 0.15*	1^{o}C day^{-1} *0.58 ± 0.09*	5.02	4	0.044
			0.5^{o}C day^{-1} *1.16 ± 0.02*	1^{o}C day^{-1} *0.58 ± 0.09*	5.31	4	0.036
			0.3^{o}C day^{-1} *1.26 ± 0.15*	Cntrl *0.63 ± 0.12*	8.74	4	0.006

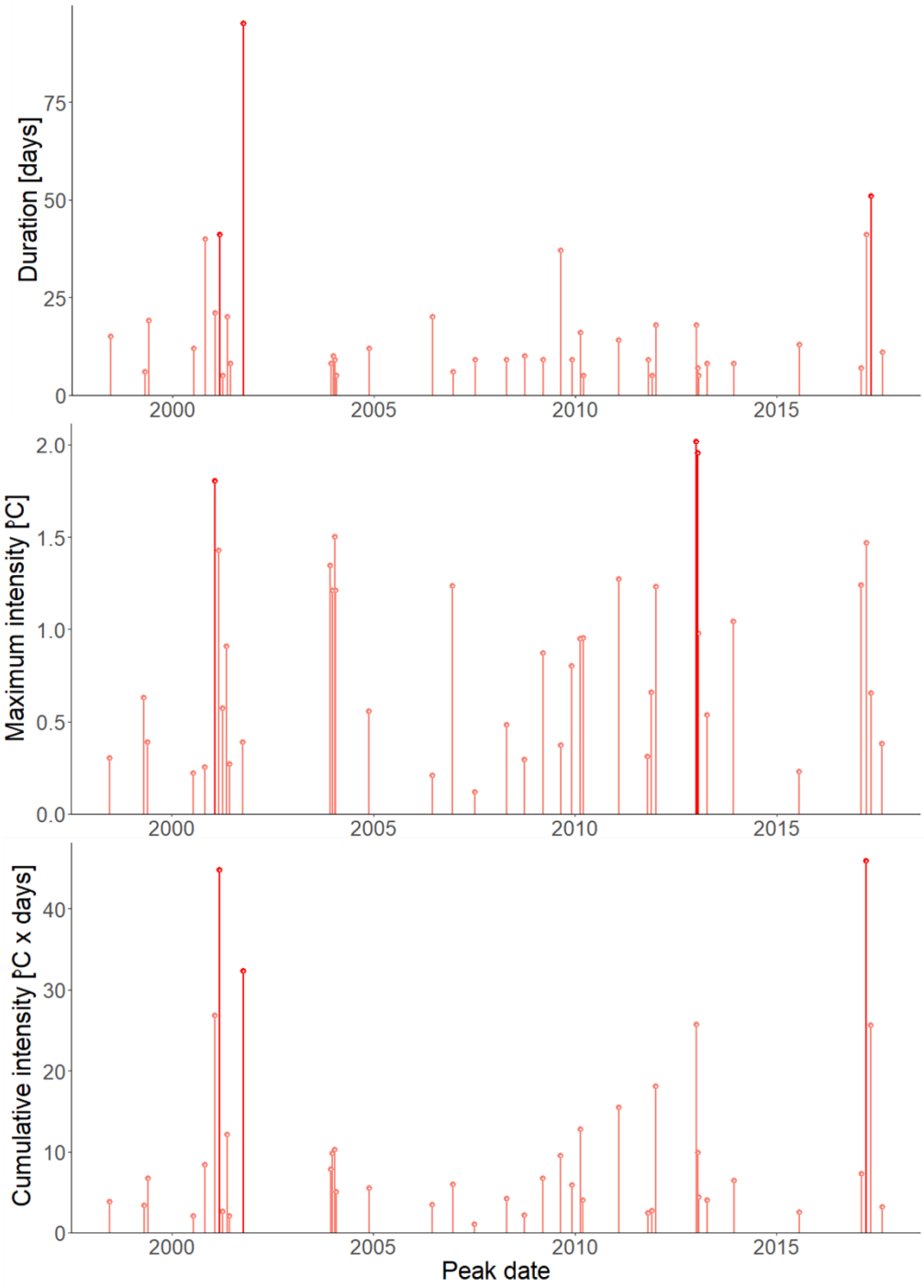

Figure A2: Characteristics of warming events occurring in Ryder Bay, Antarctica from 1997 – 2018. Y-axis indicates a) duration of the warming event in days, b) the maximum temperature reached during the warming event in ^{o}C, and c) the cumulative intensity of the warming event in terms of the integral of intensity over the duration of the event, and is equivalent to previously used metrics such as degree heating days (Hobday et al. 2016). X-axis indicates time at which the warming event occurred.

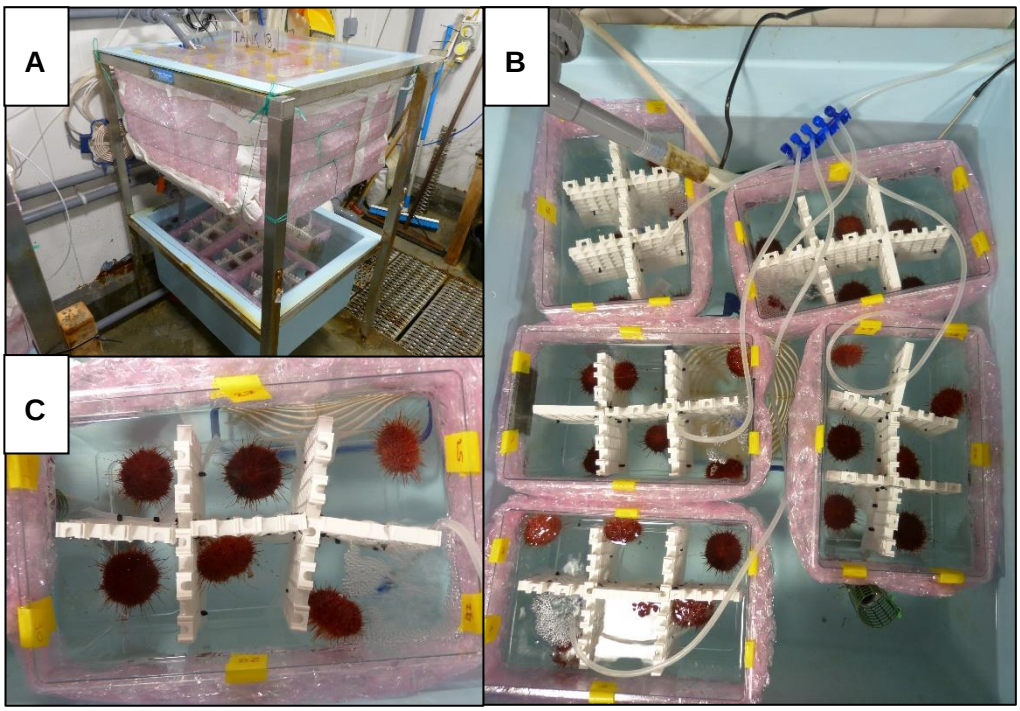

Figure A3: Experimental tank set-up a) Large water bath (Kingfisher Aquaculture) per treatment temperature containing five replicate small tanks. Bubble-wrap and foam insulated tank temperatures and limited heat transfer between treatments surrounding aquaria; b) five replicate tanks supplied with air stone with temperature changes governed through coil heaters (:hager ADC906F; LS502; ESD225; EK083) placed within water baths, circulating water by aquaria pumps (EHEIM compactON 300) and air stones; c) Within each replicate tank, each of the six pseudo replicate urchins separated using aquaria egg crate and fine mesh.

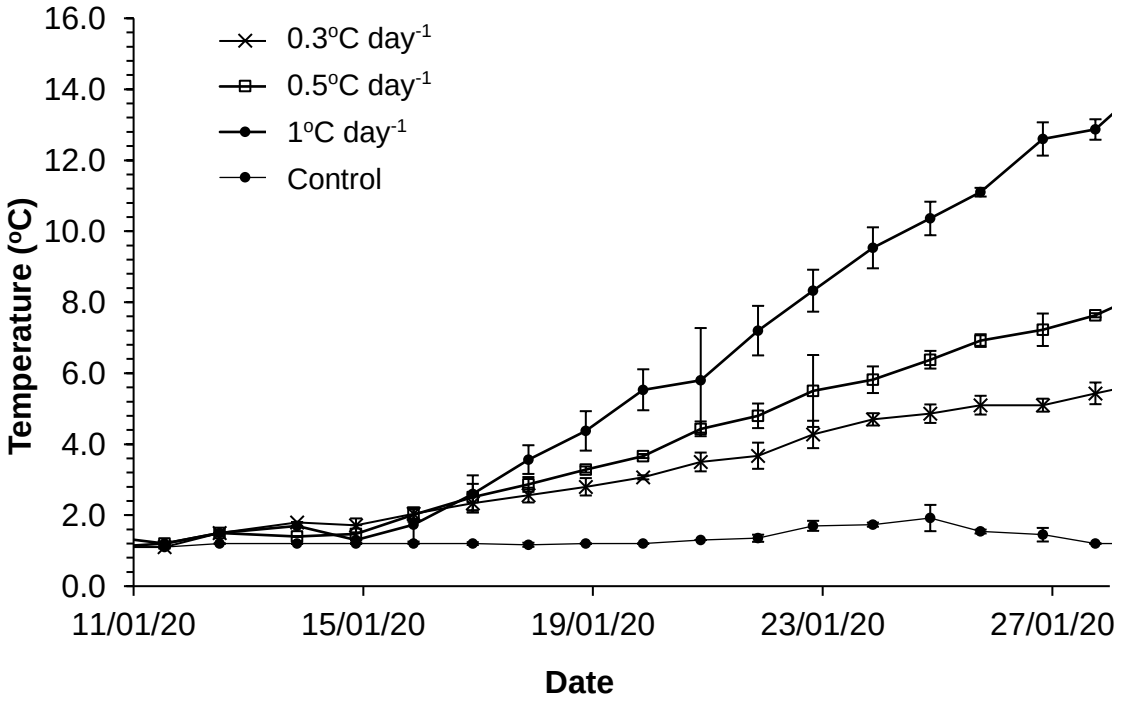

Figure A4: Mean temperature of water baths for each treatment throughout the experiment. Error bars are ± standard deviation.

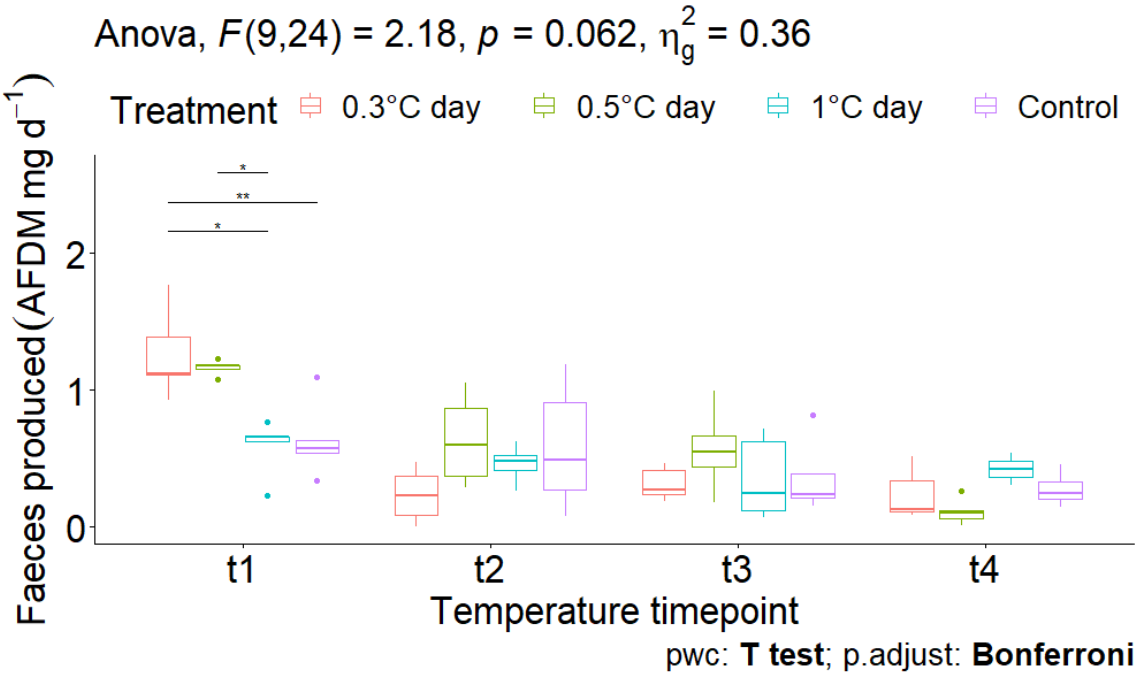

Figure A5: Repeat measures ANOVA analysis for faeces produced as AFDM mg day^{-1}, where significant differences are indicated with asterisks. Temperature time points represent the incremental increases in temperature where faecal production was measured at comparable temperatures in animals in treatment conditions, and

temperature timepoints for controls equate to periodic measurements of faecal production throughout the experimental period.

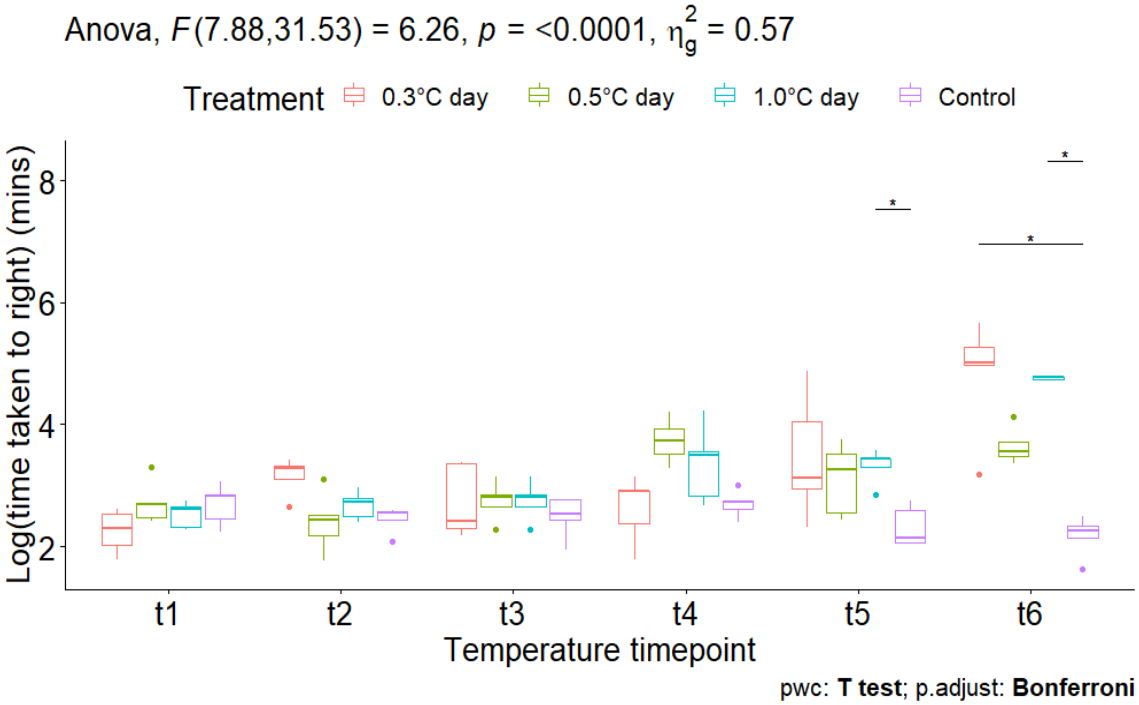

Figure A6: Repeat measures ANOVA analysis for log transformed time taken to right where significant differences are indicated with asterisks. Temperature time points represent the incremental increases in temperature where righting was measured in animals in treatment conditions, and temperature timepoints for controls equate to periodic measurements of righting throughout the experimental period.

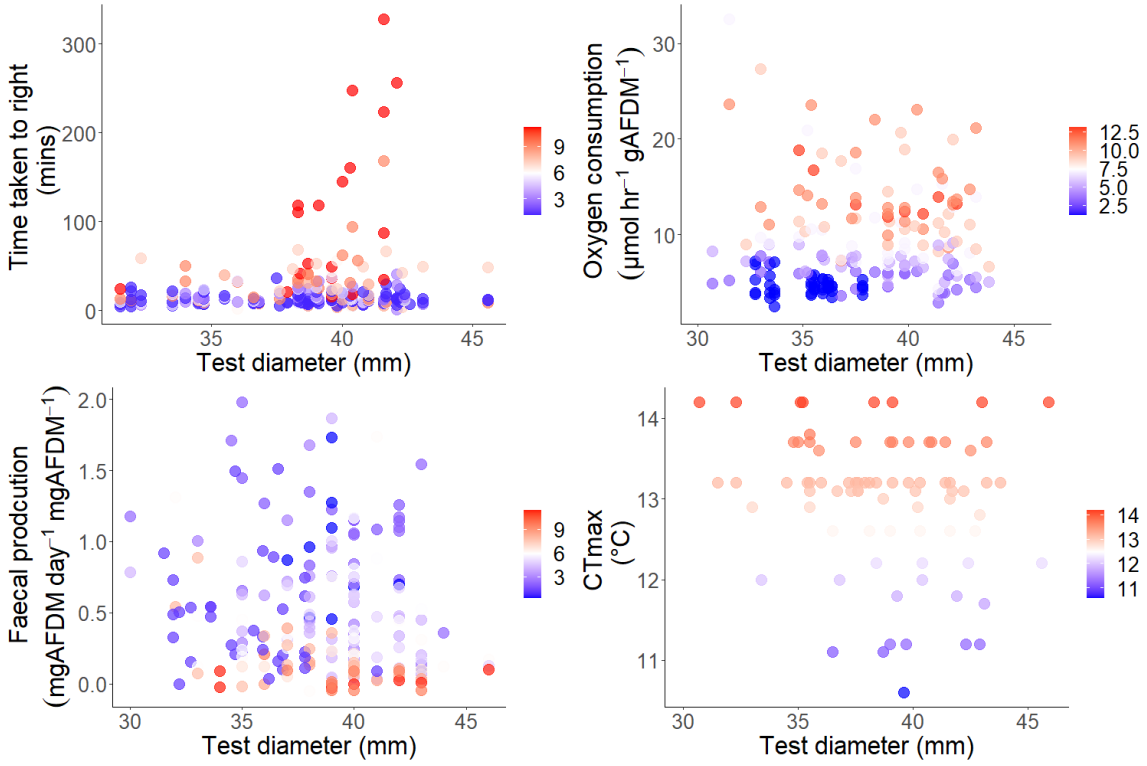

Figure A7: Effect of size of urchin (as test diameter) on function measured displayed as scatter plots, where the temperature at which the function was measured is indicated by a temperature colour gradient (low temperatures, relative to scale = blue, high temperature, relative to scale = red). Temperature scale bars are illustrated on the right of each plot.

Table A3: Linear mixed model results for the model: $\log(\text{Righting}_i) = \beta_0 + \beta_1 \text{Test diamter}_i \text{Temperature}_i + u_i + \varepsilon_i$, where u_i = random intercept for replicate tank ID and ε_i = random effect replicate tank ID. p-values are highlighted in bold where a significant effect occurs ($p < 0.05$).

	Effects of urchin size on time taken to right		
Predictors	*Estimates*	*CI*	*p*
(Intercept)	2.64	0.79 – 4.50	**0.005**
Test diameter	-0.01	-0.06 – 0.04	0.649
Temperature	-0.24	-0.59 – 0.10	0.170
Test diameter*Temperature	0.01	0.00 – 0.02	**0.035**
Random Effects			
σ^2	0.52		
$\tau_{00\ tank\_id}$	0.00		
ICC	0.01		
N_{tank_id}	20		
Observations	210		
Marginal R^2 / Conditional R^2	0.311 / 0.316		

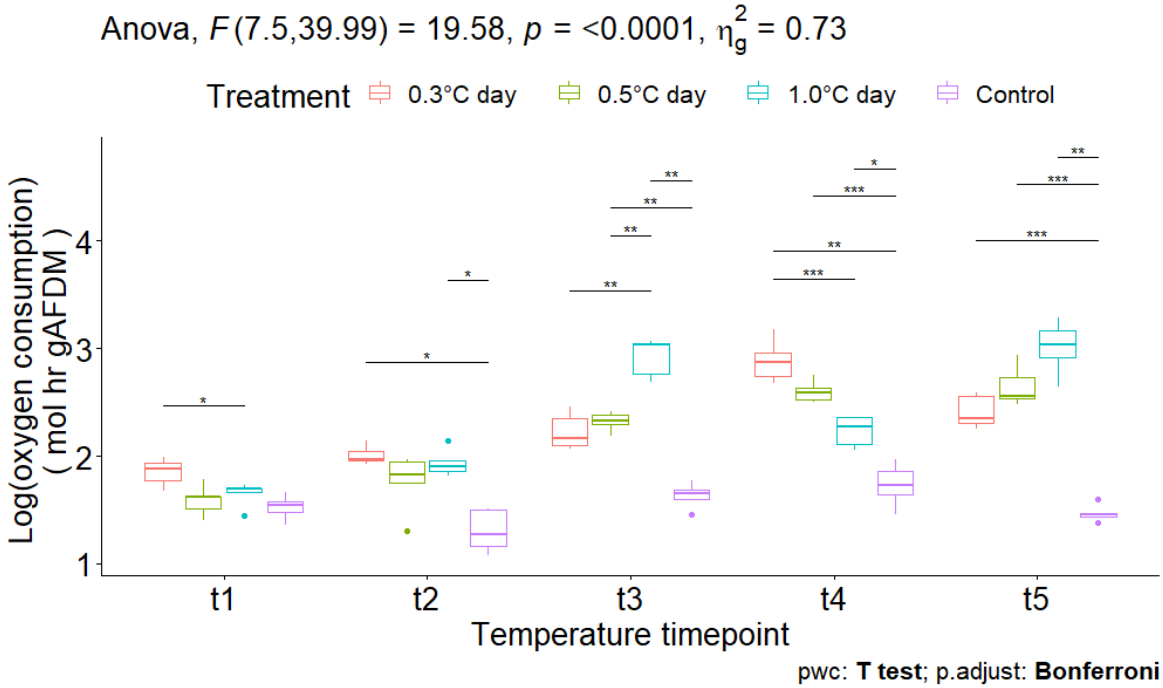

Figure A8: Repeat measures ANOVA analysis for log transformed oxygen consumption where significant differences are indicated with asterisks. Temperature time points represent the incremental increases in temperature where oxygen consumption was measured in animals in treatment conditions, and temperature timepoints for controls equate to periodic measurements of oxygen consumption throughout the experimental period.

Appendix C

Supplementary for Chapter 4

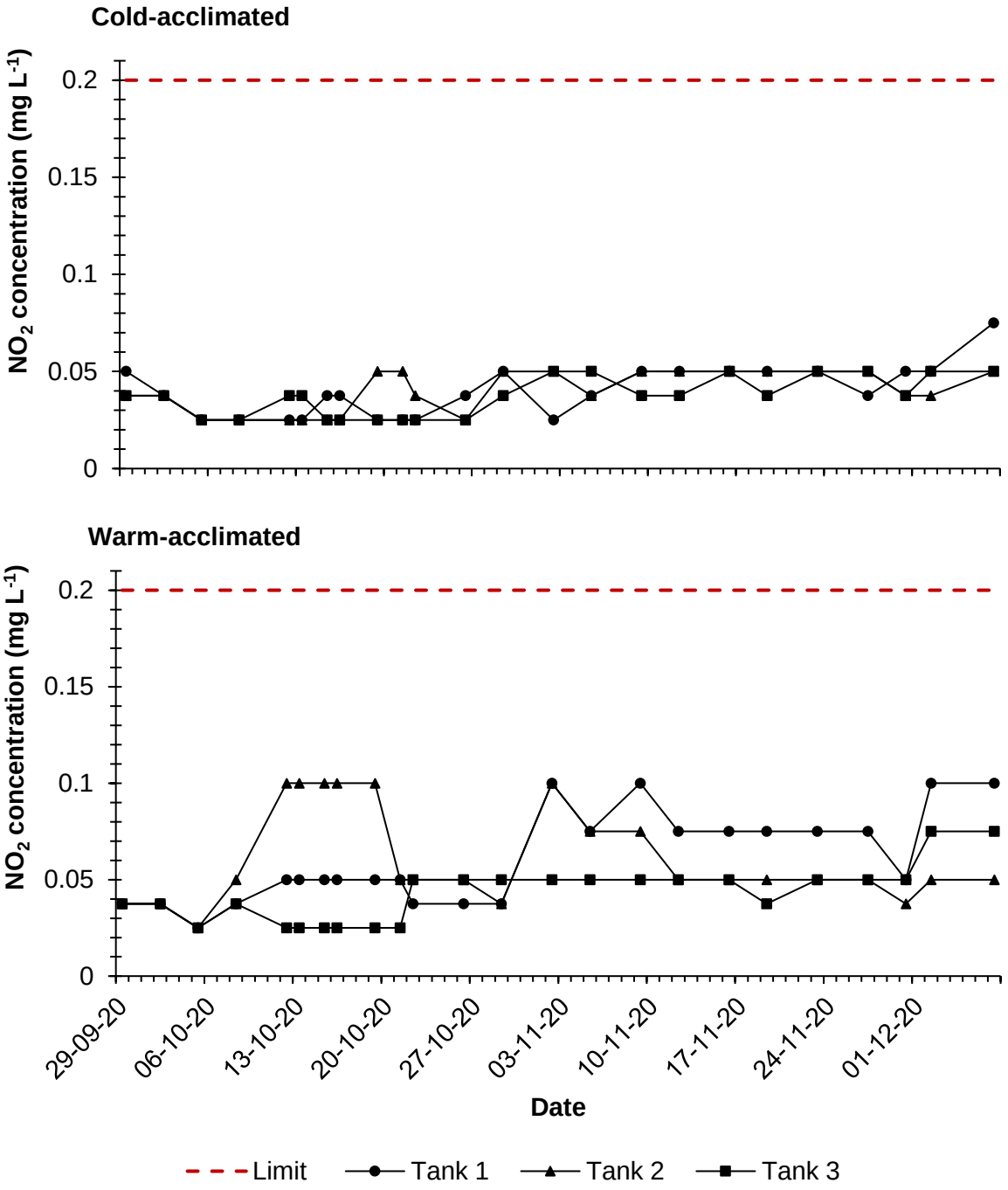

Figure A1: Nitrite (NO_2^-) concentrations in replicate tanks in cold-acclimated and warm-acclimated treatments, in relation to the upper concentration limits allowed (red dashed line).

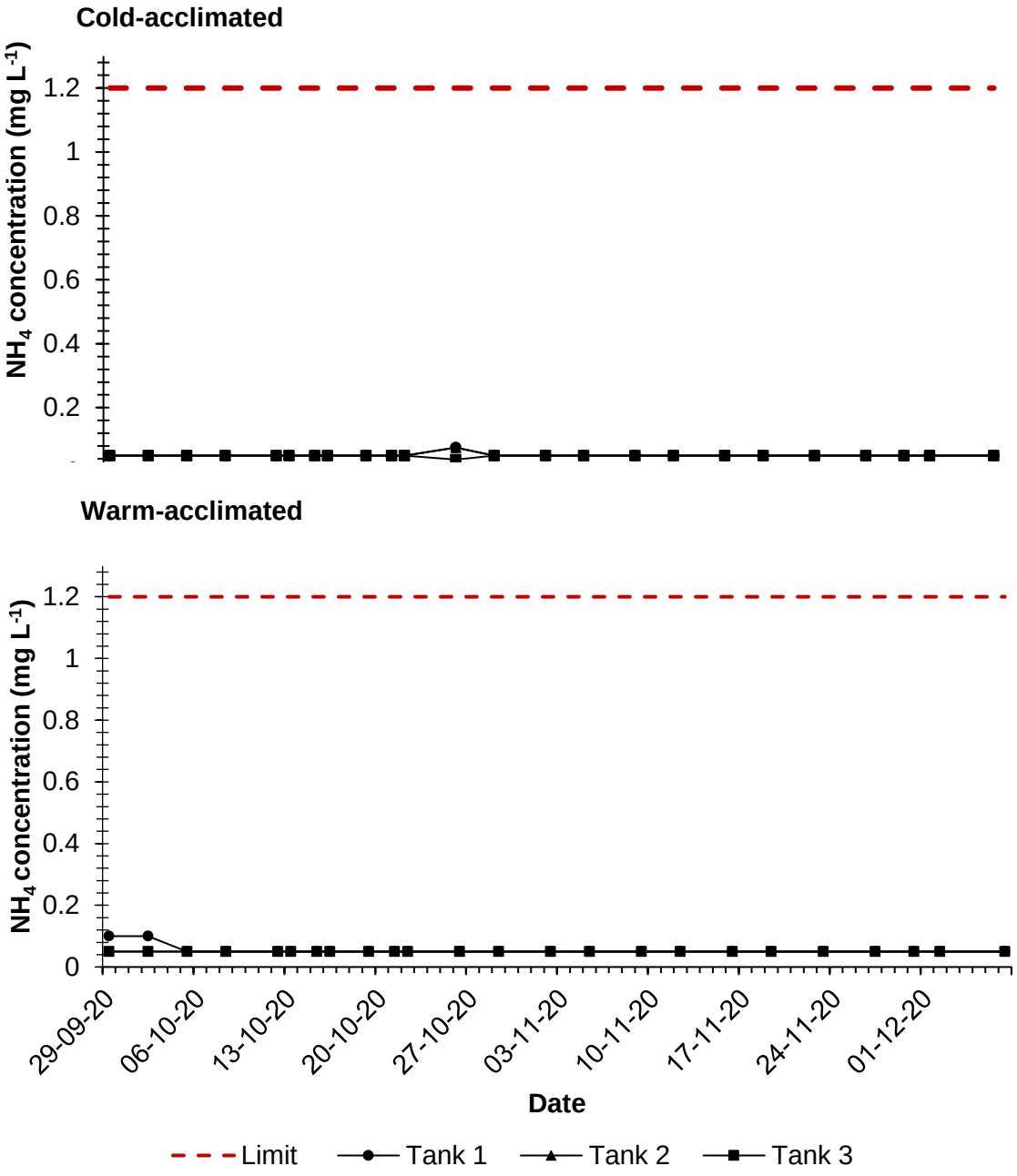

Figure A2: Ammonia (NH_4^+) concentrations in replicate tanks in cold-acclimated and warm-acclimated treatments, in relation to the upper concentration limits allowed (red dashed line).

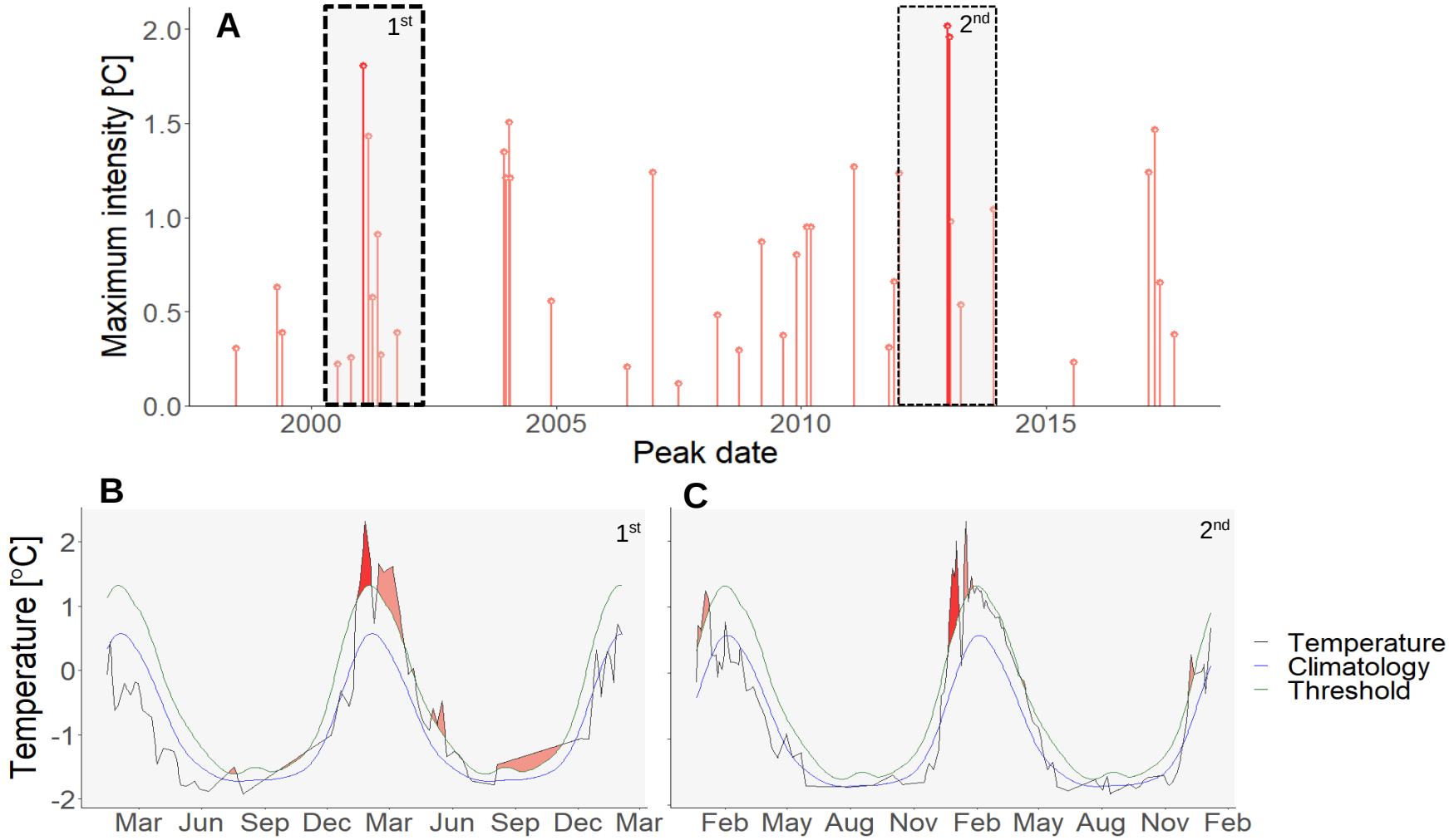

Figure A3: Marine Heatwave detection graphics from 'Heatwave R' package. Dotted outlines of events in panel A are shown in more detail in panels B and C (corresponding to events in 1st period in panel B and events in 2nd period in panel C).

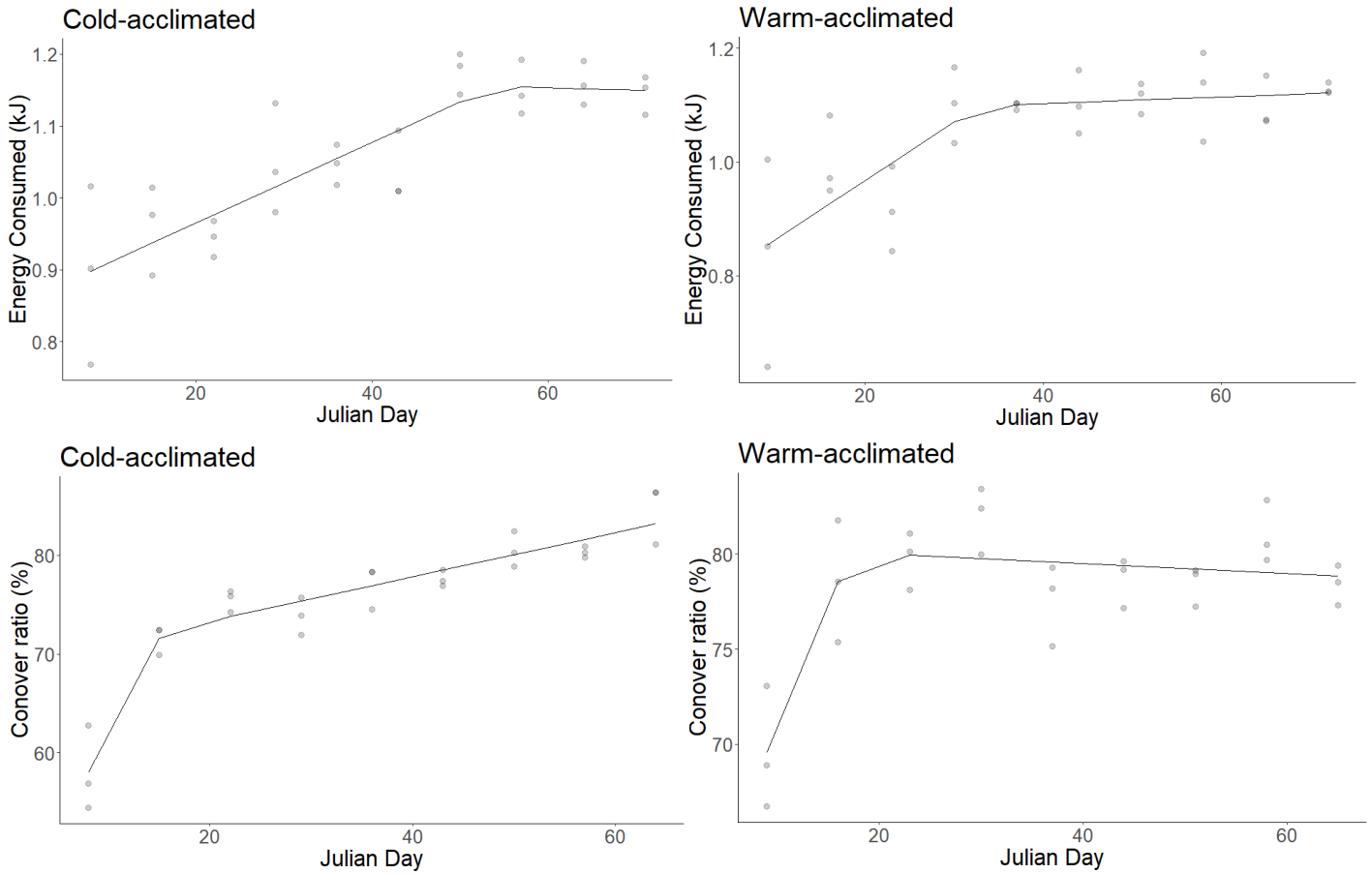

Figure A4: Linear regressions and breakpoints identified for the energy consumed (cold- and warm-acclimated) and Conover ratio (cold- and warm-acclimated) of animals feeding across three replicates in experimental treatments. Data were pooled within tank replicates for each time-point (n=5). Breakpoint locations and statistics for each regression detailed in Table S2.

Table A1: Nutritional content and equivalent energy content of artificial diet (Vitalis© Marine Grazer) fed to experiment population of *Sterechinus neumayeri*. AFDM = Ash Free Dry Mass.

Nutrition	**% in AFDM Diet**	**Equivalent Energy (kJ g^{-1})**	**Energy in Diet (kJ $AFDMg^{-1}$)**
Protein	65.9	17	11.20
Lipid	24.8	37	9.17
Carbohydrate	9.3	8	0.74
Total			21.12

Table A2: Results from t-tests comparing functional response (oxygen consumption, time taken to right, energy assimilation, Conover ratio and energy consumption) between cold- and warm-acclimated treatments at pre- peak- and post- marine heat wave simulations.

	Oxygen consumption Cold- vs Warm-acclimated	Time taken to right Cold- vs Warm-acclimated	Energy assimilation Cold- vs Warm-acclimated	Conover ratio Cold- vs Warm-acclimated	Energy consumption Cold- vs Warm-acclimated
Pre-MHW	$t_{(4)} = 2.4$, $p = 0.074$	$t_{(4)} = 1.4$, $p = 0.233$	$t_{(28)} = -2.98$, $p = 0.006$*	$t_{(22)} = 0.50$, $p = 0.626$	$t_{(28)} = -0.035$, $p = 0.972$
Peak-MHW	$t_{(57)} = 3.6$, $p < 0.001$*	$t_{(57)} = 0.74$, $p = 0.460$	$t_{(4)} = -0.29$, $p = 0.787$	$t_{(85)} = 2.46$, $p = 0.016$*	$t_{(88)} = -0.52$, $p = 0.601$
Post-MHW	$t_{(58)} = 2.2$, $p = 0.034$*	$t_{(4)} = 0.60$, $p = 0.584$	$t_{(79)} = -3.89$, $p < 0.001$*	$t_{(88)} = -0.812$, $p = 0.419$	$t_{(118)} = -0.26$, $p = 0.794$
Peak-MHW1	$t_{(4)} = 2.4$, $p = 0.074$	$t_{(17)} = 1.40$, $p = 0.179$	$t_{(4)} = -0.89$, $p = 0.426$	$t_{(27)} = 2.98$, $p = 0.006$*	$t_{(26)} = -0.62$, $p = 0.540$
Post-MHW1	$t_{(18)} = 0.97$, $p = 0.347$	$t_{(4)} = 1.67$, $p = 0.176$	$t_{(4)} = -2.83$, $p = 0.047$*	$t_{(28)} = 1.55$, $p = 0.133$	$t_{(28)} = -0.26$, $p = 0.799$
Peak-MHW2	$t_{(17)} = 1.9$, $p = 0.071$	$t_{(18)} = 0.83$, $p = 0.418$	$t_{(4)} = 1.16$, $p = 0.312$	$t_{(27)} = 4.05$, $p < 0.001$*	$t_{(26)} = 0.96$, $p = 0.347$

Post-MHW2	$t_{(18)} = 1.03$, $p = 0.319$	$t_{(4)} = 0.88$, $p = 0.425$	$t_{(28)} = -2.39$, $p = 0.024$*	$t_{(28)} = 0.51$, $p = 0.617$	$t_{(26)} = 1.11$, $p = 0.275$
Peak-MHW3	$t_{(4)} = 1.2$, $p = 0.288$	$t_{(4)} = -0.62$, $p = 0.573$	$t_{(28)} = -0.252$, $p = 0.803$	$t_{(4)} = -1.60$, $p = 0.183$	$t_{(28)} = -1.21$, $p = 0.237$
Post-MHW3	$t_{(18)} = 1.6$, $p = 0.124$	$t_{(17)} = -2.17$, $p = 0.045$*	$t_{(28)} = -0.557$, $p = 0.582$	$t_{(28)} = -2.43$, $p = 0.022$*	$t_{(28)} = -1.36$, $p = 0.186$
2^{o}C Warming	$t_{(74)} = -0.9$, $p = 0.355$	$t_{(75)} = 1.45$, $p = 0.151$	$t_{(6)} = 2.52$, $p = 0.045$*	$t_{(134)} = 2.95$, $p = 0.004$*	NA

Table A3: Results from ANOVA or non-parametric equivalent, as well as post-hoc tests, comparing functional response (oxygen consumption, time taken to right, energy assimilation, Conover ratio and energy consumption) between time points during the experiment (pre, peak and post MHW), between the peaks of MHW events (peak1, peak2 and peak3), and between recovery periods following MHW events (post1, post2 and post3).

	Oxygen consumption		Time taken to right		Energy assimilation		Conover		Energy consumption	
	Cold	Warm	Cold	Warm	Cold	Warm	Cold	Warm	Cold	Warm
Time	P < **0.001*** F= 9.70 df = 2, 65	p **< 0.001*** F= 21.6 df = 2, 63	p = 0.086 F= 2.56 df = 2,65	p = 0.607 F= 0.504 df = 2, 61	p **< 0.001*** F = 26.5 df = 2, 139	p **< 0.001*** F = 14.9 df = 2, 143	p **< 0.001*** F = 19.0 df = 2, 139	p **< 0.001*** F = 33.9 df = 2, 140	p = 0.082 F = 3.12 df = 1, 64	p = 0.142 F = 2.213 df = 1, 64
Pre-MHW vs Peak-MHW	**p < 0.001***	**p <0.001***			**p < 0.001***	**p < 0.001***	**p = 0.006***	**p < 0.001***	NA	
Pre-MHW vs Post-MHW	p = 0.156	p = 0.163			**p < 0.001***	**p < 0.001***	**p < 0.001***	**p < 0.001***		
Peak-MHW vs Post-MHW	**p =0.008***	**p <0.001***			**p = 0.001***	**p = 0.015***	**p = 0.004***	p = 0.275		
Peak MHWS	p = 0.477 F= 0.764 df = 2, 25	p = 0.892 F= 0.115 df = 2, 24	p = **0.018*** F= 4.76 df = 2, 25	p = 0.937 F= 0.07 df = 2, 24	p = **0.006*** F= 5.97 df = 2, 38	p **< 0.001** F = 14.54 df = 2, 39	p **< 0.001*** F = 44.3 df = 2, 39	p < **0.001*** F = 9.87 df = 2, 38	p **= 0.001*** F = 7.67 df = 2, 41	p = **0.001*** F = 8.08 df = 2, 41
MHW1 vs MHW2			p =0.991		p = 0.108	**p < 0.001***	**p < 0.001***	**p < 0.001***	p = 0.074	**p =0.003***
MHW1 vs MHW3			**p =0.031***		**p = 0.003***	**p = 0.013***	**p < 0.001***	**p = 0.017***	**p = 0.001***	**p = .002***
MHW2 vs MHW3			**p =0.043***		p = 0.347	p = 0.947	**p = 0.009***	p = 0.272	p = 0.233	p = 0.996

Post MHWS	p = 0.704 F= 0.356 df = 2, 25	p = 0.959 F= 0.042 df = 2, 25	p = 0.322 F= 1.185 df = 2, 25	p = 0.082 F= 2.81 df = 2, 22	p = **0.041*** F= 3.33 df = 2, 85	p **< 0.001*** F = 15.5 df = 2, 85	p < **0.001*** F = 7.69 df = 2, 84	p = 0.387 F = 0.961 df = 2, 84	p **< 0.001*** F = 9.75 df = 2, 86	p < **0.001*** F = 10.2 df = 2, 86
MHW1 vs MHW2					p = 0.091	**p < 0.001***	p = 0.307		p = 0.105	**p <0.001***
MHW1 vs MHW3					**p = 0.029***	**p < 0.001***	**p < 0.001***		**p <0.001***	**p <0.001***
MHW2 vs MHW3					p = 0.871	p = 0.379	**p = 0.010***		**p = 0.050***	p = 0.967

A4: Summary statistics for segmented linear regression relationships between energy consumed and the Conover ratio of *Sterechinus neumayeri* and experimental duration, expressed as Julian day, date, MHW ID and temperature. β indicates the slope of the linear regression lines before the breakpoint (Slope_1) and after the breakpoint (Slope_2); SE_a indicates standard error for the intercept and slopes; df = degrees of freedom; bold p-values indicate significant relationships ($p < 0.05$) between temperature and the variable measured and bold Davies p-values represent a significant change ($p < 0.05$) in the gradient of the slope of segmented regressions. Values in the column BP indicate the localisation of the breakpoint; SE_b (standard error) and R^2 refers to the goodness of fit for the entire model.

	β	SE_a	p-value	BP	SE_b	R^2	Davies p-value
Energy Consumed, Cold (Intercept) Slope_1 Slope_2	 0.853 0.006 -0.000	 0.029 0.001 0.003	df=26 <0.001 **<0.001** 0.923	53.9 JD 20/11/20 Peak MHW3 2.0°C	0.059	0.703	0.153
Energy Consumed, Warm (Intercept) Slope_1 Slope_2	 0.761 0.010 0.001	 0.062 0.003 0.002	df=26 <0.001 **<0.001** 0.712	32.7 JD 30/10/20 Peak MHW2 3.5°C	0.080	0.544	**0.027**
Conover ratio, Cold (Intercept) Slope_1 Slope_2	 42.5 1.94 0.22	 3.157 0.263 0.035	df=23 <0.001 **<0.001** **<0.001**	15.4 JD 13/10/20 Post MHW1 1.0°C	2.252	0.911	**< 0.001**
Conover ratio, Warm (Intercept) Slope_1 Slope_2	 58.0 1.28 -0.03	 3.41 0.263 0.035	df=23 <0.001 **<0.001** 0.476	17.2 JD 15/10/20 Peak MHW1 4.0°C	2.254	0.646	**< 0.001**

Table A5: Magnitude of increase (%) in mean oxygen consumption rate (µmol/hr/gAFDM) of cold- and warm-acclimated *Sterechinus neumayeri* during simulated heatwave events (MHW), relative to the previous recovery period (pre/post-MHW).

	Cold-acclimated		**Warm-acclimated**	
	Oxygen consumption rate (µmol/hr/gAFDM)	% increase	Oxygen consumption rate (µmol/hr/gAFDM)	% increase
Pre-MHW	1.18		1.76	
Peak-MHW1	2.23	89.7	3.40	93.2
Post-MHW1	2.04		2.32	
Peak-MHW2	2.76	35.0	3.53	52.6
Post-MHW2	1.75		2.13	
Peak-MHW3	2.71	54.7	3.42	60.7

Appendix D

Supplementary for reproductive data, Chapter 3 and 4

Text A1: The following data presented are results from experiments conducted in Chapter 3 and 4 concerning the reproductive impacts of warming. These data are to support the findings reported in the data chapters, but also provide novel insights that provide a basis for future work and experimentation. Results are first presented from the experiment carried out for Chapter 3, where temperatures were raised at three onset rates (0.3^{o}C day^{-1}, 0.5^{o}C day^{-1} and 1 ^{o}C day^{-1}). In these treatments, urchins were collected and preserved once the reached their critical thermal maximum (CT_{max}) (n = 30). Urchins were also collected and preserved from control treatments on the last day of the experiment, when all urchins from the warming treatment had reached CT_{max} (n = 20). As a references for maturation occurring during the experiment, urchins were preserved at the start of the experiment (n = 20). All methods for gonad index, oocyte size and male maturity were carried out as per Chapter 2. I addition to this, urchins were collected from the environment at the start of the experiment and at the end, to understand how aquarium conditions affected the urchins. The second half of the results presented are from the experiment carried out for Chapter 4, where urchins were initially acclimated to 0^{o}C and 2^{o}C before being exposed to three consecutive acute warming of +2^{o}C above acclimated temperatures. Urchins were collected and preserved following acclimation (n = 20) and then following the exposure to the acute warming events (n = 20). As above, all methods for gonad index, oocyte size and male maturity were carried out as per Chapter 2.

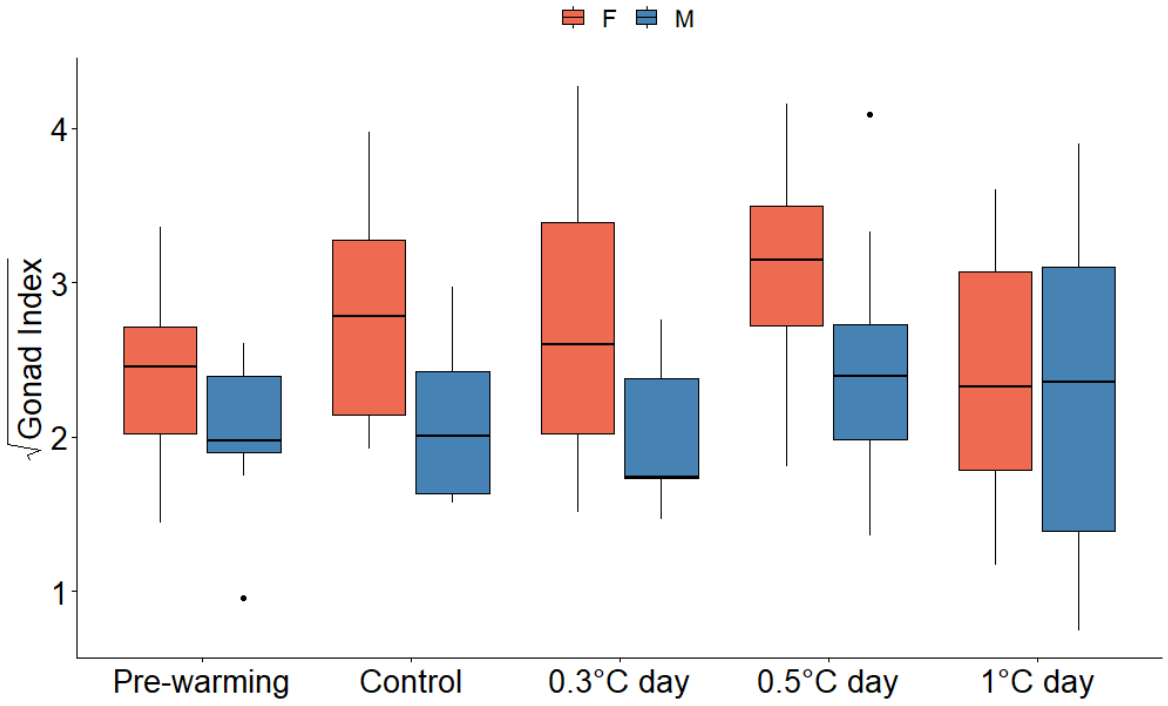

Figure A1**:** Gonad index *Sterechinus neumayeri* pre-warming (14th January) and post-warming at three warming rates where temperature increased by 0.3ºC day^{-1}, 0.5ºC day^{-1} and 1ºC day^{-1} and control treatments where urchins were not warmed. Post-warming urchins were sampled when CT_{max} was reached (0.3ºC day^{-1} = 16th – 23rd February, 0.5ºC day^{-1} = 4th – 8th February, 1ºC day^{-1} = 26th – 28th January), and control urchins were sampled at the end of the experiment (24th February). Gonad index has been square root transformed. Data are displayed as boxplots with the central line in the boxes representing the median value, the upper and lower hinges representing the 25th and 75th percentiles, and the upper/lower whiskers representing the largest/smallest value, no further than 1.5 times the interquartile range from the hinge. All data outside these ranges are plotted as points. Males and females plotted separately, where red boxes representing females and blue boxes representing males.

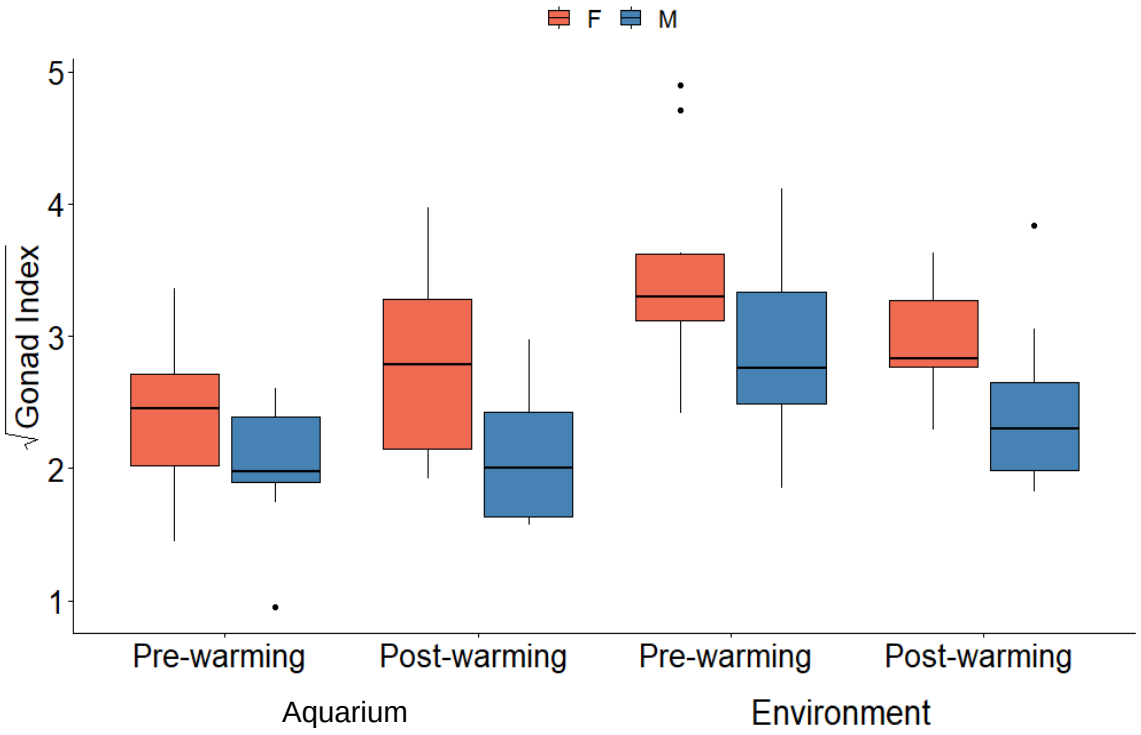

Figure A2**:** Gonad index *Sterechinus neumayeri* sampled from the aquarium, pre-warming experiment (14th January) and post-warming experiment (24th February), and sampled from the environment, pre-warming experiment (14th January) and post-warming experiment (25th February) (NB these urchins were controls and were not warmed). Gonad index has been square root transformed. Data are displayed as boxplots with the central line in the boxes representing the median value, the upper and lower hinges representing the 25th and 75th percentiles, and the upper/lower whiskers representing the largest/smallest value, no further than 1.5 times the interquartile range from the hinge. All data outside these ranges are plotted as points. Males and females plotted separately, where red boxes representing females and blue boxes representing males.

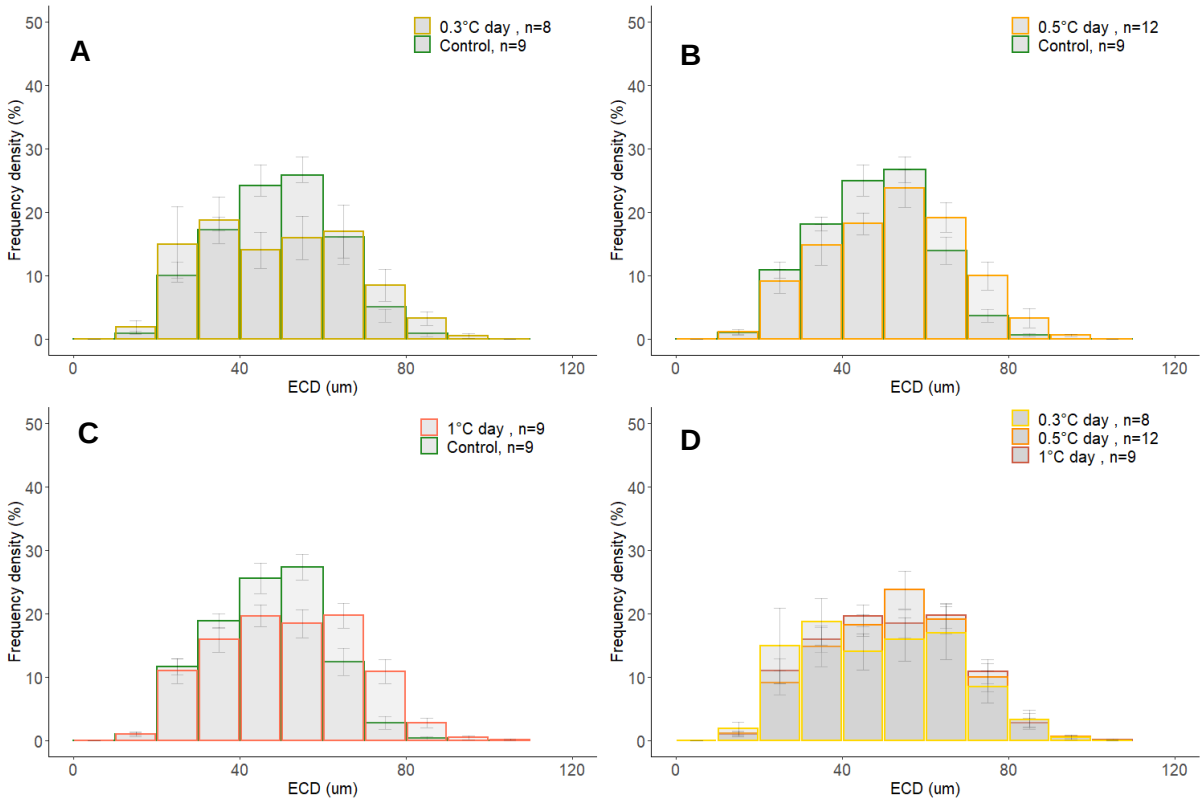

Figure A3: Oocyte size distributions (based on the calculation of Equivalent Circular Diameter, µm) of *Sterechinus neumayeri* displayed as histograms of female oocyte size percentage frequencies (%) in A) ambient controls overlayed with treatment where temperature increased by 0.3ºC day^{-1} warming, B) ambient controls overlayed with treatment where temperature increased by 0.5ºC day^{-1}, C) ambient controls overlayed with treatment where temperature increased by 1ºC day^{-1}, and D) warming treatments where temperature increased by 0.3ºC day-1, 0.5ºC day^{-1} and 1ºC day^{-1}. Control ECD size distributions were estimated to align with the sample dates of the warming treatments, where each bin frequency was estimated based the linear trajectory from pre-warming (4th January) to post-warming (24th February). Error bars are ± standard error. n = total number of females included in the distribution.

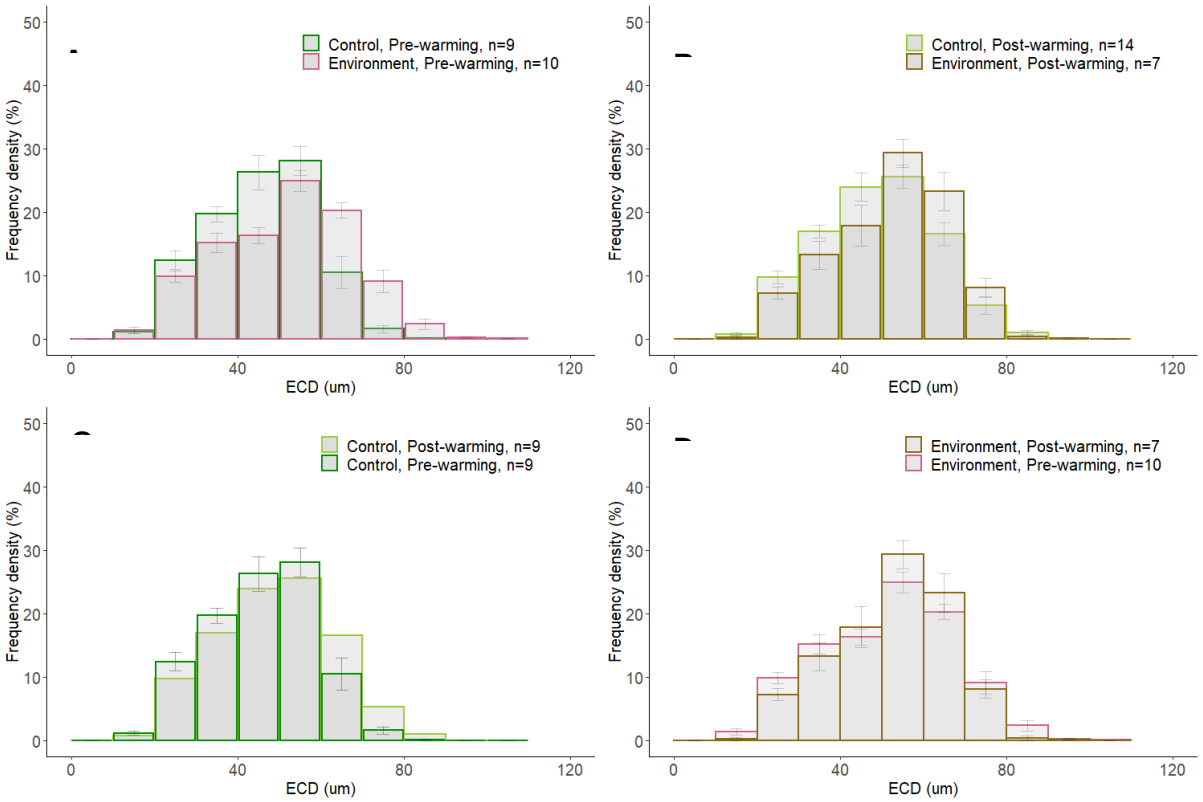

Figure A4: Oocyte size distributions (based on the calculation of Equivalent Circular Diameter, µm) of *Sterechinus neumayeri* displayed as histograms of female oocyte size percentage frequencies (%) in A) ambient controls overlayed with urchins sampled from the environment, pre-warming experiment (14th January) B) ambient controls overlayed with urchins sampled from the environment, post-warming experiment (24th and 25th February), C) ambient controls pre- and post-warming experiment, D) urchins sampled from the environment, pre- and post-warming experiment. (NB these urchins were controls and were not warmed). Error bars are ± standard error. n = total number of females included in the distribution.

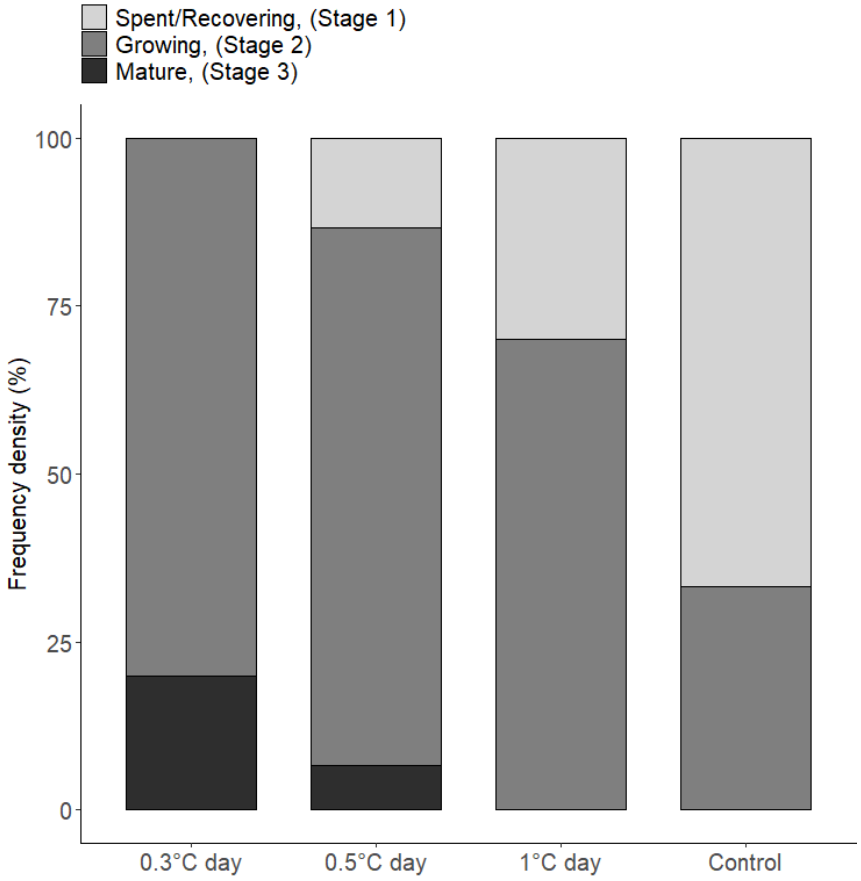

Figure A5: Male maturity stages of *Sterechinus neumayeri* in three different warming rates and ambient control conditions. Urchins were sampled when CT_{max} was reached (0.3°C day^{-1} = 16th – 23rd February, 0.5°C day^{-1} = 4th – 8th February, 1°C day^{-1} = 26th – 28th January), and control urchins were sampled at the end of the experiment (24th February).

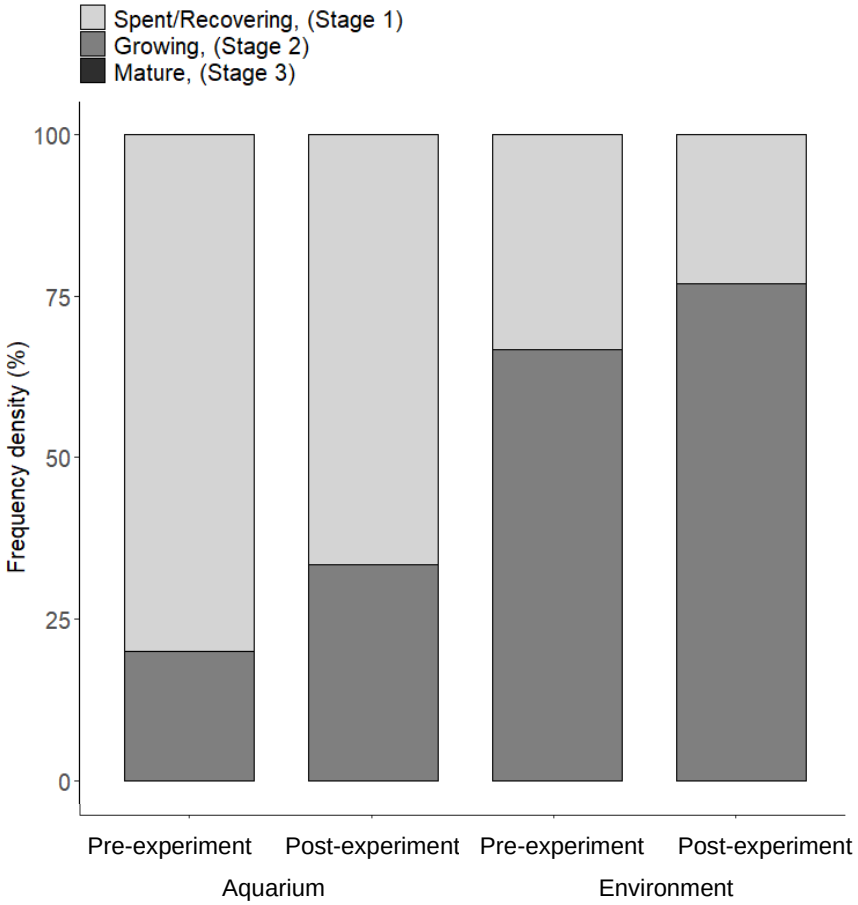

Figure A6: Male maturity stages of *Sterechinus neumayeri* sampled from the aquarium, pre-experiment (14th January) and post- experiment (24th February), and sampled from the environment, pre-experiment (14th January) and post-experiment (25th February) (NB these urchins were controls and were not warmed).

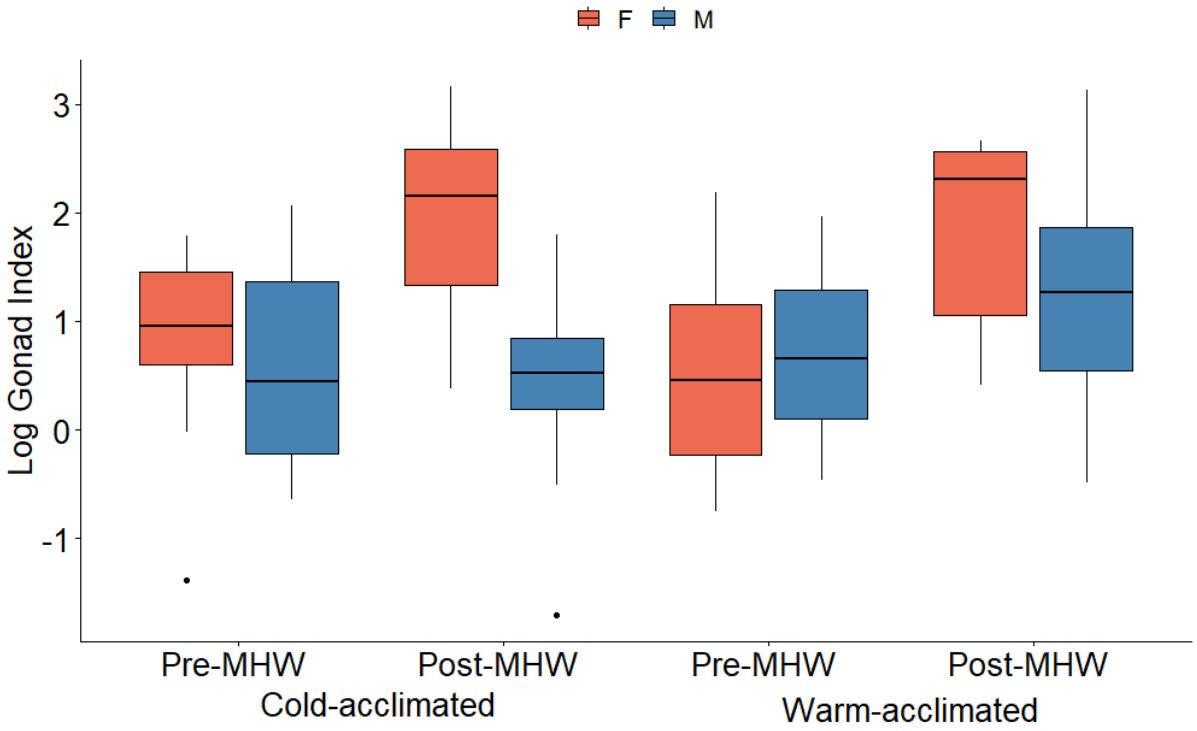

Figure A7**:** Gonad index *Sterechinus neumayeri* sampled from cold-acclimated urchins (0ºC for 8 months) and warm-acclimated urchins (2ºC for 8 months) prior to marine heatwave simulations (pre-MHW), and after three marine heatwave simulations (post-MHW). Gonad index has been log transformed. Data are displayed as boxplots with the central line in the boxes representing the median value, the upper and lower hinges representing the 25th and 75th percentiles, and the upper/lower whiskers representing the largest/smallest value, no further than 1.5 times the interquartile range from the hinge. All data outside these ranges are plotted as points. Males and females plotted separately, where red boxes representing females and blue boxes representing males.

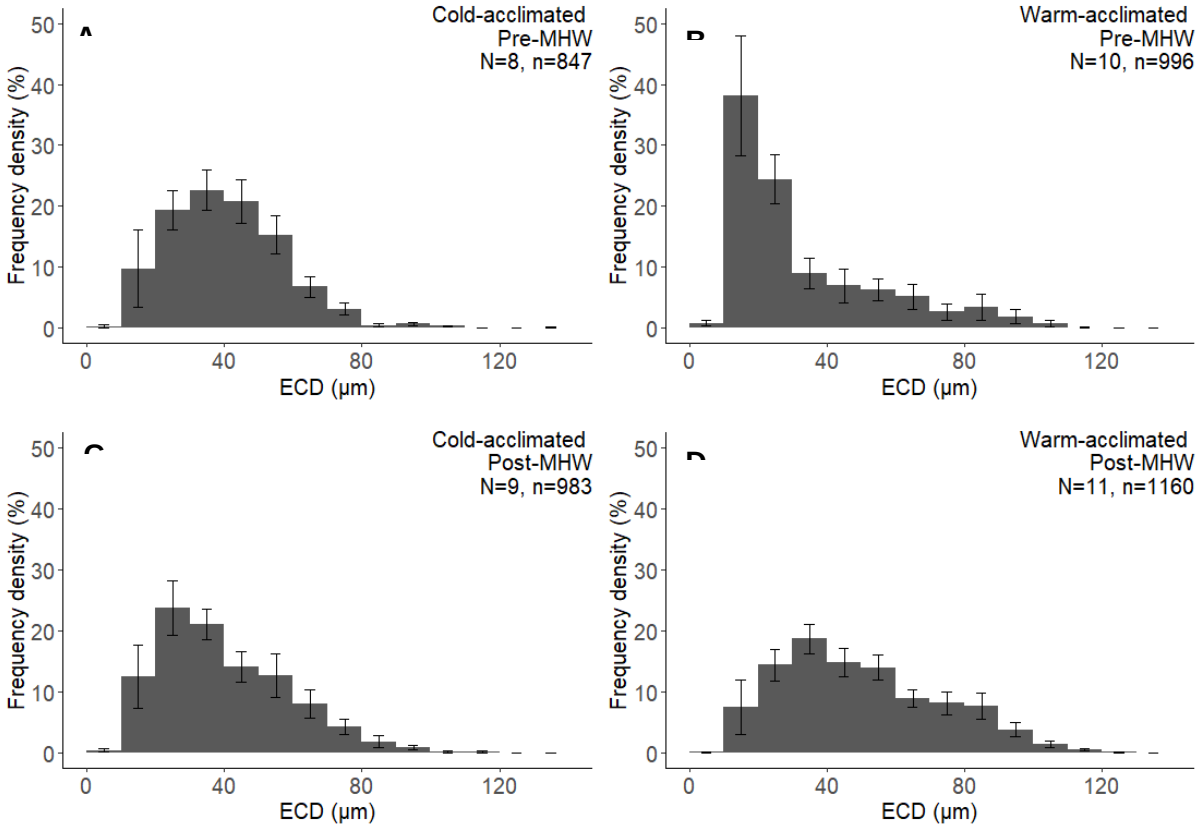

Figure A8: Oocyte size distributions (based on the calculation of Equivalent Circular Diameter, µm) displayed as histograms of female oocyte size percentage frequencies (%) for A) cold-acclimated urchins (0ºC for 8 months), pre-MHW (prior to marine heatwave simulations), B) warm-acclimated urchins (2ºC for 8 months), pre-MHW, C) cold-acclimated urchins, post-MHW (after three marine heatwave simulations), D) warm-acclimated urchins, post-MHW. Error bars are ± standard error. N = total number of females included in the distribution, n = total number of oocytes measured in the distribution.

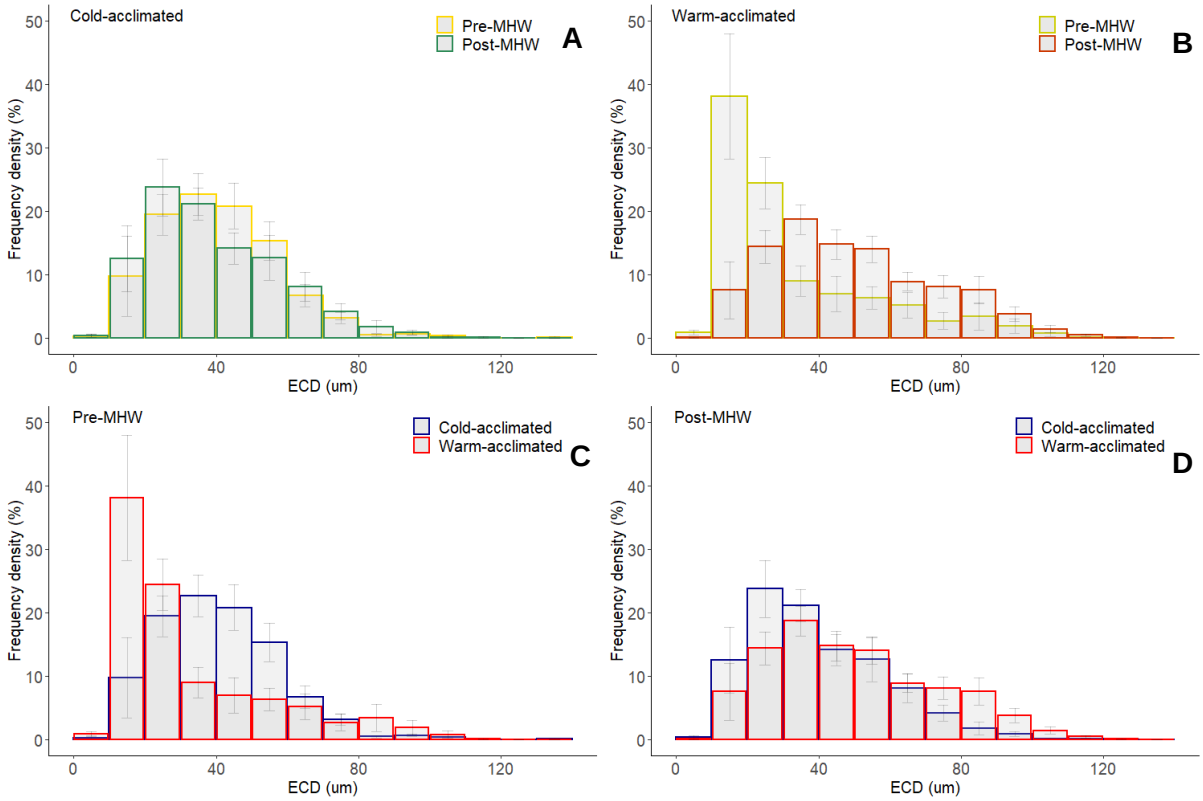

Figure A9: Oocyte size distributions (based on the calculation of Equivalent Circular Diameter, µm) of *Sterechinus neumayeri* displayed as histograms of female oocyte size percentage frequencies (%) in A) cold-acclimated urchins (0ºC for 8 months), pre-MHW (prior to marine heatwave simulations) and post-MHW (after three marine heatwave simulations), (B) warm-acclimated urchins (2ºC for 8 months), pre-MHW and post-MHW, C) cold- and warm-acclimated urchins, pre-MHWs, and D) cold- and warm-acclimated urchins, post-MHWs. Error bars are ± standard error. n = total number of females included in the distribution.

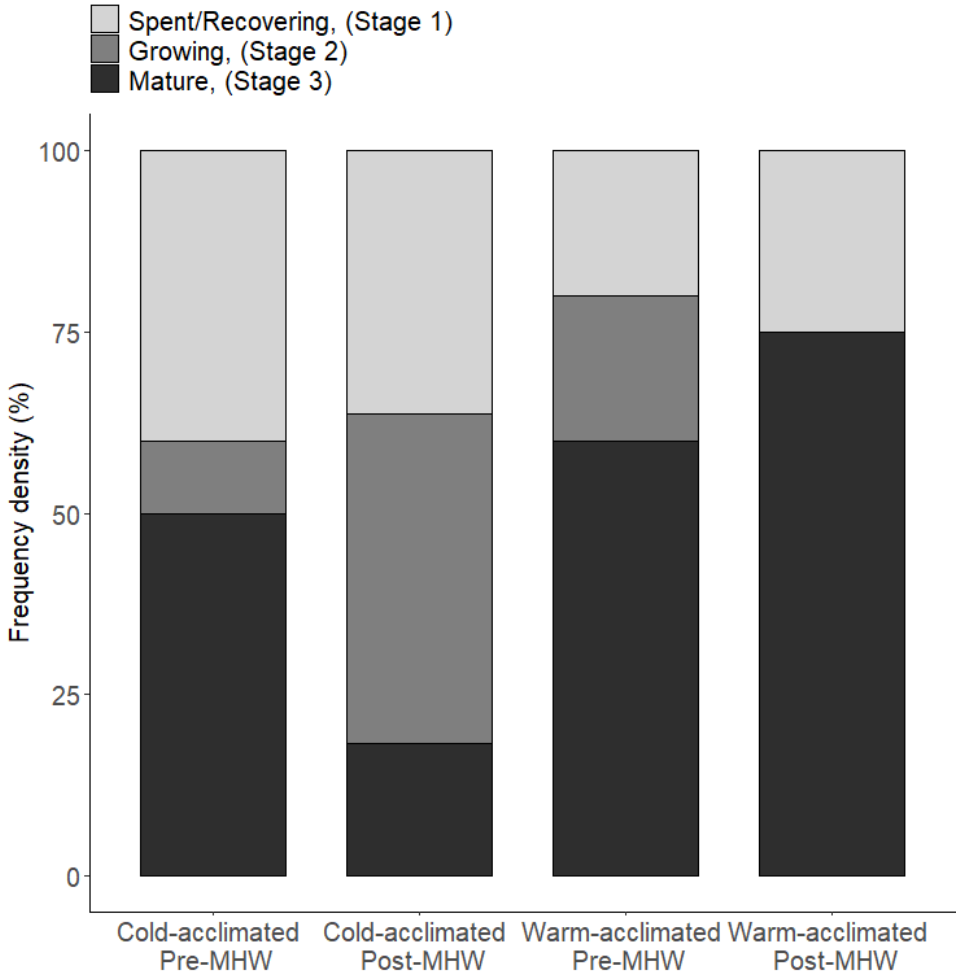

Figure A10: Male maturity stages of *Sterechinus neumayeri* in cold-acclimated urchins (0°C for 8 months), pre-MHW (prior to marine heatwave simulations) and post-MHW (after three marine heatwave simulations), and warm-acclimated urchins (2°C for 8 months), pre-MHW and post-MHW.

List of References

Abele, D., Tesch, C., Wencke, P., & Pörtner, H. O. (2001). How does oxidative stress relate to thermal tolerance in the Antarctic bivalve Yoldia eightsi? *Antarctic Science*, *13*(2), 111–118. https://doi.org/10.1017/S0954102001000189

Abram, N. J., McGregor, H. V., Tierney, J. E., Evans, M. N., McKay, N. P., Kaufman, D. S., Thirumalai, K., Martrat, B., Goosse, H., Phipps, S. J., Steig, E. J., Kilbourne, K. H., Saenger, C. P., Zinke, J., Leduc, G., Addison, J. A., Mortyn, P. G., Seidenkrantz, M. S., Sicre, M. A., … Von Gunten, L. (2016). Early onset of industrial-era warming across the oceans and continents. *Nature*, *536*(7617), 411–418. https://doi.org/10.1038/nature19082

Agüera, A., Ahn, I. Y., Guillaumot, C., & Danis, B. (2017). A Dynamic Energy Budget (DEB) model to describe Laternula elliptica (King, 1832) seasonal feeding and metabolism. *PLoS ONE*, *12*(8), 1–5. https://doi.org/10.1371/journal.pone.0183848

Ahmed, M., Anchukaitis, K. J., Asrat, A., Borgaonkar, H. P., Braida, M., Buckley, B. M., Büntgen, U., Chase, B. M., Christie, D. A., Cook, E. R., Curran, M. A. J., Diaz, H. F., Esper, J., Fan, Z. X., Gaire, N. P., Ge, Q., Gergis, J., González-Rouco, J. F., Goosse, H., … Zorita, E. (2013). Continental-scale temperature variability during the past two millennia. *Nature Geoscience*, *6*(5), 339–346. https://doi.org/10.1038/ngeo1797

Ainley, D. G., Nur, N., Eastman, J. T., Ballard, G., Parkinson, C. L., Evans, C. W., & Devries, A. L. (2013). Decadal trends in abundance, size and condition of Antarctic toothfish in McMurdo Sound, Antarctica, 1972 – 2011. *Fish and Fisheries*, *14*, 343–363. https://doi.org/10.1111/j.1467-2979.2012.00474.x

Allen, J. L., Chown, S. L., Janion-Scheepers, C., & Clusella-Trullas, S. (2016). Interactions between rates of temperature change and acclimation affect latitudinal patterns of warming tolerance. *Conservation Physiology*, *4*(1), 1–14. https://doi.org/10.1093/conphys/cow053

Allen, M., Babiker, M., Chen, Y., Coninck, H. de, Connors, S., Diemen, R. van, Dube, O. P., Ebi, K., Engelbrecht, F., Ferrat, M., & Zickfeld, K. (2018). Global Warming of 1.5°C: Summary for Policymakers. *IPCC*. https://www.ipcc.ch/sr15/chapter/summary-for-policy-makers/

Alley, R. B. (2000). Ice-core evidence of abrupt climate changes. *Proceedings of the National Academy of Sciences of the United States of America*, *97*(4), 1331–1334. https://doi.org/10.1073/pnas.97.4.1331

Alturkistani, H. A., Tashkandi, F. M., & Mohammedsaleh, Z. M. (2015). Histological Stains: A Literature Review and Case Study. *Global Journal of Health Science*, *8*(3), 72–79. https://doi.org/10.5539/gjhs.v8n3p72

Angilletta M. J., (2001) Thermal and physiological constraints on energy assimilation in a widespread lizard *(Sceloporus undulatus*). *Ecology,* 82:3044–3056. https://doi.org/10.2307/2679833

Ardor Bellucci, L. M., & Smith, N. F. (2019). Crawling and righting behavior of the subtropical sea star *Echinaster (Othilia) graminicola*: effects of elevated temperature. *Marine Biology*, *166*(11), 1–9. https://doi.org/10.1007/s00227-019-3591-4

Arntz, W. E., Brey, T., Gerdes, D., Gorny, M., Gutt, J., Hain, S., & Klages, M. (1992). Patterns of life history and population dynamics of benthic invertebrates under the high Antarctic conditions of the Weddel Sea. *Marine Eutrophication and Population Dynamics*, *370*, 221–230.

Aronson, R. B., Thatje, S., Clarke, A., Peck, L. S., Blake, D. B., Wilga, C. D., & Seibel, B. A. (2007). Climate Change and Invasibility of the Antarctic Benthos. *Annual Review of Ecology, Evolution, and Systematics*, *38*(1), 129–154. https://doi.org/10.1146/annurev.ecolsys.38.091206.095525

Azad, A. K., Pearce, C. M., & McKinley, R. S. (2011). Effects of diet and temperature on ingestion, absorption, assimilation, gonad yield, and gonad quality of the purple sea urchin (Strongylocentrotus purpuratus). *Aquaculture*, *317*(1–4), 187–196. https://doi.org/10.1016/j.aquaculture.2011.03.019

Azra, M. N., Chen, J. C., Ikhwanuddin, M., & Abol-Munafi, A. B. (2018). Thermal tolerance and locomotor activity of blue swimmer crab *Portunus pelagicus* instar reared at different temperatures. *Journal of Thermal Biology*, *74*(January), 234–240. https://doi.org/10.1016/j.jtherbio.2018.04.002

Bailey, D. M. (2001). *The thermal dependence of swimming and muscle physiology in temperate and Antarctic scallops Submitted for the degree of Doctor of Philosophy to the University of St . Andrews by ,*. University of St Andrews.

Baird, H. P., & Stark, J. S. (2013). Population dynamics of the ubiquitous Antarctic benthic amphipod Orchomenella franklini and its vulnerability to environmental change. *Polar Biology*, *36*(2), 155–167. https://doi.org/10.1007/s00300-012-1246-8

Balogh, R., Wolfe, K., & Byrne, M. (2019). Gonad development and spawning of the vulnerable commercial sea cucumber, *Stichopus herrmanni*, in the southern Great Barrier Reef. *Journal of the Marine Biological Association of the United Kingdom*,

99(2), 487–495. https://doi.org/10.1017/S0025315418000061

Bard, B., & Kieffer, J. (2019). The effects of repeat acute thermal stress on the critical thermal maximum (CTmax) and physiology of juvenile shortnose sturgeon *Acipenser brevirostrum* Journal: *Canadian Journal of Zoology*, *97*(6), 567–572. https://doi.org/10.1139/cjz-2018-0157

Barnes, D. K. A., & Brockington, S. (2003). Zoobenthic biodiversity, biomass and abundance at Adelaide Island, Antarctica. *Marine Ecology Progress Series*, *249*(Gray 2001), 145–155. https://doi.org/10.3354/meps249145

Barnes, D. K. A., Webb, K. E., & Linse, K. (2007). Growth rate and its variability in erect Antarctic bryozoans. *Polar Biology*, *30*(8), 1069–1081. https://doi.org/10.1007/s00300-007-0266-2

Bell, G. (2017). Evolutionary Rescue. *Annual Review of Ecology, Evolution, and Systematics*, *48*, 605–627. https://doi.org/10.1146/annurev-ecolsys-110316-023011

Bigatti, C., Penchaszadeh, P. E., & Mercuri, G. (2001). Aspects of the gonadal cycle in the Antarctic bivalve Laternula elliptica. *Journal of Shellfish Research*, *20*(1), 283–287.

Bilbao, R. A. F., Gregory, J. M., Bouttes, N., Palmer, M. D., & Stott, P. (2019). Attribution of ocean temperature change to anthropogenic and natural forcings using the temporal , vertical and geographical structure. *Climate Dynamics*, *53*(9), 5389–5413. https://doi.org/10.1007/s00382-019-04910-1

Bilyk, K. T., & DeVries, A. L. (2011). Heat tolerance and its plasticity in Antarctic fishes. *Comparative Biochemistry and Physiology - A Molecular and Integrative Physiology*, *158*(4), 382–390. https://doi.org/10.1016/j.cbpa.2010.12.010

Bilyk, K. T., Evans, C. W., & DeVries, A. L. (2012a). Heat hardening in Antarctic notothenioid fishes. *Polar Biology*, *35*(9), 1447–1451. https://doi.org/10.1007/s00300-012-1189-0

Bilyk, K. T., Evans, C. W., & DeVries, A. L. (2012b). Heat hardening in Antarctic notothenioid fishes. *Polar Biology*, *35*(9), 1447–1451. https://doi.org/10.1007/s00300-012-1189-0

Bopp, L., Resplandy, L., Orr, J. C., Doney, S. C., Dunne, J. P., Gehlen, M., Halloran, P., Heinze, C., Ilyina, T., Séférian, R., Tjiputra, J., & Vichi, M. (2013). Multiple stressors of ocean ecosystems in the 21st century: Projections with CMIP5 models. *Biogeosciences*, *10*(10), 6225–6245. https://doi.org/10.5194/bg-10-6225-2013

Bosch, I., Beauchamp, K. A., Steele, M. E., & Pearse, J. S. (1987). Development,

metamorphosis, and seasonal abundance of embryos and larvae of the Antarctic sea urchin *Sterechinus Neumayeri*. *The Biological Bulletin*, *173*(1), 126–135. https://doi.org/10.2307/1541867

Bowden, D. A., Clarke, A., Peck, L. S., & Barnes, D. K. A. (2006). Antarctic sessile marine benthos: Colonisation and growth on artificial substrata over three years. *Marine Ecology Progress Series*, *316*(July), 1–16. https://doi.org/10.3354/meps316001

Bowler, K. (2005). Acclimation, heat shock and hardening. *Journal of Thermal Biology*, *30*(2), 125–130. https://doi.org/10.1016/j.jtherbio.2004.09.001

Boyce, S. J., Murray, A. W. A., & Peck, L. S. (2000). Digestion rate, gut passage time and absorption efficiency in the Antarctic spiny plunderfish. *Journal of Fish Biology*, *57*(4), 908–929. https://doi.org/10.1006/jfbi.2000.1357

Brey, T., Pearse, J., Basch, L., McClintock, J., & Slattery, M. (1995). Growth and production of Sterechinus neumayeri (Echinoidea: Echinodermata) in McMurdo Sound, Antarctica. *Marine Biology*, *124*(2), 279–292. https://doi.org/10.1007/BF00347132

Brey, Thomas, & Clarke, A. (1993). Population dynamics of marine benthic invertebrates in Antarctic and subantarctic environments: Are there unique adaptations? *Antarctic Science*, *5*(3), 253–266. https://doi.org/10.1017/S0954102093000343

Brockington, S. (2001). *The seasonal ecology and physiology of* Sterechinus neumayeri *(Echinodermata; Echinoidea) at Adelaide Island, Antarctica. PhD thesis The Open University.*

Brockington, S., & Clarke, A. (2001). The relative influence of temperature and food on the metabolism of a marine invertebrate. *Journal of Experimental Marine Biology and Ecology*, *258*(1), 87–99. https://doi.org/10.1016/S0022-0981(00)00347-6

Brockington, S., Clarke, A., & Chapman, A. L. G. (2001). Seasonality of feeding and nutritional status during the austral winter in the Antarctic sea urchin *Sterechinus neumayeri*. *Marine Biology*, *139*(1), 127–138. https://doi.org/10.1007/s002270100561

Brockington, S., Peck, L. S., & Tyler, P. A. (2007). Gametogenesis and gonad mass cycles in the common circumpolar Antarctic echinoid *Sterechinus neumayeri*. *Marine Ecology Progress Series*, *330*, 139–147. https://doi.org/10.3354/meps330139

Bronstein, O., Kroh, A., & Loya, Y. (2016). Reproduction of the long-spined sea urchin *Diadema setosum* in the Gulf of Aqaba - Implications for the use of gonad-indexes. *Scientific Reports*, *6*(May), 1–11. https://doi.org/10.1038/srep29569

Brothers, C. J., & McClintock, J. (2015). The effects of climate-induced elevated seawater temperature on the covering behavior, righting response, and Aristotle's lantern reflex of the sea urchin *Lytechinus variegatus*. *Journal of Experimental Marine Biology and Ecology*, *467*, 33–38. https://doi.org/10.1016/j.jembe.2015.02.019

Brown, J., Gillooly, J. ., Allen, A. ., Savage, V. ., & West, G. . (2004). Towards a metabolic theory of ecology. *Ecology*, *85*(7), 1771–1789.

Brown, M., Kawaguchi, S., Candy, S., Yoshida, T., Virtue, P., & Nicol, S. (2013). Long-term effect of photoperiod , temperature and feeding regimes on the respiration rates of Antarctic Krill (*Euphausia superba*). *Open Journal of Marine Science*, *3*, 40–51. https://doi.org/10.4236/ojms.2013.32A005

Burger, J. R., Hou, C., & Brown, J. (2019). Toward a metabolic theory of life history. *Proceedings of the National Academy of Sciences of the United States of America*, *116*(52), 26653–26661. https://doi.org/10.1073/pnas.1907702116

Burnham, K. P., & Anderson, D. R. (2002). Model selection and multimodel inference. A practical information-theoretical approach. In *Model Selection and Multimodel Inference* (Second). Springer. https://doi.org/10.1007/978-0-387-22456-5_7

Burrows, M. T., Schoeman, D. S., Buckley, L. B., Moore, P., Poloczanska, E. S., Brander, K. M., Brown, C., Bruno, J. F., Duarte, C. M., Halpern, B. S., Holding, J., Kappel, C. V., Kiessling, W., O'Connor, M. I., Pandolfi, J. M., Parmesan, C., Schwing, F. B., Sydeman, W. J., & Richardson, A. J. (2011). The pace of shifting climate in marine and terrestrial ecosystems. *Science*, *334*, 652–655. https://doi.org/10.1126/science.1210288

Calosi, P., Bilton, D. T., & Spicer, J. I. (2008). Thermal tolerance, acclimatory capacity and vulnerability to global climate change. *Biology Letters*, *4*(1), 99–102. https://doi.org/10.1098/rsbl.2007.0408

Calosi, P., Bilton, D. T., Spicer, J. I., Votier, S. C., & Atfield, A. (2010). What determines a species' geographical range? Thermal biology and latitudinal range size relationships in European diving beetles (Coleoptera: Dytiscidae). *Journal of Animal Ecology*, *79*(1), 194–204. https://doi.org/10.1111/j.1365-2656.2009.01611.x

Caputi, N., Jackson, G., & Peace, A. (2014). The marine heat wave off Western Australia during the summer of 2010/11 – 2 years on. In *Fisheries Research Report [Western Australia]* (Issue 250).

Cavanagh, R. D., Murphy, E. J., Bracegirdle, T. J., Turner, J., Knowland, C. A., Corney, S. P., Smith, W. O., Waluda, C. M., Johnston, N. M., Bellerby, R. G. J., Constable, A. J.,

Costa, D. P., Hofmann, E. E., Jackson, J. A., Staniland, I. J., Wolf-Gladrow, D., & Xavier, J. C. (2017). A synergistic approach for evaluating climate model output for ecological applications. *Frontiers in Marine Science*, *4*. https://doi.org/10.3389/fmars.2017.00308

Chapelle, G., Peck, L. S., & Clarke, A. (1994). Effects of feeding and starvation on the metabolic rate of the necrophagous Antarctic amphipod Waldeckia obesa (Chevreux, 1905). *Journal of Experimental Marine Biology and Ecology*, *183*(1), 63–76. https://doi.org/10.1016/0022-0981(94)90157-0

Charnov, E. L., Warne, R., & Moses, M. (2007). Lifetime reproductive effort. *American Naturalist*, *170*(6). https://doi.org/10.1086/522840

Cheng, M. C. F., Sarà, G., & Williams, G. A. (2018). Combined effects of thermal conditions and food availability on thermal tolerance of the marine bivalve, *Perna viridis*. *Journal of Thermal Biology*, *78*(May), 270–276. https://doi.org/10.1016/j.jtherbio.2018.10.014

Clark, G., Stark, J. S., Johnston, E. L., Runcie, J. W., Goldsworthy, P. M., Raymond, B., & Riddle, M. J. (2013). Light-driven tipping points in polar ecosystems. *Global Change Biology*, *19*(12), 3749–3761. https://doi.org/10.1111/gcb.12337

Clark, M. S., Fraser, K. P. P., & Peck, L. S. (2008). Lack of an HSP70 heat shock response in two Antarctic marine invertebrates. *Polar Biology*, *31*(9), 1059–1065. https://doi.org/10.1007/s00300-008-0447-7

Clark, M. S., Husmann, G., Thorne, M. A. S., Burns, G., Truebano, M., Peck, L. S., Abele, D., & Philipp, E. E. R. (2013). Hypoxia impacts large adults first: Consequences in a warming world. *Global Change Biology*, *19*(7), 2251–2263. https://doi.org/10.1111/gcb.12197

Clark, M. S., & Peck, L. S. (2009). Triggers of the HSP70 stress response: environmental responses and laboratory manipulation in an Antarctic marine invertebrate (*Nacella concinna*). *Cell Stress & Chaperones*, *14*(6), 649–660. https://doi.org/10.1007/s12192-009-0117-x

Clark, M. S., Peck, L. S., & Thyrring, J. (2021). Resilience in Greenland intertidal Mytilus: The hidden stress defense. *Science of the Total Environment*, *767*, 144366. https://doi.org/10.1016/j.scitotenv.2020.144366

Clark, M. S., Sommer, U., Sihra, J. K., Thorne, M. A. S., Morley, S. A., King, M., Viant, M. R., & Peck, L. S. (2017). Biodiversity in marine invertebrate responses to acute warming revealed by a comparative multi-omics approach. *Global Change Biology*,

23(1), 318–330. https://doi.org/10.1111/gcb.13357

Clark, M. S., Suckling, C. C., Cavallo, A., Mackenzie, C. L., Thorne, M. A. ., Davies, A. J., & Peck, L. S. (2019a). Molecular mechanisms underpinning transgenerational plasticity in the green sea urchin Psammechinus miliaris. *Scientific Reports*, *9*(1), 1–12. https://doi.org/10.1038/s41598-018-37255-6

Clark, M. S., Thorne, M. A. S., King, M., Hipperson, H., Hoffman, J. I., & Peck, L. S. (2018). Life in the intertidal: Cellular responses, methylation and epigenetics. *Functional Ecology*, *32*(8), 1982–1994. https://doi.org/10.1111/1365-2435.13077

Clark, M. S., Villota Nieva, L., Hoffman, J. I., Davies, A. J., Trivedi, U. H., Turner, F., Ashton, G. V, & Peck, L. S. (2019b). Lack of long-term acclimation in Antarctic encrusting species suggests vulnerability to warming. *Nature Communications*, *10*(1), 1–10. https://doi.org/10.1038/s41467-019-11348-w

Clarke, A. (1983). Life in cold water - The physiological ecology of Polar marine ectotherms. *Oceanography and Marine Biology*, *21*, 341–453.

Clarke, A., Meredith, M. P., Wallace, M. I., Brandon, M. A., & Thomas, D. N. (2008). Seasonal and interannual variability in temperature, chlorophyll and macronutrients in northern Marguerite Bay, Antarctica. *Deep-Sea Research Part II: Topical Studies in Oceanography*, *55*(18–19), 1988–2006. https://doi.org/10.1016/j.dsr2.2008.04.035

Clarke, A., Prothero-Thomas, E., Beaumont, J. C., Chapman, A. L., & Brey, T. (2004). Growth in the limpet Nacella concinna from contrasting sites in Antarctica. *Polar Biology*, *28*(1), 62–71. https://doi.org/10.1007/s00300-004-0647-8

Clem, K. R., Fogt, R. L., Turner, J., Lintner, B. R., Marshall, G. J., Miller, J. R., & Renwick, J. A. (2020). Record warming at the South Pole during the past three decades. *Nature Climate Change*. https://doi.org/10.1038/s41558-020-0815-z

Cleveland, W. S. (1979). Robust locally weighted regression and smoothing scatterplots. *Journal of the American Statistical Association*, *74*(368), 829–836. https://doi.org/10.2307/2286407

Clusella-Trullas, S., Boardman, L., Faulkner, K. T., Peck, L. S., & Chown, S. L. (2013). Effects of temperature on heat-shock responses and survival of two species of marine invertebrates from sub-Antarctic Marion Island. *Antarctic Science*, *26*(2), 145–152. https://doi.org/10.1017/S0954102013000473

Collins, M., Peck, L. S., & Clark, M. S. (2021). Large within, and between, species differences in marine cellular responses: Unpredictability in a changing environment.

Science of the Total Environment, *794*, 148594. https://doi.org/10.1016/j.scitotenv.2021.148594

Collins, M., Truebano, M., Verberk, W. C. E. P., & Spicer, J. I. (2021). Do aquatic ectotherms perform better under hypoxia after warm acclimation? *Journal of Experimental Biology*, *224*(3). https://doi.org/10.1242/jeb.232512

Conde, A., & Prado, M. (2018). Changes in phytoplankton vertical distribution during an El Niño event. *Ecological Indicators*, *90*, 201–205. https://doi.org/10.1016/j.ecolind.2018.03.015

Conover, R. (1966). Assimilation of organic matter by zooplankton. *Limnology and Oceanography*, *11*, 338–345.

Constable, A. J., Melbourne-Thomas, J., Corney, S. P., Arrigo, K. R., Barbraud, C., Barnes, D. K. A., Bindoff, N. L., Boyd, P. W., Brandt, A., Costa, D. P., Davidson, A. T., Ducklow, H. W., Emmerson, L., Fukuchi, M., Gutt, J., Hindell, M. A., Hofmann, E. E., Hosie, G. W., Iida, T., … Ziegler, P. (2014). Climate change and Southern Ocean ecosystems I: How changes in physical habitats directly affect marine biota. *Global Change Biology*, *20*(10), 3004–3025. https://doi.org/10.1111/gcb.12623

Convey, P., Bindschadler, R., Di Prisco, G., Fahrbach, E., Gutt, J., Hodgson, D. A., Mayewski, P. A., Summerhayes, C. P., Turner, J., Abram, N. J., Adams, B., Ainley, D. G., Anderson, J., Arbetter, T., Arthern, R., Atkinson, A., Barbante, C., Bargagli, R., Bargelloni, L., … Zane, L. (2009). Antarctic climate change and the environment. *Antarctic Science*, *21*(6), 541–563. https://doi.org/10.1017/S0954102009990642

Convey, P., & Peck, L. S. (2019). Antarctic environmental change and biological responses. *Science Advances*, *5*(11). https://doi.org/10.1126/sciadv.aaz0888

D'Amario, S. C., Rearick, D. C., Fasching, C., Kembel, S. W., Porter-Goff, E., Spooner, D. E., Williams, C. J., Wilson, H. F., & Xenopoulos, M. A. (2019). The prevalence of nonlinearity and detection of ecological breakpoints across a land use gradient in streams. *Scientific Reports*, *9*(1), 1–11. https://doi.org/10.1038/s41598-019-40349-4

David, B., Choné, T., Festeau, A., Mooi, R., & de Ridder, C. (2005). Biodiversity of Antarctic echinoids: A comprehensive and interactive database. *Scientia Marina*, *69*(SUPPL. 2), 201–203. https://doi.org/10.3989/scimar.2005.69s2201

De Broyer, C., Lowry, J. K., Jażdżewski, K., & Robert, H. (2007). SYNOPSIS OF THE AMPHIPODA OF THE SOUTHERN OCEAN Part 1. Catalogue of the Gammaridean and Corophiidean Amphipoda (Crustacea) of the Southern Ocean with distribution and ecological data. *Bulletin De L'Institut Royal Des Sciences Naturelles De*

Belgique, *77*, 1–325.

De Leij, R. (2021). *Functional response of the Antarctic sea urchin,* Sterechinus neumayeri*, to environmental change and extreme events in the context of a warming climate.* PhD Thesis, University of Southampton.

De Leij, R., Peck, L. S., & Grange, L. J. (2021). Multiyear trend in reproduction underpins interannual variation in gametogenic development of an Antarctic urchin. *Scientific Reports*, *11*(1), 1–13. https://doi.org/10.1038/s41598-021-98444-4

Deere, J. A., & Chown, S. L. (2006). Testing the beneficial acclimation hypothesis and its alternatives for locomotor performance. *American Naturalist*, *168*(5), 630–644. https://doi.org/10.1086/508026

Deschaseaux, E. S. M., Taylor, A. M., Maher, W. A., & Davis, A. R. (2010). Cellular responses of encapsulated gastropod embryos to multiple stressors associated with climate change. *Journal of Experimental Marine Biology and Ecology*, *383*(2), 130–136. https://doi.org/10.1016/j.jembe.2009.12.013

Deser, C., Phillips, A., & Bourdette, V. (2012). *Uncertainty in climate change projections : the role of internal variability*. 527–546. https://doi.org/10.1007/s00382-010-0977-x

Dethier, M. N., Hoins, G., Kobelt, J., Lowe, A. T., Galloway, A. W. E., Schram, J. B., Raymore, M., & Duggins, D. O. (2019). Feces as food: The nutritional value of urchin feces and implications for benthic food webs. *Journal of Experimental Marine Biology and Ecology*, *514–515*(December 2018), 95–102. https://doi.org/10.1016/j.jembe.2019.03.016

Donelson, J. M., Munday, P. L., McCormick, M. I., & Pitcher, C. R. (2012). Rapid transgenerational acclimation of a tropical reef fish to climate change. *Nature Climate Change*, *2*(1), 30–32. https://doi.org/10.1038/nclimate1323

Doney, S. C., Ruckelshaus, M., Duffy, J. E., Barry, J. P., Chan, F., English, C. A., Galindo, H. M., Grebmeier, J. M., Hollowed, A. B., Knowlton, N., Polovina, J., Rabalais, N. N., Sydeman, W. J., & Talley, L. D. (2012). Climate Change Impacts on Marine Ecosystems. *Annual Review of Marine Science*, *4*, 11–37. https://doi.org/10.1146/annurev-marine-041911-111611

Dunlop, K. M., Barnes, D. K. A., & Bailey, D. M. (2014). Variation of scavenger richness and abundance between sites of high and low iceberg scour frequency in Ryder Bay, West Antarctic Peninsula. *Polar Biology*, *37*(12), 1741–1754.

Emilio, L., Cajado, B., Santos-da-Silva, C., Hora, J. da, Porto, U., & Vasconcellos, V.

(2018). Is the Orton's rule still valid? Tropical sponge fecundity, rather than periodicity, is modulated by temperature and other proximal cues. *Hydrobiologia*, *815*, 187–205. https://doi.org/10.1007/s10750-018-3562-7

Epherra, L., Gil, D. G., Rubilar, T., Perez-Gallo, S., Reartes, M. B., & Tolosano, J. A. (2015). Temporal and spatial differences in the reproductive biology of the sea urchin Arbacia dufresnii. *Marine and Freshwater Research*, *66*(4), 329–342. https://doi.org/10.1071/MF14080

Ferrarini, A. (2011). Detecting ecological breakpoints: a new tool for piecewise regression. *Computational Ecology and Software*, *1*(2), 121–124. www.iaees.org

Fisher, R., Wilson, S. K., Sin, T. M., Lee, A. C., & Langlois, T. J. (2018). A simple function for full-subsets multiple regression in ecology with R. *Ecology and Evolution*, *8*, 6104–6113. https://doi.org/10.1002/ece3.4134

Fitzgibbon, Q. P., Simon, C. J., Smith, G. G., Carter, C. G., & Battaglene, S. C. (2017). Temperature dependent growth , feeding , nutritional condition and aerobic metabolism of juvenile spiny lobster, *Sagmariasus verreauxi*. *Comparative Biochemistry and Physiology, Part A*, *207*, 13–20. https://doi.org/10.1016/j.cbpa.2017.02.003

Fogt, R. L., Bromwich, D. H., & Hines, K. M. (2011). Understanding the SAM influence on the South Pacific ENSO teleconnection. *Climate Dynamics*, *36*(7), 1555–1576. https://doi.org/10.1007/s00382-010-0905-0

Foo, S. A., & Byrne, M. (2017). Marine gametes in a changing ocean: Impacts of climate change stressors on fecundity and the egg. *Marine Environmental Research*, *128*, 12–24. https://doi.org/10.1016/j.marenvres.2017.02.004

Fraser, K. P. P., Clarke, A., & Peck, L. S. (2007). Growth in the slow lane: Protein metabolism in the Antarctic limpet Nacella concinna (Strebel 1908). *Journal of Experimental Biology*, *210*(15), 2691–2699. https://doi.org/10.1242/jeb.003715

Frölicher, T. L., Fischer, E. M., & Gruber, N. (2018). Marine heatwaves under global warming. *Nature*, *560*, 360–366. https://doi.org/10.1038/s41586-018-0383-9

Frölicher, T. L., & Laufkötter, C. (2018). Emerging risks from marine heat waves. *Nature Communications*, *9*(1), 2015–2018. https://doi.org/10.1038/s41467-018-03163-6

Frölicher, T. L., & Paynter, D. J. (2015). Extending the relationship between global warming and cumulative carbon emissions to multi-millennial timescales. *Environmental Research Letters*, *10*(7). https://doi.org/10.1088/1748-

9326/10/7/075002

Fuenzalida, G., Poulin, E., Gonzalez-Wevar, C., Molina, C., & Cardenas, L. (2014). Next-generation transcriptome characterization in three Nacella species (Patellogastropoda: Nacellidae) from South America and Antarctica. *Marine Genomics*, *18*, 89–91. https://doi.org/https://doi.org/10.1016/j.margen.2014.06.004

Galley, E. A., Tyler, P. A., Smith, C. R., & Clarke, A. (2008). Reproductive biology of two species of holothurian from the deep-sea order Elasipoda, on the Antarctic continental shelf. *Deep-Sea Research Part II: Topical Studies in Oceanography*, *55*(22–23), 2515–2526. https://doi.org/10.1016/j.dsr2.2008.07.002

Garland, M. A., Stillman, J. H., & Tomanek, L. (2015). The proteomic response of cheliped myofibril tissue in the eurythermal porcelain crab *Petrolisthes cinctipes* to heat shock following acclimation to daily temperature fluctuations. *Journal of Experimental Biology*, *218*(3), 388–403. https://doi.org/10.1242/jeb.112250

Garrabou, J., Coma, R., Bensoussan, N., Bally, M., Chevaldonné, P., Cigliano, M., Diaz, D., Harmelin, J. G., Gambi, M. C., Kersting, D. K., Ledoux, J. B., Lejeusne, C., Linares, C., Marschal, C., Pérez, T., Ribes, M., Romano, J. C., Serrano, E., Teixido, N., … Cerrano, C. (2009). Mass mortality in Northwestern Mediterranean rocky benthic communities: Effects of the 2003 heat wave. *Global Change Biology*, *15*(5), 1090–1103. https://doi.org/10.1111/j.1365-2486.2008.01823.x

Gillooly, J. F., Brown, J., West, G. B., Savage, V. M., & Charnov, E. L. (2001). Effects of size and temperature on metabolic rate. *Science*, *293*(5538), 2248–2251. https://doi.org/10.1126/science.1061967

Giomi, F., Mandaglio, C., Ganmanee, M., Han, G. D., Dong, Y. W., Williams, G. A., & Sara, G. (2016). The importance of thermal history: Costs and benefits of heat exposure in a tropical, rocky shore oyster. *Journal of Experimental Biology*, *219*(5), 686–694. https://doi.org/10.1242/jeb.128892

Gómez-Robles, E., & Saucedo, P. E. (2009). Evaluation of quality indices of the gonad and somatic tissues involved in reproduction of the pearl oyster *Pinctada mazatlanica* with histochemistry and digital image analysis. *Journal of Shellfish Research*, *28*(2), 329–335.

Gómez-Valdez, M., Ocampo, L., Carvalho-Saucedo, L., & Gutiérrez-González, J. (2021). Reproductive activity and seasonal variability in the biochemical composition of a pen shell, *Atrina maura*. *Marine Ecology Progress Series*, *663*, 99–113. https://doi.org/10.3354/meps13623

González-Aravena, M., Calfio, C., Mercado, L., Morales-Lange, B., Bethke, J., De Lorgeril, J., & Cárdenas, C. A. (2018). HSP70 from the Antarctic sea urchin Sterechinus neumayeri: Molecular characterization and expression in response to heat stress. *Biological Research*, *51*(1), 1–10. https://doi.org/10.1186/s40659-018-0156-9

Grange, L. J., Peck, L. S., & Tyler, P. A. (2011). Reproductive ecology of the circumpolar Antarctic nemertean *Parborlasia corrugatus*: No evidence for inter-annual variation. *Journal of Experimental Marine Biology and Ecology*, *404*(1–2), 98–107. https://doi.org/10.1016/j.jembe.2011.04.011

Grange, L. J., Tyler, P. A., & Peck, L. S. (2007). Multi-year observations on the gametogenic ecology of the Antarctic seastar *Odontaster validus*. *Marine Biology*, *153*(1), 15–23. https://doi.org/10.1007/s00227-007-0776-z

Grange, L. J., Tyler, P. A., Peck, L. S., & Cornelius, N. (2004). Long-term interannual cycles of the gametogenic ecology of the Antarctic brittle star *Ophionotus victoriae*. *Marine Ecology Progress Series*, *278*, 141–155. https://doi.org/10.3354/meps278141

Griffiths, H. J. (2010). Antarctic marine biodiversity - what do we know about the distribution of life in the southern ocean? *PLoS ONE*, *5*(8). https://doi.org/10.1371/journal.pone.0011683

Halberg, F., Shankaraiah, K., & Giese, A. . (1987). The chronobiology of marine invertebrates: methods of analysis. In *Reproduction of marine invertebrates, Vol IX. General aspects: seeking unity in diversity* (pp. 331–384). The Boxwood Press.

Hamby, R. J. A. Y. (1975). Heat Effects on a Marine Snail. *Biological Bulletin*, *149*(2), 331–347.

Harper, E. M., & Peck, L. S. (2003). Predatory behaviour and metabolic costs in the Antarctic muricid gastropod *Trophon longstaffi*. *Polar Biology*, *26*(3), 208–217. https://doi.org/10.1007/s00300-002-0455-y

Harrington, L. H., Walker, C. W., & Lesser, M. P. (2007). Stereological analysis of nutritive phagocytes and gametogenic cells during the annual reproductive cycle of the green sea urchin, *Strongylocentrotus droebachiensis*. *Invertebrate Biology*, *126*(2), 202–209. https://doi.org/10.1111/j.1744-7410.2007.00090.x

Henriques, P., Delgado, J., & Sousa, R. (2017). Patellid Limpets: An Overview of the Biology and Conservation of Keystone Species of the Rocky Shores. *Organismal and Molecular Malacology*, *August*. https://doi.org/10.5772/67862

Hernandez, E., Vázquez, O. A., Torruco, A., & Rahman, M. S. (2020). Reproductive cycle

and gonadal development of the Atlantic sea urchin *Arbacia punctulata* in the Gulf of Mexico: changes in nutritive phagocytes in relation to gametogenesis. *Marine Biology Research*, *16*(3), 177–194. https://doi.org/10.1080/17451000.2020.1731758

Hobday, A. J., Alexander, L. V., Perkins, S. E., Smale, D. A., Straub, S. C., Oliver, E. C. J., Benthuysen, J. A., Burrows, M. T., Donat, M. G., Feng, M., Holbrook, N. J., Moore, P. J., Scannell, H. A., Sen Gupta, A., & Wernberg, T. (2016). A hierarchical approach to defining marine heatwaves. *Progress in Oceanography*, *141*, 227–238. https://doi.org/10.1016/j.pocean.2015.12.014

Hochachka, P., & Somero, G. (2002). *Bio-Chemical Adaptation: Mechanism and Process in Physiological Evolution* (Vol. 30). New York: Oxford University Press.

Holbrook, N. J., Scannell, H. A., Sen Gupta, A., Benthuysen, J. A., Feng, M., Oliver, E. C. J., Alexander, L. V., Burrows, M. T., Donat, M. G., Hobday, A. J., Moore, P. J., Perkins-Kirkpatrick, S. E., Smale, D. A., Straub, S. C., & Wernberg, T. (2019). A global assessment of marine heatwaves and their drivers. *Nature Communications*, *10*(1), 1–14. https://doi.org/10.1038/s41467-019-10206-z

IPCC. (2014). *Climate Change 2014: Synthesis Report. Contribution of Working Groups I, II and III to the Fifth Assessment Report of the Intergovernmental Panel on Climate Change* (Core Writing Team Pachauri RK and Meyer LA (ed.)). papers3://publication/uuid/73613368-F884-4F20-B937-5302445B00E5

IPCC. (2019). *Summary for Policymakers. In: Climate Change and Land: an IPCC special report on climate change, desertification, land degradation, sustainable land management, food security, and greenhouse gas fluxes in terrestrial ecosystems* (J. Shukla PR, Skea J, Calvo Buendia E, Masson-Delmotte V, Pörtner HO, Roberts DC, Zhai P, Slade R, Connors S, van Diemen R, Ferrat M, Haughey E, Luz S, Neogi S, Pathak M, Petzold J, Portugal Pereira J, Vyas P, Huntley E, Kissick K, Malley (ed.)). *In Press*. https://report.ipcc.ch/srocc/pdf/SROCC_SPM_Approved.pdf

IPCC. (2021). Climate Change 2021: The Physical Science Basis. Contribution of Working Group I to the Sixth Assessment Report of the Intergovernmental Panel on Climate Change [Masson-Delmotte, V., P. Zhai, A. Pirani, S. L. Connors, C. Péan, S. Berger, N. Caud, Y. Chen,. *Cambridge University Press*, *In Press*, 3949. https://www.ipcc.ch/report/ar6/wg1/downloads/report/IPCC_AR6_WGI_Full_Report.pdf

Jager, T., Ravagnan, E., & Dupont, S. (2016). Near-future ocean acidification impacts maintenance costs in sea-urchin larvae: Identification of stress factors and tipping points using a DEB modelling approach. *Journal of Experimental Marine Biology and*

Ecology, *474*, 11–17. https://doi.org/10.1016/j.jembe.2015.09.016

Janecki, T., Kidawa, A., & Potocka, M. (2010a). The effects of temperature and salinity on vital biological functions of the Antarctic crustacean *Serolis polita*. *Polar Biology*, *33*(8), 1013–1020. https://doi.org/10.1007/s00300-010-0779-y

Janecki, T., Kidawa, A., & Potocka, M. (2010b). The effects of temperature and salinity on vital biological functions of the Antarctic crustacean Serolis polita. *Polar Biology*, *33*(8), 1013–1020. https://doi.org/10.1007/s00300-010-0779-y

Johnson, G. C., Lyman, J. M., Boyer, T. P., Cheng, L., Domingues, C. M., Gilson, J., Ishii, M., Killick, R. E., Monselesan, D., Purkey, S. G., & Wijffels, S. E. (2020). Ocean heat content [in"State of the climate in 2019"]. *Bulletin of the American Meteorological Society*, *101*(8), S185–S238. https://doi.org/10.1175/BAMS-D-20-0105.1.

Joyce, W., Axelsson, M., Egginton, S., Farrell, A. P., Crockett, E. L., & O'Brien, K. M. (2018). The effects of thermal acclimation on cardio-respiratory performance in an Antarctic fish (*Notothenia coriiceps*). *Conservation Physiology*, *6*(1), 1–12. https://doi.org/10.1093/conphys/coy069

Kaiser, S., Brandão, S. N., Brix, S., Barnes, D. K. A., Bowden, D. A., Ingels, J., Leese, F., Schiaparelli, S., Arango, C. P., Badhe, R., Bax, N., Blazewicz-Paszkowycz, M., Brandt, A., Brenke, N., Catarino, A. I., David, B., De Ridder, C., Dubois, P., Ellingsen, K. E., … Yasuhara, M. (2013). Patterns, processes and vulnerability of Southern Ocean benthos: A decadal leap in knowledge and understanding. *Marine Biology*, *160*(9), 2295–2317. https://doi.org/10.1007/s00227-013-2232-6

Kelly, M. S. (2001). Environmental parameters controlling gametogenesis in the echinoid *Psammechinus miliaris*. *Journal of Experimental Marine Biology and Ecology*, *266*(1), 67–80. https://doi.org/10.1016/S0022-0981(01)00338-0

Kidawa, A., Potocka, M., & Janecki, T. (2010). The effects of temperature on the behaviour of the Antarctic sea star *Odontaster validus*. *Polish Polar Research*, *31*(3), 273–284. https://doi.org/10.2478/v10183−010−0003−3

Kingsolver, J. G., & Umbanhowar, J. (2018). The analysis and interpretation of critical temperatures. *The Journal of Experimental Biology*, *221*. https://doi.org/10.1242/jeb.167858

Kolzenburg, R., D'Amore, F., McCoy, S. J., & Ragazzola, F. (2021). Marginal populations show physiological adaptations and resilience to future climatic changes across a North Atlantic distribution. *Environmental and Experimental Botany*, *188*(March), 104522. https://doi.org/10.1016/j.envexpbot.2021.104522

Kooijman, S. A. L. M., Sousa, T., Pecquerie, L., Van Der Meer, J., & Jager, T. (2008). From food-dependent statistics to metabolic parameters, a practical guide to the use of dynamic energy budget theory. *Biological Reviews*, *83*(4), 533–552. https://doi.org/10.1111/j.1469-185X.2008.00053.x

Kuklinski, P., Berge, J., McFadden, L., Dmoch, K., Zajaczkowski, M., Nygård, H., Piwosz, K., & Tatarek, A. (2013). Seasonality of occurrence and recruitment of Arctic marine benthic invertebrate larvae in relation to environmental variables. *Polar Biology*, *36*(4), 549–560. https://doi.org/10.1007/s00300-012-1283-3

Kwok, R., & Comiso, J. C. (2002). Spatial patterns of variability in Antarctic surface temperature: Connections to the Southern Hemisphere Annular Mode and the Southern Oscillation. *Geophysical Research Letters*, *29*(14), 2–5. https://doi.org/10.1029/2002GL015415

La, H. S., Park, K., Wåhlin, A., Arrigo, K. R., Kim, D. S., Yang, E. J., Atkinson, A., Fielding, S., Im, J., Kim, T. W., Shin, H. C., Lee, S. H., & Ha, H. K. (2019). Zooplankton and micronekton respond to climate fluctuations in the Amundsen Sea polynya, Antarctica. *Scientific Reports*, *9*(1), 1–7. https://doi.org/10.1038/s41598-019-46423-1

Lau, S. C. Y., Grange, L. J., Peck, L. S., & Reed, A. J. (2018). The reproductive ecology of the Antarctic bivalve *Aequiyoldia eightsii* (Protobranchia: Sareptidae) follows neither Antarctic nor taxonomic patterns. *Polar Biology*, *41*(9), 1693–1706. https://doi.org/10.1007/s00300-018-2309-2

Lee, T., Hobbs, W. R., Willis, J. K., Halkides, D., Fukumori, I., Armstrong, E. M., Hayashi, A. K., Liu, W. T., Patzert, W., & Wang, O. (2010). Record warming in the South Pacific and western Antarctica associated with the strong central-Pacific El Nio in 2009-10. *Geophysical Research Letters*, *37*(19). https://doi.org/10.1029/2010GL044865

Lemoine N. P., Burkepile D. E., (2012) Temperature-induced mismatches between consumption and metabolism reduce consumer fitness. *Ecology*, 93:2483–2489. https://doi.org/10.1890/12-0375.1

Lenihan, H. S., Peterson, C. H., Miller, R. J., Kayal, M., & Potoski, M. (2018). Biotic disturbance mitigates effects of multiple stressors in a marine benthic community. *Ecosphere*, *9*(6). https://doi.org/10.1002/ecs2.2314

Leroi, A. M., Bennett, A. F., & Lenski, R. E. (1994). Temperature acclimation and competitive fitness: An experimental test of the beneficial acclimation assumption. *Proceedings of the National Academy of Sciences of the United States of America*,

91(5), 1917–1921. https://doi.org/10.1073/pnas.91.5.1917

Levitus, S., Antonov, J. I., Boyer, T. P., Baranova, O. K., Garcia, H. E., Locarnini, R. A., Mishonov, A. V., Reagan, J. R., Seidov, D., Yarosh, E. S., & Zweng, M. M. (2012a). World ocean heat content and thermosteric sea level change (0-2000m), 1955-2010. *Geophysical Research Letters*, *39*(10), 1–5. https://doi.org/10.1029/2012GL051106

Levitus, S., Antonov, J. I., Boyer, T. P., Baranova, O. K., Garcia, H. E., Locarnini, R. A., Mishonov, A. V, Reagan, J. R., Seidov, D., Yarosh, E. S., & Zweng, M. M. (2012b). *World ocean heat content and thermosteric sea level change (0 – 2000 m), 1955 – 2010*. *39*, 1–5. https://doi.org/10.1029/2012GL051106

Liu, H., Kelly, M. S., Cook, E. J., Black, K., Orr, H., Zhu, J. X., & Dong, S. L. (2007). The effect of diet type on growth and fatty-acid composition of sea urchin larvae, I. Paracentrotus lividus (Lamarck, 1816) (Echinodermata). *Aquaculture*, *264*(1–4), 247–262. https://doi.org/10.1016/j.aquaculture.2006.12.021

Loeb, V. J., Hofmann, E. E., Klinck, J. M., Holm-Hansen, O., & White, W. B. (2009). ENSO and variability of the antarctic peninsula pelagic marine ecosystem. *Antarctic Science*, *21*(2), 135–148. https://doi.org/10.1017/S0954102008001636

Loeb, V. J., & Santora, J. A. (2012). Population dynamics of *Salpa thompsoni* near the Antarctic Peninsula: Growth rates and interannual variations in reproductive activity (1993-2009). *Progress in Oceanography*, *96*(1), 93–107. https://doi.org/10.1016/j.pocean.2011.11.001

Louthan, A. M., Peterson, M. L., & Shoemaker, L. G. (2021). Climate sensitivity across latitude: scaling physiology to communities. *Trends in Ecology & Evolution*, *36*(10), 931–942. https://doi.org/10.1016/j.tree.2021.05.008

Magniez, P. (1983). Reproductive cycle of the brooding echinoid *Abatus cordatus* (Echinodermata) in Kerguelen (Antarctic Ocean): changes in the organ indices, biochemical composition and caloric content of the gonads. *Marine Biology*, *74*(1), 55–64. https://doi.org/10.1007/BF00394275

Magozzi, S., & Calosi, P. (2015). Integrating metabolic performance, thermal tolerance, and plasticity enables for more accurate predictions on species vulnerability to acute and chronic effects of global warming. *Global Change Biology*, *21*(1), 181–194. https://doi.org/10.1111/gcb.12695

Marshall, J., Scott, J. R., Armour, K. C., Campin, J. M., Kelley, M., & Romanou, A. (2015). The ocean's role in the transient response of climate to abrupt greenhouse gas forcing. *Climate Dynamics*, *44*(7–8), 2287–2299. https://doi.org/10.1007/s00382-014-

2308-0

McClintock, J. (1994). Trophic biology of Antarctic shallow-water echinoderms. *Marine Ecology Progress Series*, *111*(1–2), 191–202. https://doi.org/10.3354/meps111191

McWhorter, T. J., Gerson, A. R., Talbot, W. A., Smith, E. K., McKechnie, A. E., & Wolf, B. O. (2018). Avian thermoregulation in the heat: Evaporative cooling capacity and thermal tolerance in two Australian parrots. *Journal of Experimental Biology*, *221*(6). https://doi.org/10.1242/jeb.168930

Meidlinger, K., Tyler, P. A., & Peck, L. S. (1998). Reproductive patterns in the Antarctic brachiopod Liothyrella uva. *Marine Biology*, *132*(1), 153–162. https://doi.org/10.1007/s002270050381

Melzner, F., Stange, P., Trubenbach, K., Thomsen, J., Casties, I., Panknin, U., Gorb, S. N., & Gutowska, M. A. (2011). Food Supply and Seawater pCO2 Impact Calcification and Internal Shell Dissolution in the Blue Mussel <i>Mytilus edulis<i/>. *PLoS ONE*, *6*(9), e24223. https://doi.org/10.1371/journal.pone.0024223

Mercier, A., & Hamel, J. F. (2009). Endogenous and exogenous control of gametogenesis and spawning in echinoderms: Chapter 1. *Advances in Marine Biology*, *55*, 1–6. https://doi.org/10.1016/S0065-2881(09)55001-8

Mercier, A., & Hamel, J. F. (2010). Synchronized breeding events in sympatric marine invertebrates: Role of behavior and fine temporal windows in maintaining reproductive isolation. *Behavioral Ecology and Sociobiology*, *64*(11), 1749–1765. https://doi.org/10.1007/s00265-010-0987-z

Meredith, M. P., & King, J. C. (2005). Rapid climate change in the ocean west of the Antarctic Peninsula during the second half of the 20th century. *Geophysical Research Letters*, *32*(19), 1–5. https://doi.org/10.1029/2005GL024042

Montgomery, D., & Peck, E. (1992). *Introduction to linear regression analysis*. Wiley.

Moran, A. L., McAlister, J. S., & Whitehill, E. A. G. (2013). Eggs as energy: Revisiting the scaling of egg size and energetic content among echinoderms. *Biological Bulletin*, *224*(3), 184–191. https://doi.org/10.1086/BBLv224n3p184

Morley, S. A., Bates, A. E., Lamare, M., Richard, J., Nguyen, K. D., Brown, J., & Peck, L. S. (2016). Rates of warming and the global sensitivity of shallow water marine invertebrates to elevated temperature. *Journal of the Marine Biological Association of the United Kingdom*, *96*(1), 159–165. https://doi.org/10.1017/S0025315414000307

Morley, S. A., Hirse, T., Pörtner, H.-O., & Peck, L. S. (2009). Geographical variation in

thermal tolerance within Southern Ocean marine ectotherms. *Comparative Biochemistry and Physiology Part A: Molecular & Integrative Physiology*, *153*(2), 154–161. https://doi.org/https://doi.org/10.1016/j.cbpa.2009.02.001

Morley, S. A., Lai, C. H., Clarke, A., Tan, K. S., Thorne, M. A. S., & Peck, L. S. (2014). Limpet feeding rate and the consistency of physiological response to temperature. *Journal of Comparative Physiology B: Biochemical, Systemic, and Environmental Physiology*, *184*(5), 563–570. https://doi.org/10.1007/s00360-014-0814-3

Morley, S. A., Lemmon, V., Obermüller, B. E., Spicer, J. I., Clark, M. S., & Peck, L. S. (2011). Duration tenacity: A method for assessing acclimatory capacity of the Antarctic limpet, Nacella concinna. *Journal of Experimental Marine Biology and Ecology*, *399*(1), 39–42. https://doi.org/https://doi.org/10.1016/j.jembe.2011.01.013

Morley, S. A., Martin, S. M., Bates, A. E., Clark, M. S., Ericson, J., Lamare, M., & Peck, L. S. (2012a). Spatial and temporal variation in the heat tolerance limits of two abundant Southern Ocean invertebrates. *Marine Ecology Progress Series*, *450*, 81–92. https://doi.org/10.3354/meps09577

Morley, S. A., Martin, S. M., Day, R. W., Ericson, J., Lai, C. H., Lamare, M., Tan, K. S., Thorne, M. A. S., & Peck, L. S. (2012b). Thermal Reaction Norms and the Scale of Temperature Variation: Latitudinal Vulnerability of Intertidal Nacellid Limpets to Climate Change. *PLoS ONE*, *7*(12), 7–10. https://doi.org/10.1371/journal.pone.0052818

Morley, S. A., Nguyen, K. D., Peck, L. S., Lai, C. H., & Tan, K. S. (2017). Can acclimation of thermal tolerance, in adults and across generations, act as a buffer against climate change in tropical marine ectotherms? *Journal of Thermal Biology*, *68*(January 2016), 195–199. https://doi.org/10.1016/j.jtherbio.2016.09.007

Morley, S. A., Peck, L. S., Sunday, J., Heiser, S., & Bates, A. E. (2019). Physiological acclimation and persistence of ectothermic species under extreme heat events. *Global Ecology and Biogeography*, *28*(7), 1018–1037. https://doi.org/10.1111/geb.12911

Morley, S. A., Suckling, C. C., Clark, M. S., Cross, E. L., & Peck, L. S. (2016). Long-term effects of altered pH and temperature on the feeding energetics of the Antarctic sea urchin, *Sterechinus neumayeri*. *Biodiversity*, *17*(1–2), 34–45. https://doi.org/10.1080/14888386.2016.1174956

Muggeo, V. M. R. (2008). segmented: An R Package to Fit Regression Models with Broken-Line Relationships. *R News*, *3*(6), 343–344.

https://doi.org/10.1159/000323281

Muthiga, N. A. (2006). The reproductive biology of a new species of sea cucumber, *Holothuria (Mertensiothuria) arenacava* in a Kenyan marine protected area: The possible role of light and temperature on gametogenesis and spawning. *Marine Biology*, *149*(3), 585–593. https://doi.org/10.1007/s00227-005-0224-x

Muthiga, N. A., & Kawaka, J. (2008). The effects of temperature and light on the gametogenesis and spawning of four sea urchin and one sea cucumber species on coral reefs in Kenya. *Wildlife Conservation*, *11*, 7–11.

Myrvoll-Nilsen, E., Fredriksen, H. B., Sørbye, S. H., & Rypdal, M. (2019). Warming Trends and Long-Range Dependent Climate Variability Since Year 1900: A Bayesian Approach. *Frontiers in Earth Science*, *7*(August), 1–8. https://doi.org/10.3389/feart.2019.00214

Ndhlovu, A., & Mcquaid, C. D. (2021). Science of the Total Environment Ectoparasites reduce scope for growth in a rocky-shore mussel (*Perna perna*) by raising maintenance costs. *Science of the Total Environment*, *753*, 142020. https://doi.org/10.1016/j.scitotenv.2020.142020

Nicholas, B. A., Cronin, M. F., Freeland, H., & Mantua, N. (2015). Causes and impacts of the 2014 warm anomaly in the NE Pacific. *Geophysical Research Letters*, *42*, 3414–3420,. https://doi.org/10.1002/2015GL063306

Nowicki, R., Heithaus, M., Thomson, J., Burkholder, D., Gastrich, K., & Wirsing, A. (2019). Indirect legacy effects of an extreme climatic event on a marine megafaunal community. *Ecological Monographs*, *89*(3), 1–20. https://doi.org/10.1002/ecm.1365

Obermüller, B. E., Morley, S. A., Barnes, D. K. A., & Peck, L. S. (2010). Seasonal physiology and ecology of Antarctic marine benthic predators and scavengers. *Marine Ecology Progress Series*, *415*, 109–126. https://doi.org/10.3354/meps08735

Oliver, E. C. J., Burrows, M. T., Donat, M. G., Sen Gupta, A., Alexander, L. V., Perkins-Kirkpatrick, S. E., Benthuysen, J. A., Hobday, A. J., Holbrook, N. J., Moore, P. J., Thomsen, M. S., Wernberg, T., & Smale, D. A. (2019). Projected Marine Heatwaves in the 21st Century and the Potential for Ecological Impact. *Frontiers in Marine Science*, *6*(December), 1–12. https://doi.org/10.3389/fmars.2019.00734

Oliver, E. C. J., Donat, M. G., Burrows, M. T., Moore, P. J., Smale, D. A., Alexander, L. V., Benthuysen, J. A., Feng, M., Sen Gupta, A., Hobday, A. J., Holbrook, N. J., Perkins-Kirkpatrick, S. E., Scannell, H. A., Straub, S. C., & Wernberg, T. (2018). Longer and more frequent marine heatwaves over the past century. *Nature Communications*,

9(1), 1–12. https://doi.org/10.1038/s41467-018-03732-9

Oschlies, A., Brandt, P., Stramma, L., & Schmidtko, S. (2018). Drivers and mechanisms of ocean deoxygenation. *Nature Geoscience*, *11*(7), 467–473. https://doi.org/10.1038/s41561-018-0152-2

Pansch, C., Scotti, M., Barboza, F. R., Al-Janabi, B., Brakel, J., Briski, E., Bucholz, B., Franz, M., Ito, M., Paiva, F., Saha, M., Sawall, Y., Weinberger, F., & Wahl, M. (2018). Heat waves and their significance for a temperate benthic community: A near-natural experimental approach. *Global Change Biology*, *24*(9), 4357–4367. https://doi.org/10.1111/gcb.14282

Payton, S. L., Johnson, P. D., & Jenny, M. J. (2016). Comparative physiological, biochemical and molecular thermal stress response profiles for two unionid freshwater mussel species. *Journal of Experimental Biology*, *219*(22), 3562–3574. https://doi.org/10.1242/jeb.140129

Pearce, A. F., & Feng, M. (2013). The rise and fall of the “marine heat wave” off Western Australia during the summer of 2010/2011. *Journal of Marine Systems*, *111–112*, 139–156. https://doi.org/10.1016/j.jmarsys.2012.10.009

Peck, L. S. (1989). Temperature and basal metabolism in two Antarctic marine herbivores. *Journal of Experimental Marine Biology and Ecology*, *127*(1), 1–12. https://doi.org/10.1016/0022-0981(89)90205-0

Peck, L. S. (2002). Ecophysiology of Antarctic marine ectotherms: Limits to life. *Polar Biology*, *25*(1), 31–40. https://doi.org/10.1007/s003000100308

Peck, L. S. (2005). Prospects for survival in the Southern Ocean: Vulnerability of benthic species to temperature change. *Antarctic Science*, *17*(4), 497–507. https://doi.org/10.1017/S0954102005002920

Peck, L. S. (2011). Organisms and responses to environmental change. *Marine Genomics*, *4*(4), 237–243. https://doi.org/10.1016/j.margen.2011.07.001

Peck, L. S. (2016). A Cold Limit to Adaptation in the Sea. *Trends in Ecology and Evolution*, *31*(1), 13–26. https://doi.org/10.1016/j.tree.2015.09.014

Peck, L. S. (2018). Antarctic Marine Biodiversity: Adaptations, Environments and Responses to Change. *Oceanography and Marine Biology: An Annual Review*, *56*, 105–236. https://doi.org/10.1201/9780429454455-3

Peck, L. S., & Bullough, L. W. (1993). Growth and population structure in the infaunal bivalve Yoldia eightsi in relation to iceberg activity at Signy Island, Antarctica. *Marine*

Biology, *117*(2), 235–241. https://doi.org/10.1007/BF00345668

Peck, L. S., Clark, M. S., Morley, S. A., Massey, A., & Rossetti, H. (2009). Animal temperature limits and ecological relevance: Effects of size, activity and rates of change. *Functional Ecology*, *23*(2), 248–256. https://doi.org/10.1111/j.1365-2435.2008.01537.x

Peck, L. S., Morley, S. A., & Clark, M. S. (2010). Poor acclimation capacities in Antarctic marine ectotherms. *Marine Biology*, *157*(9), 2051–2059. https://doi.org/10.1007/s00227-010-1473-x

Peck, L. S., Morley, S. A., Pörtner, H.-O., & Clark, M. S. (2007). Thermal limits of burrowing capacity are linked to oxygen availability and size in the Antarctic clam Laternula elliptica. *Oecologia*, *154*(3), 479–484. https://doi.org/10.1007/s00442-007-0858-0

Peck, L. S., Morley, S. A., Richard, J., & Clark, M. S. (2014). Acclimation and thermal tolerance in Antarctic marine ectotherms. *Journal of Experimental Biology*, *217*(1), 16–22. https://doi.org/10.1242/jeb.089946

Peck, L. S., Pörtner, H.-O., & Hardewig, I. (2002). Metabolic demand, oxygen supply, and critical temperatures in the Antarctic bivalve *Laternula elliptica*. *Physiological and Biochemical Zoology*, *75*(2), 123–133. https://doi.org/10.1086/340990

Peck, L. S., Webb, K. E., & Bailey, D. M. (2004). Extreme sensitivity of biological function to temperature. *Functional Ecology*, *18*, 625–630.

Peck, L. S., Webb, K. E., Miller, A., Clark, M. S., & Hill, T. (2008). Temperature limits to activity, feeding and metabolism in the Antarctic starfish Odontaster validus. *Marine Ecology Progress Series*, *358*, 181–189. https://doi.org/10.3354/meps07336

Pérez, A. F., Morriconi, E., Boy, C., & Calvo, J. (2008). Seasonal changes in energy allocation to somatic and reproductive body components of the common cold temperature sea urchin *Loxechinus albus* in a Sub-Antarctic environment. *Polar Biology*, *31*(4), 443–449. https://doi.org/10.1007/s00300-007-0370-3

Piepho, H. P., & Ogutu, J. O. (2003). Inference for the break point in segmented regression with application to longitudinal data. *Biometrical Journal*, *45*(5), 591–601. https://doi.org/10.1002/bimj.200390035

Pierrat, B., Saucède, T., Laffont, R., De Ridder, C., Festeau, A., & David, B. (2012). Large-scale distribution analysis of Antarctic echinoids using ecological niche modelling. *Marine Ecology Progress Series*, *463*(August), 215–230.

https://doi.org/10.3354/meps09842

Pörtner, H.-O., Bock, C., & Mark, F. C. (2017). Oxygen- & capacity-limited thermal tolerance: Bridging ecology & physiology. *Journal of Experimental Biology*, *220*(15), 2685–2696. https://doi.org/10.1242/jeb.134585

Pörtner, H.-O., Peck, L. S., & Hirse, T. (2006). Hyperoxia alleviates thermal stress in the Antarctic bivalve, *Laternula elliptica*: Evidence for oxygen limited thermal tolerance. *Polar Biology*, *29*(8), 688–693. https://doi.org/10.1007/s00300-005-0106-1

Pörtner, H.-O., Peck, L. S., & Somero, G. (2007). Thermal limits and adaptation in marine Antarctic ectotherms: An integrative view. *Philosophical Transactions of the Royal Society B: Biological Sciences*, *362*(1488), 2233–2258. https://doi.org/10.1098/rstb.2006.1947

Precht, H., Christophersen, J., & Hensel, H. (1955). Temperatur und Leben. In *Springer-Verlag.*

Rastrick, S. P. S., & Whiteley, N. M. (2013). Influence of Natural Thermal Gradients on Whole Animal Rates of Protein Synthesis in Marine Gammarid Amphipods. *PLoS ONE*, *8*(3). https://doi.org/10.1371/journal.pone.0060050

Reed, A. J., Morris, J. P., Linse, K., & Thatje, S. (2014). Reproductive morphology of the deep-sea protobranch bivalves *Yoldiella ecaudata, Yoldiella sabrina*, and *Yoldiella valettei* (Yoldiidae) from the Southern Ocean. *Polar Biology*, *37*(10), 1383–1392. https://doi.org/10.1007/s00300-014-1528-4

Robertson, R., El-Haj, A. J., Clarke, A., Peck, L. S., & Taylor, E. (2001). The effects of temperature on metabolic rate and protein synthesis following a meal in the isopod Glyptonotus antarcticus Eights (1852). *Polar Biology*, *24*(9), 677–686. https://doi.org/10.1007/s003000100268

Rohr, J. R., Civitello, D. J., Cohen, J. M., Roznik, E. A., Sinervo, B., & Dell, A. I. (2018). The complex drivers of thermal acclimation and breadth in ectotherms. *Ecology Letters*, *21*(9), 1425–1439. https://doi.org/10.1111/ele.13107

Román-González, A., Scourse, J. D., Butler, P. G., Reynolds, D. J., Richardson, C. A., Peck, L. S., Brey, T., & Hall, I. R. (2017). Analysis of ontogenetic growth trends in two marine Antarctic bivalves *Yoldia eightsi* and *Laternula elliptica*: Implications for sclerochronology. *Palaeogeography, Palaeoclimatology, Palaeoecology*, *465*, 300–306. https://doi.org/10.1016/j.palaeo.2016.05.004

Rozema, P. D., Venables, H. J., van de Poll, W. H., Clarke, A., Meredith, M. P., & Buma,

A. G. J. (2017). Interannual variability in phytoplankton biomass and species composition in northern Marguerite Bay (West Antarctic Peninsula) is governed by both winter sea ice cover and summer stratification. *Limnology and Oceanography*, *62*(1), 235–252. https://doi.org/10.1002/lno.10391

Rubio-Portillo, E., Izquierdo-Muñoz, A., Gago, J. F., Rosselló-Mora, R., Antón, J., & Ramos-Esplá, A. A. (2016). Effects of the 2015 heat wave on benthic invertebrates in the Tabarca Marine Protected Area (southeast Spain). *Marine Environmental Research*, *122*, 135–142. https://doi.org/10.1016/j.marenvres.2016.10.004

Rueden, C. T., Schindelin, J., Hiner, M. C., DeZonia, B. E., Walter, A. E., Arena, E. T., & Eliceiri, K. W. (2017). ImageJ2: ImageJ for the next generation of scientific image data. *BMC Bioinformatics*, *18*(1), 1–26. https://doi.org/10.1186/s12859-017-1934-z

Ryan, J. P., Kudela, R. M., Birch, J. M., Blum, M., Bowers, H. A., Chavez, F. P., Doucette, G. J., Hayashi, K., Marin, R., Mikulski, C. M., Pennington, J. T., Scholin, C. A., Smith, G. J., Woods, A., & Zhang, Y. (2017). Causality of an extreme harmful algal bloom in Monterey Bay, California, during the 2014–2016 northeast Pacific warm anomaly. *Geophysical Research Letters*, *44*(11), 5571–5579. https://doi.org/10.1002/2017GL072637

Saba, G. K., Fraser, W. R., Saba, V. S., Iannuzzi, R. A., Coleman, K. E., Doney, S. C., Ducklow, H. W., Martinson, D. G., Miles, T. N., Patterson-Fraser, D. L., Stammerjohn, S. E., Steinberg, D. K., & Schofield, O. M. (2014). Winter and spring controls on the summer food web of the coastal West Antarctic Peninsula. *Nature Communications*, *5*(July), 1–8. https://doi.org/10.1038/ncomms5318

Saha, M., Barboza, F. R., Somerfield, P. J., Al-Janabi, B., Beck, M., Brakel, J., Ito, M., Pansch, C., Nascimento-Schulze, J. C., Jakobsson Thor, S., Weinberger, F., & Sawall, Y. (2020). Response of foundation macrophytes to near-natural simulated marine heatwaves. *Global Change Biology*, *26*(2), 417–430. https://doi.org/10.1111/gcb.14801

Salin, K., Auer, S. K., Anderson, G. J., Selman, C., & Metcalfe, N. B. (2016). *Inadequate food intake at high temperatures is related to depressed mitochondrial respiratory capacity*. 1356–1362. https://doi.org/10.1242/jeb.133025

Salinas, S., & Munch, S. B. (2012). Thermal legacies: Transgenerational effects of temperature on growth in a vertebrate. *Ecology Letters*, *15*(2), 159–163. https://doi.org/10.1111/j.1461-0248.2011.01721.x

Sandersfeld, T., Davison, W., Lamare, M. D., Knust, R., & Richter, C. (2015). Elevated

temperature causes metabolic trade-offs at the wholeorganism level in the Antarctic fish *Trematomus bernacchii*. *Journal of Experimental Biology*, *218*(15), 2373–2381. https://doi.org/10.1242/jeb.122804

Sandoval-Castillo, J., Gates, K., Brauer, C. J., Smith, S., Bernatchez, L., & Beheregaray, L. B. (2020). Adaptation of plasticity to projected maximum temperatures and across climatically defined bioregions. *Proceedings of the National Academy of Sciences of the United States of America*, *117*(29), 17112–17121. https://doi.org/10.1073/pnas.1921124117

Santamaría-del-Ángel, E., Cañon-Páez, M. L., Sebastiá-Frasquet, M. T., González-Silveira, A., Gutierrez, A. L., Aguilar-Maldonado, J. A., López-Calderón, J., Camacho-Ibar, V., Franco-Herrera, A., & Castillo-Ramírez, A. (2021). Interannual climate variability in the west antarctic peninsula under austral summer conditions. *Remote Sensing*, *13*(6). https://doi.org/10.3390/rs13061122

Santidrián Tomillo, P., Fonseca, L. G., Ward, M., Tankersley, N., Robinson, N. J., Orrego, C. M., Paladino, F. V., & Saba, V. S. (2020). The impacts of extreme El Niño events on sea turtle nesting populations. *Climatic Change*. https://doi.org/10.1007/s10584-020-02658-w

Santora, J. A., Mantua, N. J., Schroeder, I. D., Field, J. C., Hazen, E. L., Bograd, S. J., Sydeman, W. J., Wells, B. K., Calambokidis, J., Saez, L., Lawson, D., & Forney, K. A. (2020). Habitat compression and ecosystem shifts as potential links between marine heatwave and record whale entanglements. *Nature Communications*, *11*(1), 1–12. https://doi.org/10.1038/s41467-019-14215-w

Schiaparelli, S., & Linse, K. (2006). A reassessment of the distribution of the common Antarctic scallop Adamussium colbecki (Smith, 1902). *Deep-Sea Research Part II-Topical Studies in Oceanography*, *53*(8–10), 912–920. https://doi.org/10.1016/j.dsr2.2006.02.004

Schindelin, J., Arganda-Carreras, I., Frise, E., Kaynig, V., Longair, M., Pietzsch, T., Preibisch, S., Rueden, C., Saalfeld, S., Schmid, B., Tinevez, J. Y., White, D. J., Hartenstein, V., Eliceiri, K., Tomancak, P., & Cardona, A. (2012). Fiji: An open-source platform for biological-image analysis. *Nature Methods*, *9*(7), 676–682. https://doi.org/10.1038/nmeth.2019

Schlegel, R. W., & Smit, A. J. (2018). heatwaveR: A central algorithm for the detection of heatwaves and cold-spells. *Journal of Open Source Software*, *3*(27), 821. https://doi.org/https://doi.org/10.21105/joss.00821

Schneider, D. P., Okumura, Y., & Deser, C. (2012). Observed Antarctic interannual climate variability and tropical linkages. *Journal of Climate*, *25*(12), 4048–4066. https://doi.org/10.1175/JCLI-D-11-00273.1

Seebacher, F., White, C. R., & Franklin, C. E. (2015). Physiological plasticity increases resilience of ectothermic animals to climate change. *Nature Climate Change*, *5*(1), 61–66. https://doi.org/10.1038/nclimate2457

Smale, D. A., & Wernberg, T. (2013). *Extreme climatic event drives range contraction of a habitat-forming species Subject collections*. *May 2014*. https://doi.org/10.1098/rspb.2012.2829

Smale, D. A., Yunnie, A. L. E., Vance, T., & Widdicombe, S. (2015). Disentangling the impacts of heat wave magnitude, duration and timing on the structure and diversity of sessile marine assemblages. *PeerJ*, *3*. https://doi.org/10.7717/peerj.863

Smart, T. I., Young, C. M., & Emlet, R. B. (2012). Environmental cues and seasonal reproduction in a temperate estuary: A case study of *Owenia collaris* (Annelida: Polychaeta, Oweniidae). *Marine Ecology*, *33*(3), 290–301. https://doi.org/10.1111/j.1439-0485.2011.00493.x

Somero, G. N. (2010). The physiology of climate change: How potentials for acclimatization and genetic adaptation will determine “winners” and “losers.” *Journal of Experimental Biology*, *213*(6), 912–920. https://doi.org/10.1242/jeb.037473

Sorte, C. J. B., Jones, S. J., & Miller, L. P. (2011). Geographic variation in temperature tolerance as an indicator of potential population responses to climate change. *Journal of Experimental Marine Biology and Ecology*, *400*(1–2), 209–217. https://doi.org/10.1016/j.jembe.2011.02.009

Souster, T. A., Morley, S. A., & Peck, L. S. (2018). Seasonality of oxygen consumption in five common Antarctic benthic marine invertebrates. *Polar Biology*, *41*(5), 897–908. https://doi.org/10.1007/s00300-018-2251-3

Spence, P., Holmes, R. M., Hogg, A. M. C., Griffies, S. M., Stewart, K. D., & England, M. H. (2017). Localized rapid warming of West Antarctic subsurface waters by remote winds. *Nature Climate Change*, *7*(8), 595–603. https://doi.org/10.1038/NCLIMATE3335

Spicer, J. I., Morley, S. A., & Bozinovic, F. (2019). Physiological diversity, biodiversity patterns and global climate change: Testing key hypotheses involving temperature and oxygen. *Philosophical Transactions of the Royal Society B: Biological Sciences*, *374*(1778), 8–11. https://doi.org/10.1098/rstb.2019.0032

St.Gelais, A. T., Chaves-Fonnegra, A., Moulding, A. L., Kosmynin, V. N., & Gilliam, D. S. (2016). *Siderastrea siderea* spawning and oocyte resorption at high latitude. *Invertebrate Reproduction and Development*, *60*(3), 212–222. https://doi.org/10.1080/07924259.2016.1194334

Stanwell-Smith, D., & Peck, L. S. (1998). Temperature and embryonic development in relation to spawning and field occurrence of larvae of three Antarctic echinoderms. *Biological Bulletin*, *194*(1), 44–52. https://doi.org/10.2307/1542512

Stanwell-Smith, D., Peck, L. S., Clarke, A., Murray, A. W. A., & Todd, C. D. (1999). The distribution, abundance and seasonality of pelagic marine invertebrate larvae in the maritime Antarctic. *Philosophical Transactions of the Royal Society B: Biological Sciences*, *354*(1382), 471–484. https://doi.org/10.1098/rstb.1999.0398

Starr, M., Himmelman, J. H., & Therriault, J. (1990). Direct coupling of marine invertebrate spawning with phytoplankton blooms. *Science*, *247*(4946), 1071–1074. https://doi.org/10.1126/science.247.4946.1071

Steinberg, D. K., Ruck, K. E., Gleiber, M. R., Garzio, L. M., Cope, J. S., Bernard, K. S., Stammerjohn, S. E., Schofield, O. M. E., Quetin, L. B., & Ross, R. M. (2015). Long-term (1993-2013) changes in macrozooplankton off the Western Antarctic Peninsula. *Deep-Sea Research Part I: Oceanographic Research Papers*, *101*, 54–70. https://doi.org/10.1016/j.dsr.2015.02.009

Stenseth, N. C., Ottersen, G., Hurrell, J. W., Mysterud, A., Lima, M., Chan, K. S., Yoccoz, N. G., & Ådlandsvik, B. (2003). Studying climate effects on ecology through the use of climate indices: The North Atlantic Oscillation, El Niño Southern Oscillation and beyond. *Proceedings of the Royal Society B: Biological Sciences*, *270*(1529), 2087–2096. https://doi.org/10.1098/rspb.2003.2415

Stevens, G. C. (1989). The Latitudinal Gradient in Geographical Range : How so Many Species Coexist in the Tropics Author (s): George C . Stevens Reviewed work (s): Source : The American Naturalist , Vol . 133 , No . 2 (Feb ., 1989), pp . 240-256 Published by : The Univer. *The American Naturalist*, *133*(2), 240–256.

Stevens, M. M., Jackson, S., Bester, S. A., Terblanche, J. S., & Chown, S. L. (2010). Oxygen limitation and thermal tolerance in two terrestrial arthropod species. *Journal of Experimental Biology*, *213*(13), 2209–2218. https://doi.org/10.1242/jeb.040170

Stillman, J. H. (2003). Acclimation capacity underlies susceptibility to climate change. *Science*, *301*(5629), 65. https://doi.org/10.1126/science.1083073

Stott, P. A., Stone, D. A., & Allen, M. R. (2004). *Human contribution to the European*

heatwave of 2003. *432*(December). https://doi.org/10.1029/2001JB001029

Suckling, C. C., Clark, M. S., Beveridge, C., Brunner, L., Hughes, A. D., Harper, E. M., Cook, E. J., Davies, A. J., & Peck, L. S. (2014). Experimental influence of pH on the early life-stages of sea urchins II: Increasing parental exposure times gives rise to different responses. *Invertebrate Reproduction and Development*, *58*(3), 161–175. https://doi.org/10.1080/07924259.2013.875951

Suckling, C. C., Clark, M. S., Richard, J., Morley, S. A., Thorne, M. A. S., Harper, E. M., & Peck, L. S. (2015). Adult acclimation to combined temperature and pH stressors significantly enhances reproductive outcomes compared to short-term exposures. *Journal of Animal Ecology*, *84*(3), 773–784. https://doi.org/10.1111/1365-2656.12316

Sunday, J., Bennett, J. M., Calosi, P., Clusella-Trullas, S., Gravel, S., Hargreaves, A. L., Leiva, F. P., Verberk, W. C. E. P., Olalla-Tárraga, M. Á., & Morales-Castilla, I. (2019). Thermal tolerance patterns across latitude and elevation. *Philosophical Transactions of the Royal Society B: Biological Sciences*, *374*(1778). https://doi.org/10.1098/rstb.2019.0036

Sunday, J. M., Bates, A. E., & Dulvy, N. K. (2011). Global analysis of thermal tolerance and latitude in ectotherms. *Proceedings of the Royal Society B: Biological Sciences*, *278*(1713), 1823–1830. https://doi.org/10.1098/rspb.2010.1295

Sunday, J. M., Bates, A. E., & Dulvy, N. K. (2012). Thermal tolerance and the global redistribution of animals. *Nature Climate Change*, *2*(6), 1–5. https://doi.org/10.1038/nclimate1539

Takemura, A., Rahman, M. S., & Park, Y. J. (2010). External and internal controls of lunar-related reproductive rhythms in fishes. *Journal of Fish Biology*, *76*(1), 7–26. https://doi.org/10.1111/j.1095-8649.2009.02481.x

Taylor, J. D., Glover, E. A., Harper, E. M., Crame, J. A., Ikebe, C., & Williams, S. T. (2018). Left in the cold? Evolutionary origin of Laternula elliptica, a keystone bivalve species of Antarctic benthos. *Biological Journal of the Linnean Society*, *123*(2), 360–376. https://doi.org/10.1093/biolinnean/blx144

Terblanche, J. S., Deere, J. A., Clusella-Trullas, S., Janion, C., & Chown, S. L. (2007). Critical thermal limits depend on methodological context. *Proceedings of the Royal Society B: Biological Sciences*, *274*(1628), 2935–2942. https://doi.org/10.1098/rspb.2007.0985

Testa, J. W., Oehlert, G., Ainley, D. G., Bengtson, J. L., Siniff, D. B., Laws, R. M., & Rounsevell, D. (1991). Temporal variability in Antarctic marine ecosystems: periodic

fluctuations in the phocid seals. *Canadian Journal of Fisheries and Aquatic Sciences*, *48*(4), 631–639. https://doi.org/10.1139/f91-081

Tett, S. F. B., Jones, G. S., Stott, P. A., Hill, D. C., Mitchell, J. F. B., Allen, M. R., Ingram, W. J., Johns, T. C., Johnson, C. E., Jones, A., Roberts, D. L., Sexton, D. M. H., & Woodage, M. J. (2002). Estimation of natural and anthropogenic contributions to twentieth century temperature change. *Journal of Geophysical Research Atmospheres*, *107*(16).

Todd, C., & Doyle, R. (1981). Reproductive Strategies of Marine Benthic Invertebrates: A Settlement-Timing Hypothesis. *Marine Ecology Progress Series*, *4*, 75–83. https://doi.org/10.3354/meps004075

Turner, J. (2004). The El Niño-Southern Oscillation and Antarctica. *International Journal of Climatology*, *24*(1), 1–31. https://doi.org/10.1002/joc.965

Turner, J., Barrand, N. E., Bracegirdle, T. J., Convey, P., Hodgson, D. A., Jarvis, M., Jenkins, A., Marshall, G., Meredith, M. P., Roscoe, H., Shanklin, J., French, J., Goosse, H., Guglielmin, M., Gutt, J., Jacobs, S., Kennicutt, M. C., Masson-Delmotte, V., Mayewski, P., … Klepikov, A. (2014). Antarctic climate change and the environment: An update. *Polar Record*, *50*(3), 237–259. https://doi.org/10.1017/S0032247413000296

Turner, J., Lu, H., White, I., King, J. C., Phillips, T., Hosking, J. S., Bracegirdle, T. J., Marshall, G. J., Mulvaney, R., & Deb, P. (2016). Absence of 21st century warming on Antarctic Peninsula consistent with natural variability. *Nature*, *535*(7612), 411–415. https://doi.org/10.1038/nature18645

Tyler, P. A., Reeves, S., Peck, L. S., Clarke, A., & Powell, D. K. (2003). Seasonal variation in the gametogenic ecology of the Antarctic scallop Adamussium colbecki. *Polar Biology*, *26*(11), 727–733. https://doi.org/10.1007/s00300-003-0548-2

van der Meer, J. (2006). An introduction to Dynamic Energy Budget (DEB) models with special emphasis on parameter estimation. *Journal of Sea Research*, *56*(2), 85–102. https://doi.org/10.1016/j.seares.2006.03.001

Venables, H. J., Clarke, A., & Meredith, M. P. (2013). Wintertime controls on summer stratification and productivity at the western Antarctic Peninsula. *Limnology and Oceanography*, *58*(3), 1035–1047. https://doi.org/10.4319/lo.2013.58.3.1035

Vergani, D. F., Labraga, J. C., Stanganelli, Z. B., & Dunn, M. (2008). The effects of El Niño-La Niña on reproductive parameters of elephant seals feeding in the Bellingshausen Sea. *Journal of Biogeography*, *35*(2), 248–256.

https://doi.org/10.1111/j.1365-2699.2007.01780.x

Walker, C. W., Lesser, M. P., & Unuma, T. (2013). Sea urchin gametogenesis - Structural, functional and molecular/genomic biology. In *Developments in Aquaculture and Fisheries Science* (Vol. 38, Issue December). Elsevier. https://doi.org/10.1016/B978-0-12-396491-5.00003-4

Walter, J., Jentsch, A., Beierkuhnlein, C., & Kreyling, J. (2013). Ecological stress memory and cross stress tolerance in plants in the face of climate extremes. *Environmental and Experimental Botany*, *94*, 3–8. https://doi.org/https://doi.org/10.1016/j.envexpbot.2012.02.009

Welch, DW, Ishida Y, Nagasawa K (1998) Thermal limits and ocean migrations of sockeye salmon (*Oncorhynchus nerka*): long-term consequences of global warming. *Canadian Journal of Fisheries Aquatic Sciences* 55:937–948. https://doi.org/10.1139/f98-023

Welhouse, L., Lazzara, M., Keller, L., Tripoli, G., & Hitchman, M. (2016). Composite analysis of the effects of ENSO events on Antarctica. *Journal of Climate*, *29*(5), 1797–1808. https://doi.org/10.1175/JCLI-D-15-0108.1

Wetherald, R. T., Stouffer, R. J., & Dixon, K. W. (2001). Committed warming and its implications for climate change. *Geophysical Research Letters*, *28*(8), 1535–1538.

White, W. B., Chen, S. C., Allan, R. J., & Stone, R. C. (2002). Positive feedbacks between the Antarctic Circumpolar Wave and the global El Niño-Southern Oscillation wave. *Journal of Geophysical Research C: Oceans*, *107*(10), 29–1. https://doi.org/10.1029/2000jc000581

Wilson, S. K., Depcyznski, M., Fisher, R., Holmes, T. H., Noble, M. M., Radford, B. T., Rule, M., Shedrawi, G., Tinkler, P., & Fulton, C. J. (2018). Climatic forcing and larval dispersal capabilities shape the replenishment of fishes and their habitat-forming biota on a tropical coral reef. *Ecology and Evolution*, *8*(3), 1918–1928. https://doi.org/10.1002/ece3.3779

Wood, S. (2011). Fast stable restricted maximum likelihood and marginal likelihood estimation of semiparametric generalized linear models. *Journal of the Royal Statistical Society*, *73*(Part 1), 3–36. https://doi.org/1369–7412/11/73003

Wood, S., Baums, I. B., Paris, C. B., Ridgwell, A., Kessler, W. S., & Hendy, E. J. (2016). El Nino and coral larval dispersal across the eastern Pacific marine barrier. *Nature Communications*, *7*(12571). https://doi.org/10.1038/ncomms12571

Woodin, S. A., Hilbish, T. J., Helmuth, B., Jones, S. J., & Wethey, D. S. (2013). *Climate change , species distribution models , and physiological performance metrics : predicting when biogeographic models are likely to fail*. https://doi.org/10.1002/ece3.680

Xuebin, Z., & Mcphaden, M. J. (2008). Eastern equatorial Pacific forcing of ENSO sea surface temperature anomalies. *Journal of Climate*, *21*, 6070–6079. https://doi.org/10.1175/2008JCLI2422.1

Young, J. S., Peck, L. S., & Matheson, T. (2006a). The effects of temperature on peripheral neuronal function in eurythermal and stenothermal crustaceans. *Journal of Experimental Biology*, *209*(10), 1976–1987. https://doi.org/10.1242/jeb.02224

Young, J. S., Peck, L. S., & Matheson, T. (2006b). The effects of temperature on walking and righting in temperate and Antarctic crustaceans. *Polar Biology*, *29*(11), 978–987. https://doi.org/10.1007/s00300-006-0140-7

Yuan, X. (2004). ENSO-related impacts on Antarctic sea ice: A synthesis of phenomenon and mechanisms. *Antarctic Science*, *16*(4), 415–425. https://doi.org/10.1017/S0954102004002238

Zachos, J., Pagani, H., Sloan, L., Thomas, E., & Billups, K. (2001). Trends, rhythms, and aberrations in global climate 65 Ma to present. *Science*, *292*(5517), 686–693. https://doi.org/10.1126/science.1059412

Zhadan, P. M., Vaschenko, M. A., & Almyashova, T. N. (2017). Effects of environmental factors on reproduction of the sea urchin *Strongylocentrotus Intermedius* . *Sea Urchin - From Environment to Aquaculture and Biomedicine*, *October*. https://doi.org/10.5772/intechopen.69511

Zhadan, P. M., Vaschenko, M. A., & Ryazanov, S. D. (2018). Assessing the effect of environmental factors on the spawning activity of the sea urchin *Strongylocentrotus intermedius* through video recording observations. *Marine Ecology Progress Series*, *588*, 101–119. https://doi.org/10.3354/meps12436

Zupo, V., Glaviano, F., Paolucci, M., Ruocco, N., Polese, G., Di Cosmo, A., Costantini, M., & Mutalipassi, M. (2019). Roe enhancement of Paracentrotus lividus: Nutritional effects of fresh and formulated diets. *Aquaculture Nutrition*, *25*(1), 26–38. https://doi.org/10.1111/anu.12826

Zuur, A., Ieno, E. N., & Smith, G. M. (2007). Analyzing Ecological Data. In W. W. M. Gail, K. Krickeberg, J. Samet, A. Tsiatis (Ed.), *Analyzing Ecological Data* (1st ed., pp. 23–47). Springer-Verlag New York.